From the characterization of human skin to the development of a skin model

Agnieszka Katarzyna Dąbrowska

ETH Zürich, 2017

DISS. ETH NO: 24048

From the characterization of human skin to the development of a skin model

A thesis submitted to attain the degree of

DOCTOR OF SCIENCES of ETH ZURICH

(Dr. sc. ETH ZURICH)

presented by

Agnieszka Katarzyna Dąbrowska

Master of Science, West Pomeranian University of Technology in Szczecin

born on 11.03.1989

citizen of Poland

accepted on the recommendation of

Prof. Dr. Nicholas D. Spencer	Examiner
Prof. Dr. Mark Rutland	Co-examiner
Dr. René M. Rossi	Co-examiner
Dr. Fabrizio Spano	Co-examiner

2017

For my parents

"Nothing in life is to be feared, it is only to be understood. Now is the time to understand more, so that we may fear less."

Maria Skłodowska Curie

Acknowledgments

Taking this opportunity, I would like to thank everyone who made this PhD project possible, efficient and pleasant.

First of all, I would like to thank my supervisors. Sharing duties among so many bosses could be difficult, but thanks to their competence and willingness to discuss, the work was easier, more effective and satisfying.

I am thankful to Nicholas D. Spencer for welcoming me into his great group. Although being such a busy man, he was always able to find time for discussion and he was always extremely fast with his meaningful feedback. He was also able to create an amazing atmosphere in the group, being not only the boss, whom people appreciate, and respect, but also a real member of the team.

I also would like to thank René Rossi for welcoming me into his laboratory, as well as for the freedom and trust that he gave me. I am really thankful for all possibilities that I got during my PhD project: willingness to start all new collaborations that I needed and chance to attend great conferences and meetings.

I am grateful to Fabrizio Spano for his commitment and expertise every single day during this project. His office was always open for me and he was always optimistic about new ideas. Besides being a great boss, he was also a fabulous colleague, always happy to talk, for example about new teas and chocolates.

I should not forget about Mark Rutland, who agreed to attend my defense as one of my examiners. I am really thankful for his time and effort.

I am also thankful to Gelu M. Rotaru, who was also involved in the project from the very beginning. I always admired his knowledge and professionalism.

I also need to thank Siegfried Derler for his involvement and accurate feedback, even when he was no longer involved in my project.

Then, I would also like to thank Christian Adlhart for a great collaboration that resulted in the paper, being the heart of my thesis. I am thankful for his time, effort and continuous smile on his face.

I will always remember my master's student, Patryk Spera, who was always curious and happy to work. He was able to bring some fresh light to my project. His work answered many questions that were always waiting to be answered.

Work is always enjoyable when the atmosphere at the workplace is nice. Therefore I would like to thank all members of the LSST and ISA groups for all the nice discussions, for their time and help. I am also thankful to the members of the Laboratory for Protection and Physiology at Empa for welcoming me into their group and for a very nice time that I had thanks to them. Here, I would like to express special thanks to my friend, Agnieszka Psikuta, for her professional opinions and help. I would also like to thank Yvonne Metzger and Josephine Baer, our administrative assistants, for being able to organize everything that I could ever need to make my work easier and more efficient.

Last but not least I would like to thank people whose help turned out to be very important for my research: James Best, Gökçe Yazgan, Brit Maike Quandt, Reto Völlmin, Braid McRae, Giuseppino Fortunato and Christian Affolter, who were always willing to help, either answering my never-ending questions, organizing important meetings, introducing me to advanced devices or discussing my language dilemmas.

The professional side of life would be nothing without a strong foundation and support from family and friends.

Firstly, I would like to thank my parents, who brought me into this world and raised me to be the human being that I am now. They always believed in me and they never skimped on good words. I always felt loved, accepted and motivated: what else would a child need from parents?

Then, of course, I would like to thank my fiancé, Tomasz Piątek. He was the one who encouraged me to apply for this position and who always believed that I am stronger than I think. He was also the one who was with me every day for the last almost twelve years, no matter whether I was nice and smiling or a little bit unbearable.

I could not forget about my grandparents, for whom even the smallest reason was enough to be so proud of me.

And finally, I would like to thank my friends, who always remembered about me and were extremely flexible to find time to meet me during my short visits to the homeland.

Abstract

Evolution gave humans their skin; a functional protective barrier perfectly adapted to the surrounding environment. Skin has accompanied human kind from the beginning of its existence and has always played a very important role in everyday life.

Not surprisingly, also today human skin remains a popular topic among researchers. Recently, more attention has been focused on the interfacial role of human skin. Skin is the first layer of contact between the human body and environmental factors and it is supposed to protect internal organs from harmful factors. On the other hand, skin properties and function can be affected by environmental conditions and contact with other materials and substances. This can result, for example, in chemical burns, skin irritation or diseases, but also in friction-related issues, such as friction burns, decubitus ulcers, discomfort or mechanical damage.

Investigations of the skin-environment interactions can be performed *in vivo*, involving human volunteers or *in vitro*, using skin models. Various skin models have been validated for different applications, but there is still a vast space for improvement and new solutions.

This thesis focuses on the influence of water on human skin properties, especially frictional behaviour, as well as the development of a physical water-responsive skin model to mimic frictional behaviour of human skin rubbed against textiles under dry conditions as well as in the presence of water.

A substantial background chapter has been developed, in order to summarize the state of the art related to human skin properties as a function of body-related and environmental factors, as well as the frictional behaviour of human skin under dry and hydrated conditions and an overview of materials used as skin models for various applications.

The first step on the way to develop a new physical skin model involved testing materials with mechanical properties similar to those of human skin, such as Pebax or polyurethanes, as well as commercially available materials with the potential to be used as skin models, such as Lorica® Soft and Stamskin Silicone. Unfortunately, focusing on mechanical and structural properties was not enough to develop a skin model that would mimic the significant increase in friction coefficients values observed for human skin rubbed against textiles in the presence of water.

The next section introduces the results of an investigation on hydration-induced changes in human skin, such as hydration level, surface roughness, *stratum corneum* thickness and interaction with other materials. Upon water uptake, the hydration level of first few μm of the *stratum corneum* increased significantly. Uptake of water and swelling led to increase in the *stratum corneum* thickness. In addition, water exposure resulted in lower surface roughness and the decrease in the dimensions of primary lines, which led to increased real contact area with other objects.

Finally, in the last step, the combination of my preliminary results and knowledge about hydration-induced changes in human skin properties, led to the development of a gelatine-based, water-responsive skin model. This skin model mimics the changes observed for human skin after prolonged contact with water: It demonstrates the same change in frictional behaviour, both according to the friction coefficient values, as well as general trends. Moreover, the gelatine-based skin model shows a significant decrease in tensile Young's modulus values after immersion in water, as was reported for human skin, and is characterised by comparable values of tensile Young's modulus in both a dry and a hydrated state. In addition, both for human skin and the skin model, surface smoothening and an increase in thickness were observed after water exposure.

The proposed skin model can be used instead of or next to *in vivo* friction measurements and can lead to better understanding of the mechanisms of human-skin friction, as well as facilitating the avoidance of friction-related injuries and irritations and leading to more comfortable usage of many everyday items.

Zusammenfassung

Die Evolution gab den Menschen ihre Haut: ein funktionelle Schutzschicht, die sich an die umgebende Umwelt perfekt angepasst hat. Die Haut begleitet Menschen seit dem Anfang ihres Lebens und spielt allzeit eine wichtige Rolle im Alltag.

Nicht überraschend bleibt auch heutzutage die Haut ein populäres Forschungsthema. In letzter Zeit ist mehr Aufmerksamkeit auf die Rolle der Haut als Grenzfläche gerichtet worden. Die Haut ist die erste Kontaktfläche zwischen dem Körper und Umweltfaktoren und soll die inneren Organe vor den schädigenden Faktoren schützen. Andererseits können die Eigenschaften und Funktionen der Haut von Umwelteinflüssen und dem Kontakt mit den anderen Materialien und Substanzen beeinflusst werden. Auswirkungen davon können, zum Beispiel, Verätzungen, Irritationen, Hautkrankheiten oder auch reibungsverursachte Probleme, wie Reibungsverbrennungen, Drückgeschwüre, Unbehagen oder mechanischer Schaden sein.

Untersuchungen der Wechselwirkungen zwischen Haut und Umwelt können *in vivo* (den Menschen involvierend) oder *in vitro* (Hautmodelle benutzend) gemacht werden. Verschiedene Hautmodelle sind bereits für verschiedene Anwendungen verifiziert worden, es gibt aber weiterhin Raum für Verbesserungen und neue Lösungen.

Diese Dissertation befasst sich zum einen mit dem Einfluss von Wasser auf die Hauteigenschaften, insbesondere das Reibungsverhalten sowie zum anderen mit der Entwicklung eines physikalischen, auf Wasser reagierenden Hautmodells um das Reibungsverhalten der Haut gegen Textilien in trockenen Bedingungen und auch in Gegenwart von Wasser zu imitieren.

Der theoretische Hintergrund wurde ausführlich bearbeitet um den Stand der Technik bezüglich der Hauteigenschaften als Funktion von Einflüssen des Körpers selbst als auch der Umwelt zusammenzufassen. Ausserdem wurde das Reibungsverhalten der Haut in trockenen und hydrierten Bedingungen und die in verschiedenen Anwendungen als Hautmodell benutzten Materialien eingeführt.

Der erste Schritt um ein neues physikalisches Hautmodell zu entwickeln schloss die Prüfung von Materialien mit hautähnlichen mechanischen Eigenschaften (z.Bsp. Pebax und Polyurethane) mit ein, sowie kommerziell verfügbare Materialien

wie Lorica® Soft und Stamskin-Silikon, die Potenzial als Hautmodell zeigen. Der Fokus auf mechanischen und strukturellen Eigenschaften war leider nicht genug um ein Hautmodell zu entwickeln, welches die signifikante Erhöhung der Reibungskoeffizienten wiederspiegelt, der für die Hautreibung gegen Textilien in Gegenwart von Wasser beobachtet wird.

Im zweiten Teil werden die Ergebnisse der Untersuchung zu den hydrierungsbedingten Veränderungen der Haut vorgestellt, wie zum Beispiel das Hydrierungsniveau, die Rauhtiefe, die *stratum corneum* Dicke und die Interaktion mit anderen Materialien.

Bezüglich der Wasseraufnahme stieg die Hydratation der ersten paar μm des *stratum corneum* bedeutend. Die Wasseraufnahme und Schwellung führte zu einer Erhöhung der *stratum corneum* Dicke. Zusätzlich führte die Wasserbehandlung zu einer kleinen Rauhtiefe und zu einer Abnahme der Größe der Primärrillen der Haut, was zu einer erhöhten effektiven Kontaktfläche mit anderen Objekten führte.

Schließlich, im letzten Schritt wurde ein Gelatine-basiertes, auf Wasser reagierendes Hautmodell aus der Kombination meiner Präliminärergebnisse mit dem gewonnenen Wissen über die hydrierungsinduzierten Veränderungen der Eigenschaften der Haut entwickelt. Dieses Hautmodell imitiert die Veränderungen, die bei der Haut nach längerem Wasserkontakt beobachtet werden. Es zeigt ebenfalls die Veränderung des Reibungsverhaltens, sowohl entsprechend der Reibwerte, als auch der allgemeinen Trends. Das Gelatine-basierte Hautmodell zeigt ausserdem eine deutliche Abnahme des Zugmoduls nach dem Eintauchen in Wasser, wie es auch für Haut berichtet wird und zeigt vergleichbare Elastizitätsmodulwerte in trockenem und hydriertem Zustand. Zusätzlich, sowohl für die Haut als auch für das Hautmodell, konnte Oberflächenglättung und eine Erhöhung der Dicke nach Wasserkontakt beobachtet werden.

Das vorgeschlagene Hautmodell kann anstelle von oder zusammen mit den *in vivo*-Reibungsmessungen benutzt werden. Dies führt zu einem besseren Verständnis des Hautreibungsmechanismus sowie reibungsverursachte Verletzungen und Reizungen verhindern und so eine komfortablere Anwendung von Alltagsgeräten ermöglichen.

Table of contents

Chapter 1

Introduction

The first chapter of the thesis provides a general introduction about the field and gives an overview of the content of the thesis. Section 1.1 focuses on our motivation for the research. Section 1.2 introduces the scope of the thesis.

1.1. General introduction

One of the main functions of skin is to protect the body from external threats. Skin plays a role of an active shelter, regulating temperature, absorbing radiation, and preventing the penetration of various biological and chemical substances [1-3]. As it is the outermost layer of the body, it remains in constant interaction with the environment and various materials. Hence, investigations focused on the influence of environmental factors on the functioning of human skin, as well as friction-related experiments, are an important topic, facilitating the avoidance of injuries and generally increasing safety in everyday life. [4-6].

Human skin, although it acts as a barrier, is not inert to all agents present in the environment [7]. Moreover, properties of human skin can vary, depending on many factors, such as age, gender, ethnicity, hydration level, foundation type, lifestyle etc. [4, 8]. The natural complexity of skin structure, properties and performance, additionally augmented by an infinite number of possible modifications caused by both skin penetration and body-dependent factors, poses a strong motivation for further research in this field [9, 10].

Water is one of the substances that can significantly influence skin properties [11, 12]. Water is not only commonly found in the environment, but it is also constantly present on the surface of the skin in the form of sweat [13]. On average two to four millions sweat glands secret sweat in a process that is mainly responsible for temperature regulation [14]. Emotions and ingestion can also trigger sweating (emotional and gustatory sweating) [15]. The sweating rate of the healthy body can even exceed 1.8 l/h during exercise in a warm environment [16]. Sweating, sweat accumulation and water coming from external sources (moisturizers, rainfall etc.) all influence skin properties. Skin, following contact with water, becomes more elastic [17], the thickness of the *stratum corneum* layer increases [18] and the dimensions of the primary lines decrease [19].

Sweating can also be directly related to the frictional behaviour of skin. It is known that hydrated human skin is characterised by higher friction-coefficient values than dry skin [11, 20, 21]. This phenomenon is commonly explained based on the adhesion theory of friction, which states that an increased amount of water leads to both smoothening and softening of the skin surface, resulting in higher real contact area and the presence of capillary bridges, higher adhesion forces and, consequently, higher

friction coefficient [20, 22-25]. According to some researchers, the high density of eccrine sweat glands present on palms and soles allows the grip to be improved during motion via elevated friction coefficient values [26]. Increased sweating rate in stressful situations is motivated by the beneficial influence of higher friction coefficient on escape speed in prehistoric times [26]. On the other hand, constant contact with a flat surface and the resulting enhanced sweating result in the formation of a lubricating water layer that leads to decreased friction coefficient [27].

As already mentioned, human skin constantly interacts with other objects. The character, effect and safety of these interactions are strictly related to the frictional behaviour of human skin. Friction influences our tactile perception [28], as well as the comfort and safety of usage of various products [29]. Therefore friction-related investigations are very important, especially when the new product is introduced into the market and is supposed to stay in contact with the skin for an extended period (tools, household items, medical equipment or functional clothes).

As frictional behaviour of human skin depends not only on skin properties and the countersurface, but also on environmental conditions, in vivo friction measurements are very difficult to perform and need many repetitions to be statistically significant. The use of skin models would appear to be a cheaper and more convenient alternative.

Skin models can be used instead of, or in addition to, *in vivo* measurements, in order to determine the response of human skin to triggers of any nature. The use of skin models can make measurements less complicated, safer, faster and cheaper. As human skin is a complex material performing many functions in everyday life, there is a tremendous variety of both existing and potential skin models [4]. Skin models mimicking the frictional behaviour of human skin constitute only one out of many specific types of skin models.

According to the literature, several materials have been used as frictional skin models, such as Lorica®, silicones, polyurethanes or polyamides [5]. Unfortunately, all existing skin models show clear limitations and perform a useful role only under specific conditions. For that reason, there is a need for more advanced skin models that can simulate frictional behaviour of dry and wet human skin, providing trustworthy results and at the same time being inexpensive and convenient to use and store.

1.2. Scope of the thesis

Human skin is a complex material, whose properties and performance depend on many internal and external factors. Despite the long history of skin-related research, there are still some missing points in our knowledge about human skin, its structure, properties, functions and the influence of possible stimuli on skin characteristics.

The role of a skin model or artificial skin is to mimic chosen properties or functions of human skin. It is important to know detailed characteristics of human skin related to a specific situation, in order to design an applicable substitute for human skin.

The main goal of this thesis is to investigate interactions between human skin and textiles in dry and hydrated conditions, as well as to examine the influence of hydration on the structure, properties and performance of human skin and, based on the collected results and literature, design a physical skin model that mimics the frictional behaviour of human skin.

The chapters of the thesis explain the influence of hydration on the structure, properties and performance of human skin and present the line of thinking about potential skin substitutes and all the steps undertaken to design and optimize the bio-mimicking physical skin model.

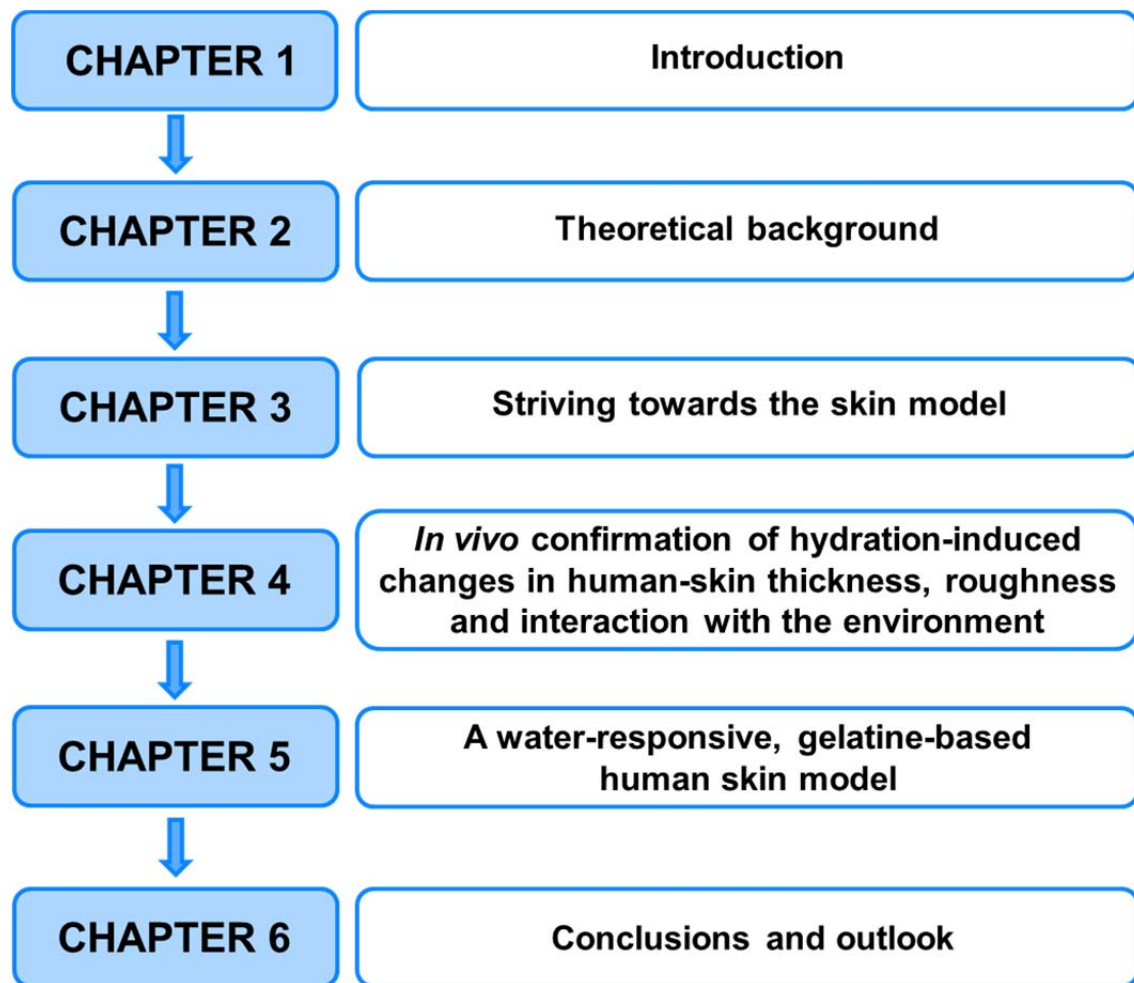Figure 1.1 summarizes the scope of the thesis.

CHAPTER 1	**Introduction**
CHAPTER 2	**Theoretical background**
CHAPTER 3	**Striving towards the skin model**
CHAPTER 4	*In vivo* confirmation of hydration-induced changes in human-skin thickness, roughness and interaction with the environment
CHAPTER 5	**A water-responsive, gelatine-based human skin model**
CHAPTER 6	**Conclusions and outlook**

Figure 1. 1. Scope of the thesis.

Chapter 1 presents a general introduction and the scope of the thesis.

Chapter 2 provides the theoretical background for human skin structure, properties and functions. It also presents the influence of body-dependent factors and penetration on human skin functioning and introduces the topic of human skin frictional behaviour. Finally, it gives an overview of various materials that have been used as skin models.

Chapter 3 presents the line of thinking on an approach to develop a new bio-mimicking skin model. It explains why some materials, especially those processed in a certain way, could act as skin substitutes. It also summarizes initial results and further research possibilities.

Chapter 4 describes how human skin takes up water and what the consequences of the change in hydration level of the skin are. It shows the link between the hydration, structure and morphology of human skin, as well as the way in which it interacts with other materials.

Chapter 5 presents our new bio-mimicking gelatine-based physical skin model to simulate the frictional behaviour of human skin. This chapter focuses on the preparation and characterization of the skin model that mimics the frictional behaviour of human skin against a chosen textile under dry and hydrated conditions over a wide range of applied normal load. Other parameters were also considered, such as Young's modulus and surface roughness, as well as changes due to forced hydration.

Chapter 6 contains general conclusions, a summary of the thesis and an outlook.

Chapter 2

Theoretical background

Chapter 2 provides a detailed theoretical background and focuses on human skin characteristics, including skin structure, properties, functions, frictional behavior, as well as factors that influence human skin in everyday life. In addition, it introduces the variety of materials used as physical skin models.

Sections 2.1 and 2.4 are based on my contribution, under the supervision of G.M. Rotaru, F.Spano, R.M.Rossi and N.D. Spencer, to Ref. [4]:

Dąbrowska AK, Rotaru GM, Derler S,

Spano F, Camenzind M, Annaheim S,

Stämpfli R, Schmid M and Rossi RM.

Materials used to simulate physical properties of human skin.

Skin Research and Technology. 2016;22:3-14

All coauthors participated in the discussions and corrections of the manuscript written by myself, G.M. Rotaru and S. Derler.

Section 2.2 is based on my own contribution under the supervision of F.Spano, G.M. Rotaru, R.M. Rossi and N.D. Spencer, to Ref. [30]:

Dąbrowska AK, Spano F, Derler S,

Adlhart C, Spencer ND and Rossi RM.

Relationship between skin functioning, barrier properties and body-dependent factors.

Submitted to Colloids and Surfaces B: Biointerfaces (November 2016)

All coauthors participated in discussions and correction of the manuscript written by myself under the supervision of F.Spano, R.M. Rossi and N.D. Spencer.

2.1. Human skin: structure, functions and properties

Human skin has complex properties and functions and is in continuous change due to environmental, biochemical, and psychological factors [9, 31]. Figure 2.1 shows schematically the human skin structure and important interactions with the environment.
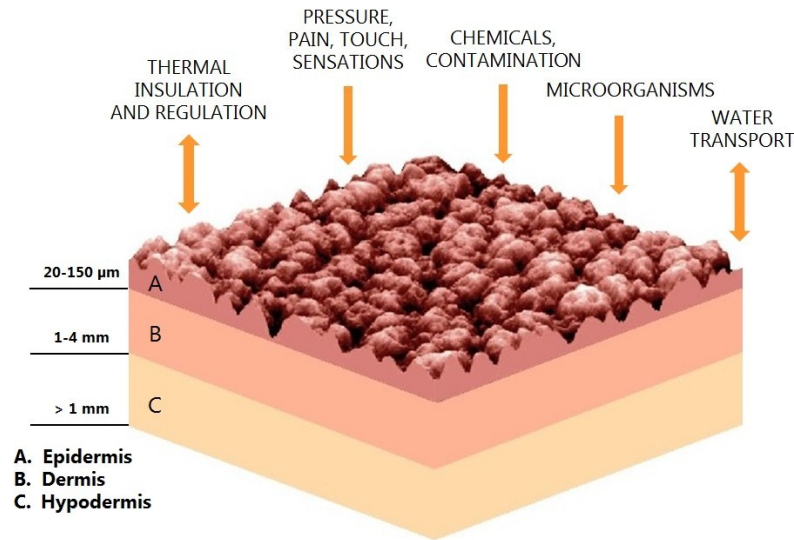

Figure 2. 1. Schematic of human skin structure and the main interactions with the environment.

As a result of this complexity, assigning exact numeric values for its properties, as is common for nonbiological materials, is of limited use. Instead, statistical investigations based on subject studies and physical and numerical simulations are more meaningful to characterise the skin. Generally, skin properties are anisotropic, as well as dependent on time, site, temperature, and measurement method. Furthermore, the presence of substances on the skin (e.g. sweat, water, dust, cosmetics) can strongly affect skin properties and interactions with the environment.

Human skin structure is organized in three main layers: *epidermis*, *dermis* and *hypodermis*. The *epidermis* is thin, with a typical thickness of about 20–150 μm [32], depending mostly on the body site except for the palms and soles that are thicker [33]. It mainly consists of keratinocytes, which differentiate in the *stratum basale* and then migrate outwards, changing their shape, physiology and function. Dead keratinocytes, the corneocytes, are stored in the outermost layer forming the *stratum corneum*, which has a thickness of about 14 μm [34]. The thickness of the *dermis* varies between 1 and 4 mm. The *dermis* is built up of collagen and keratin fibers, which provide structural

strength to the skin. The *hypodermis* or the fat layer lies below the *dermis* and helps protect the body from heat and cold, and from mechanical shocks [34, 35].

The main functions of the skin are: protection (against mechanical, thermal, and chemical impact, UV radiation, microorganisms etc.), repair and adaptation (self-healing and change in composition and structure when injured or exposed to stresses), sensation through its mechanoreceptors, thermoreceptors and nociceptors) and temperature regulation (e.g. control of the sweating and perfusion rate). The skin is also responsible for the synthesis of vitamin D3 and the excretion of water, urea, ammonia and uric acid. Besides these functions, the appearance of the skin has important implications on social interaction providing information about health, age, gender etc.

2.2. Relationship between skin functioning, barrier properties and body-dependent factors

2.2.1. Motivation

Human skin is the interface between human body and environment [35]. With a surface of some 2 m^2 and a mass equal to around 15% of total body mass, skin is the human body's largest single organ [36]. Skin is responsible for various functions that are very important for health and comfort in everyday life. The main functions of human skin are to regulate the temperature, both by insulation and sweating, to be involved in the functioning of the nervous system and the regulation of water content, and to protect the organism from mechanical injuries, microorganisms, substances and radiation present in the environment [1, 4].

The properties and condition of the skin vary with body site and can be influenced by various inherent body-dependent factors, such as skin type, ethnicity, or gender, or those that we can control, such as our lifestyle and body mass index (BMI). Skin can be also influenced by the penetration of various substances to which we are exposed [1, 8, 37]. Figure 2.2 shows how body-dependent factors and skin penetration can influence human skin.

The *stratum corneum* (SC) acts as a barrier that resist the penetration of external matter and loss of water, but it is not completely impermeable [7]. This can lead to harmful health effects of the environment [7]. On the other hand, the permeability of skin can be used for cosmetic purposes or drug delivery, which has been a developing technology since the 1970s [38, 39].

This review summarizes the different factors influencing and determining human-skin properties and performance and provides an overview of skin barrier functions and their limitations. We also discuss the absorption abilities of human skin, the mechanisms of penetration and the methods used to enable or improve drug-delivery processes. Our aim is to provide readers with an understanding of the complex relationship between all skin functions.
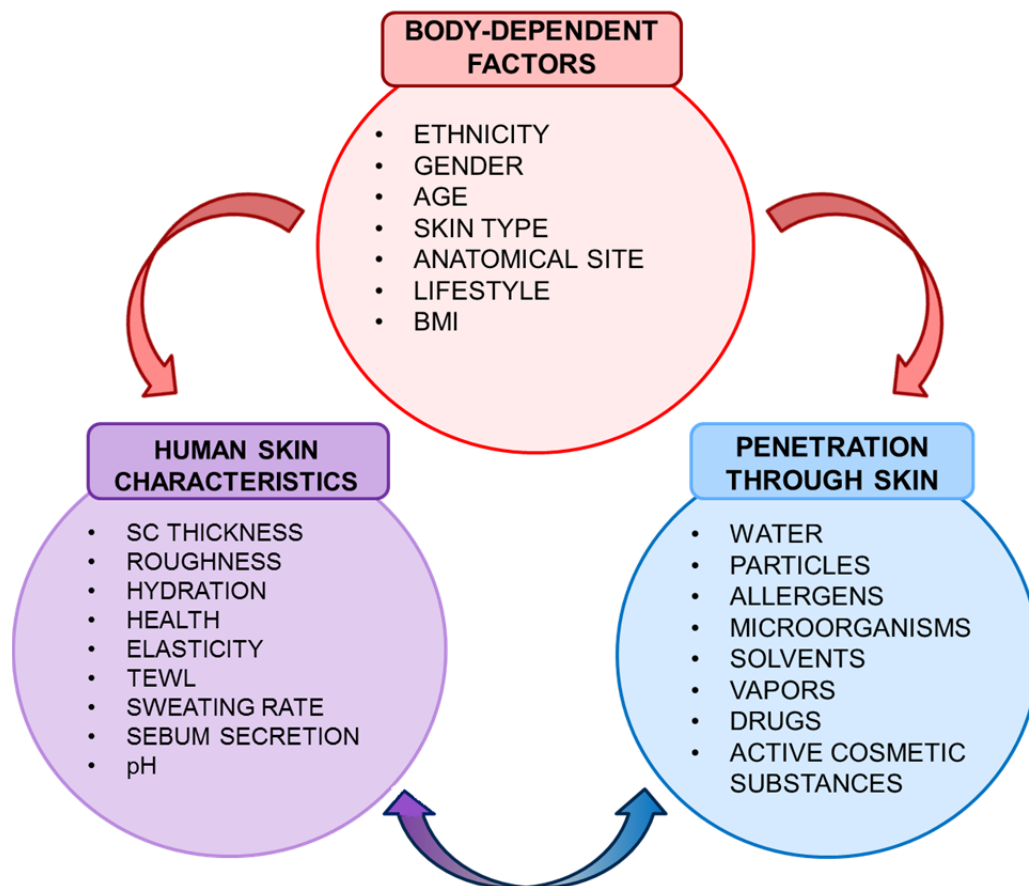
Figure 2. 2. Factors influencing human skin.

2.2.2. Body-dependent factors influencing human skin

Ethnicity

The most visible difference in skin characteristics between people coming from different ethnic groups is skin pigmentation [40, 41]. Skin tone varies due to different levels of the four chromophores responsible for skin color: hemoglobin and oxyhemoglobin, which are responsible for pinkish tones in the complexion, melanin, which correspond to brownish shades, and carotenoids, responsible for yellow-orange tones [40, 42]. Ethnicity also influences the natural hydration level of the skin as well as the decrease in hydration level with age [43-45]. It has been reported that Caucasians and African-Americans have slightly drier skin, compared to Chinese, due to the lower levels of SC natural moisturizing factors [40, 45-47]. Other experiment have shown no difference in skin hydration level between ethnic groups [48]. There is also a difference in the skin-ageing processes between different ethnic groups. Caucasians exhibit higher dryness with age than Chinese, which may be caused by different eating habits and avoidance of the sun exposure among Chinese [44, 49]. Also pigmentation changes in a different way for different ethnic groups [50]. It has been shown that darker skin is

more resistant to photo ageing processes [42]. Also the thickness of the SC was found to be greater for darker skin [49, 51]. Some studies have also indicated differences in SC thickness or in the number of layers within comparable SC thickness, suggesting that African-Americans have more cell layers within the SC than do Caucasians (16 layers reported for African-Americans compared to 9 layers reported for Caucasians), the skin thus being more resistant to chemicals and damage [52-54]. The density of the SC is comparable for Caucasians and Asians [54]. Most studies demonstrated higher transepidermal water loss (TEWL) for African-Americans than for Caucasians [46, 53, 55] as well as larger gland pore sizes and a higher level of sebum secretion [40, 56].

Gender

Skin hydration was found to be different for female and male subjects [8, 45], but other studies have presented no clear relationship between gender and hydration of the skin [57-59]. Similar results were found for TEWL: some researchers found that TEWL is higher for men, explaining this by the fact that they spend more time outdoors and their skin is more damaged [8, 60, 61], but predominantly no relationship between gender and TEWL was found [58, 62-65]. Sebum secretion is considered to be either independent of gender [58] or slightly higher in males [8, 45, 66-68], due to a higher testosterone level [8, 45, 69]. The sweating rate was found to be 30-40% higher in males than in females (taking the difference in body surface area into consideration) [70]. Measurements of the surface pH of skin in males and females have shown contradictory results. Surface pH values for women have been found to be higher than [45, 64, 71, 72], lower then [73] or comparable with those reported for men [58, 74]. A similar situation exists regarding the thickness of skin in females and males. Results show no clear relationship between gender and SC thickness [51, 75-82], but it was also found that the cellular *epidermis* is slightly thicker in males than in females [51]. Measurements have shown no statistically significant difference between the elastic properties of the skin in females and males for the same anatomical sites [8, 83-86].

Age

Age is a very important factor influencing the skin and for the body in general. Overall, the hydration level of the skin decreases significantly with age, mainly because of the decrease in the amount of natural moisturizers present in the skin [8, 45, 84]. On the other hand, there are studies showing contrary results [87]. It was also found that the influence of the skin-ageing processes on skin hydration can vary between different ethnic groups, being the most significant for Caucasians [44]. Furthermore, the

elasticity of the skin is also known to decrease, predominantly due to the decreasing amount of collagen [8, 67, 84, 88-90]. The thickness of skin initially increases with age, showing a maximum value for women at around 30-40 years of age and for men at around 40-50 years, and then significantly decreases with age [91-93]. TEWL values were observed to be lower for infants than for adults and also varied with the anatomical site [94]. However, some measurements showed no statistically significant difference in TEWL values for adults of different ages [95-97]. The amount of sebum secretion has been reported to be either independent or slightly decreasing with age [8, 58, 67, 98]. The sweating rate slightly decreases with age [99, 100]. Ageing also influences skin pH, and has been found to be higher for older subjects [45, 95, 101]. Skin morphology is also related to the skin-ageing process. Skin roughness, the dimensions of the primary lines and anisotropy were all found to increase with age [35, 102-106]. Additionally, ageing leads to the creation of wrinkles and pigmented spots (hyperpigmentation) due to the reduced amount of collagen, as well as the reduced water-binding ability of skin and its lower elasticity, which can become problematic, especially for women [50, 84, 89, 107-109].

Skin type

Skin type, its pigmentation, hydration, roughness and many other parameters are very individual. Significant variations can be observed between people from the same ethnic groups, living in the same environment and sharing the same lifestyle. As already mentioned, naturally darker skin may be considered as being more resistant to damages caused by UV light [42]. Both higher pigmentation and hydration level can slower skin-ageing processes [42, 49].

Anatomical sites

Skin differs not only between different people but also between anatomical sites for the same person [5, 110, 111]. Table 2.1 summarizes exemplary characteristics of human skin for different anatomical sites.

Table 2. 1. Dependence of main properties of human skin on the anatomical site.

Human skin characteristics	Anatomical site	Value/range (reference)
SC thickness	volar forearm	18.3 ± 4.9 µm [51]

		22.6 ± 4.33 µm [112]
	shoulder	11 ± 2.2 µm [51] 21.8 ± 3.63 µm [112]
	buttock	14.9 ± 3.4 µm [51]
	cheek	16.8 ± 2.84 µm [112]
	back of hand	29.3 ± 6.84 µm [112]
roughness Ra	forehead	12-15 µm [35]
	volar forearm	17-20 µm [35]
	index finger	19-33 µm [35]
hydration level	forehead	53.54 ± 16.49 corneometer units [8]
	Forearm	51.00 ± 15.92 corneometer units [8] *(corneometry)* 26.2 ± 3.4% [19] *(confocal Raman spectroscopy)*
	leg	37.22 ± 17.50 corneometer units [8]
	palm	40.47 ± 18.47 corneometer units [8] *(corneometry)* 30 ± 5 % [113] *(confocal Raman spectroscopy)*
TEWL	forehead	12.27 ±10.05 g/m^2/h [8]
	forearm	10.12 ± 9.54 g/m^2/h [8]
	leg	9.68 ± 9.52 g/m^2/h [8]
	palm	23.47 ± 9.67 g/m^2/h [8]
sweating rate	whole body	95 ± 13 g/m^{2}h [16] *(average for 10 subjects walking on a flat treadmill in 20 ˚C, 40% RH with a speed of 1.34 m/s)*
sebum secretion	forehead	95.65 ± 51.38 µg/cm^2 [8]
	forearm	18.45 ± 37.88 µg/cm^2 [8]
	cheek	73.39 ± 64.05 µg/cm^2 [8]

	leg	2.88 ± 6.42 µg/cm^2 [8]
	palm	9.82 ± 10.11 µg/cm^2 [8]
Elasticity	forearm	E*=8.3 ± 2.1 kPa [114] *(indentation in vivo)* E= 0.42-0.85 MPa *[115]* *(torsion test in vivo)* E= 129 ± 88 kPa *[116]* *(suction test in vivo)*
pH	forehead	6.43 ± 0.44 [95] *(average amount people at the age of 24-34 years)*
	forearm	5.30 ± 0.30 [95]
	cheek	5.07 ± 0.45 [95]

For example, the SC thickness, given by the number of cell layers, varies significantly with the investigated anatomical site [82, 117]. It was found that the thickest SC layer is to be found in heels, having 86 ± 36 cell layers, whereas the smallest number of cell layers (6 ± 2) has been observed for genital skin [82]. The SC thickness on the forearm, back and thigh lies within the range of 11-13 µm, whereas on the abdomen, the SC layer is thinner (8.7 ± 7.5 µm) [118]. The thickness of the *epidermis* depends on the body site in a similar way [33, 51]. The SC thickness is related to many other phenomena, such as surface morphology, hydration level and permeability to various substances [19, 119, 120]. Since the SC acts as a barrier layer, penetration through the skin is higher on body sites with thinner SC. This phenomenon has been observed for water and other substances [118, 121, 122]. Another parameter varying with anatomical site is surface morphology. The roughness (Ra) of the index finger lies within the range of 19 and 33 µm, whereas it is lower (12-20 µm) for the volar forearm [35, 123, 124]. Anatomical sites also differ between each other due to the presence of hair. While some body parts can be considered to be hairy (e.g. head), others can be considered as hairless (e.g. volar forearm) [35, 125, 126]. Also sebum secretion varies between different anatomical regions, not only as far as the amount is concerned, but also the chemical composition [95, 127-129]. The hydration level of the skin also depends on the body site. Due to many reasons, such as exposure to harsh environmental conditions or the frequency of washing with detergents, certain body parts, e.g. hands, are more prone to having a lower hydration level of the superficial *stratum corneum* (SSC) [112, 130]. The sweating rate and the density of sweat glands

are also dependent on the anatomical location. The highest density of sweat glands can be found on the soles of the feet (620 ± 20 sweat glands per cm^2), whereas the lowest density of sweat glands is found on the upper lips (16 sweat glands per cm^2) [131, 132]. TEWL also varies with the anatomical location. In general, the SC thickness is directly related to the TEWL and anatomical sites characterised by the thickest SC display the lowest TEWL values [133]. However, TEWL levels are also dependent on other factors, such as SC lipid content, blood flow or skin temperature [8, 133]. This explains the fact, that the TEWL of the palm (characterised by a thick SC layer but a low level of barrier lipids) is higher than that of the leg [8, 95]. Also the elastic properties of the skin vary between different anatomical sites. For example, facial skin was found to be less elastic than the skin on the arm and on the back [90]. The elastic properties of skin depend on the collagen structure in the *dermis*, the local thickness of the skin and other parameters that depend on the anatomical site [84, 134, 135]. As the properties of human skin are rarely independent of each other but work as a system, a variation in one property is generally coupled with ta variation in others. For example, the frictional behaviour of human skin varies with body sites because it depends on SC roughness, elastic properties, thickness, hydration level, sweating rate as well as on the presence of hair and sebum [28, 35, 112, 125, 136, 137].

Lifestyle and Body Mass Index

In addition to the above-mentioned factors, which are independent of everyday decisions and habits, there are additional aspects influencing our skin, such as lifestyle or body mass index.

Lifestyle is considered to be the one of the factors influencing the extrinsic ageing process, which is related to visible ageing caused by the exposure to external factors [37]. Human skin remains in constant interaction with the environment: the higher the exposure to harmful environmental factors, the lower the level of antioxidants protecting the organism from oxidative stress and inhibiting the skin-ageing process [138]. Habits preventing skin ageing are probably beneficial for overall health [37]. Proper sun protection allows the avoidance of accelerated skin ageing and the risk of skin cancer and other skin damage [139]. A healthy diet, containing significant amount of fruits and vegetables, as well as a calm, low-stress lifestyle, lead to a higher concentration of carotenoids and may result in a slower rate of skin ageing [138, 140]. Higher daily vitamin C intake has been connected to a decreased formation of wrinkles, while a higher linoleic acid dose has been associated with a lower level of dryness [141]. A study has shown that smoking is associated with a worse skin condition among women and men from different ethnic groups [37]. It also significantly increases the risk of skin diseases, such as necrosis after surgeries, as it decreases the

self-healing abilities of the skin [142-144]. The thickness of the SC was found to decrease with the number of years smoking [51]. Protection from the sun is a factor correlated with better skin appearance [37, 145]. Direct correlation between sun exposure and the number of wrinkles has been reported [139].

Skin properties are also dependent on the body mass index (BMI). TEWL is usually higher for obese people [40, 146]. Obesity is also correlated to elevated sweat gland activity and higher skin blood flow [146, 147]. According to the investigations, obesity can also increase the risk of various skin disorders [146, 147] and impaired wound healing [147]. For example, 74% of examined obese people have been found to suffer from *acanthosis nigricans*, also related to insulin resistance [147]. In another study, 40% of obese children were diagnosed with striae disease [147].

Cause and effect chain

Skin properties and performance depend on many body factors that are either provided by our genetic background or based on our choices and habits. In addition to individual factors, many external triggers and penetrating substances can simultaneously influence the skin. It has to be pointed out, that several different factors can influence the skin at the same time in everyday life. The same effect can have various origins while the same cause can result in different symptoms, depending on individuals and circumstances. An example, showing the cause and effect chain connected with the hydration level of skin, is summarized in Figure 2.3.
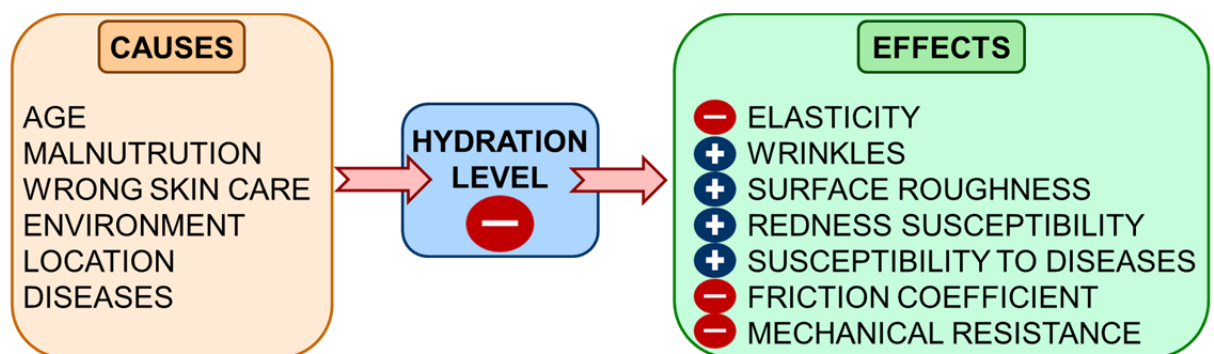

Figure 2. 3. Cause and effect chain for the example of the decrease in skin hydration level. "+" and "-"
symbolize positive and negative correlation

As skin hydration is a very important parameter responsible for skin homeostasis, all deviations from a normal hydration level can result in significant changes in human skin properties and functions [148]. Many factors can lead to a decreased hydration level of skin. Among the main causes of dry skin one can list skin

ageing [8], the wrong or no skin care [149] or malnutrition [150]. Skin hydration can also be influenced by environmental factors [151] or by anatomical location (e.g. skin on the palms and legs is drier than on the forehead) [8]. Skin dryness can also be a consequence of various diseases, not only directly related to the skin, such as atopic dermatitis, but also other health problems, e.g. hypothyroidism [152-155]. A lower hydration level results in a lower elasticity of the skin [8], faster skin ageing and wrinkles creation [124], higher surface roughness [156] and lower mechanical resistance [1]. Dry skin is also more susceptible to skin diseases and more prone to redness and itchiness [119, 157]. The frictional behaviour of human skin also depends on hydration [158]. It was reported that moist skin shows higher friction coefficient values than dry or completely wet skin. Based on the example of skin hydration, it can be concluded, that sometimes the causes of certain skin properties and their effects interact with each other, creating a self-perpetuating cycle, in particular for skin diseases.

2.2.3. Penetration through human skin

Our skin is constantly in contact with various substances that are either present in the environment or deliberately applied to the surface of the skin [159]. Numerous substances have been applied to the skin surface for medical or religious reasons since the beginning of humanity, which provides a hint that the absorption properties of the skin were already known a long time ago [160]. Depending on the circumstances, the barrier properties of human skin, given mainly by the horny layer of the skin (SC), may be perceived as either an advantage or an obstacle [161]. One of the functions of the skin is to protect the organism from both mechanical injury and harmful substances [4, 38, 162]. In everyday life, the skin can be exposed to various substances in the solid, liquid or gaseous state. Some of them, such as harmful chemicals, allergens, pathogens etc. can be dangerous and lead to irritation, rashes, burns or other health problems following the topical application or penetration of these substances into deeper layers of the skin [2, 160]. On the other hand, the skin barrier can be an obstacle for the delivery of therapeutic agents, present in drugs and cosmetics, for example [163]. Due to the skin's large surface area (around $2m^2$), the topical dosage of drugs seems to be an interesting alternative for medication, but, because of the barrier function of the skin, this method is far from straightforward [38, 162, 164].

The *epidermis* and *dermis* are the skin layers involved in the penetration processes, but the SC composition and properties are mainly responsible for the barrier function of human skin [1]. Skin protects the body from penetrating substances through various mechanisms, either mechanically blocking particles from further migration into the skin or neutralizing, attacking or degrading them [1]. Substances that penetrate

through the SC barrier layer still have to overcome many other obstacles, such as the antimicrobial barrier, immunological systems or enzymatic systems [1, 2].

There are three different pathways that can be used by substances penetrating the skin mentioned in the literature: **intercellular**, **transcellular** and **transappendageal** [38]. Figure 2.4 shows a simplified scheme of skin penetration.
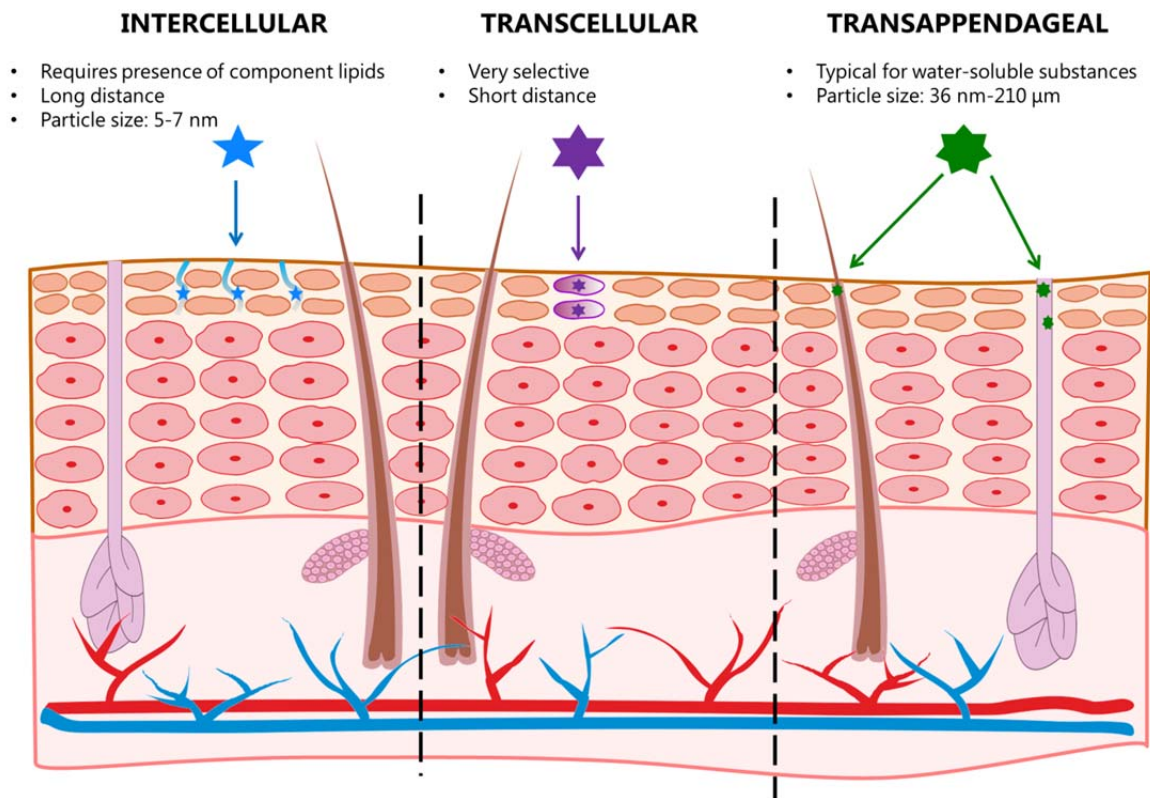

Figure 2. 4. Three penetration pathways for the skin: intercellular, transcellular and transappendageal.

The **intercellular** pathway involves the transport of substances between the cells of the SC layer [38, 165]. This mechanism plays a major role in skin permeability and requires the presence of component lipids, such as ceramides, that allow free lateral water diffusion by forming nanometric spaces via short range repulsive forces [165, 166]. The diffusion rate depends on the properties of penetrating particles, such as volume, weight, solubility, lipophilicity or hydrogen-bonding ability [39]. Small particles can move freely between the SC cells but the intercellular space is mechanically restricted to 19 nm, the average dimension of the lipid channels [39, 167]. It is assumed that particles with a size of 5-7 nm can be efficiently transported through the intercellular pathway [1]. Although the SC is a thin layer, reaching a thickness of some 20 μm for the volar forearm [51], the intercellular pathway is much longer.

According to the 20-fold rule, assuming that the effective pathway is twenty times longer than the SC thickness, it reaches 400 μm, which reduces penetration rate significantly [168-170].

The **transcellular** pathway involves keratinocytes in the transport of substances [38]. Despite the seemingly short distances involved, this pathway is very selective. Penetrating particles have to overcome various barriers that are repeated many times in the skin structure; lipophilic cell membranes, hydrophilic cellular contents with keratin and phospholipidic cell barriers [171, 172].

The **transappendageal** pathway involves appendages, such as sweat and sebaceous glands and hair follicles and is a typical route for the penetration of water-soluble substances [162, 165]. There are various opinions about the maximum size of the particles that can penetrate into deeper layers of human skin through the transappendageal pathway. Some studies have shown that the size of particles penetrating the skin through aqueous pores can be around 36 nm, whereas trans-follicularly penetrating particles can migrate distances up to 210 μm [1]. However, other researchers have argued that only particles with a size up to 40 nm [164] or even as small as 20 nm [39] can penetrate through follicles into deeper skin layers, whereas bigger particles will only be transported deep into the hair follicle.

The transappendageal pathway used to be considered as the least significant penetration passage, as the appendages cover only 0.1% of the skin surface [38, 168]. On the other hand, it is the only penetration pathway for large particles [1]. In addition, appendages may play a role as reservoirs for topically applied substances and therefore could potentially be an efficient penetration path [38]. Special treatments and substances called penetration enhancers can be used in order to increase the permeability of human skin for the purpose of drug delivery or cosmetics.

There are many factors influencing skin absorption, connected with both skin properties and characteristics of the penetrating substances. Consistent with the first part of this paper, the properties of human skin can vary significantly not only between different people but also between anatomical areas. The absorption properties of skin are subject to analogous variations, in particular, when skin barrier properties are altered due to a skin disease.

As presented in Figure 2.2, penetration through human skin depends on the body-dependent factors and also influences human skin characteristics, such as skin dryness, roughness or health.

Figure 2.5 presents the main body-dependent factors influencing skin permeability. As previously mentioned, skin characteristics depend on each other. Skin function, e.g. skin barrier properties, has to be considered as a function of skin ageing.

Influence of altered skin hydration, SC thickness or sweating rate have to be considered as well, as these parameters vary with age and have an impact on skin permeability.
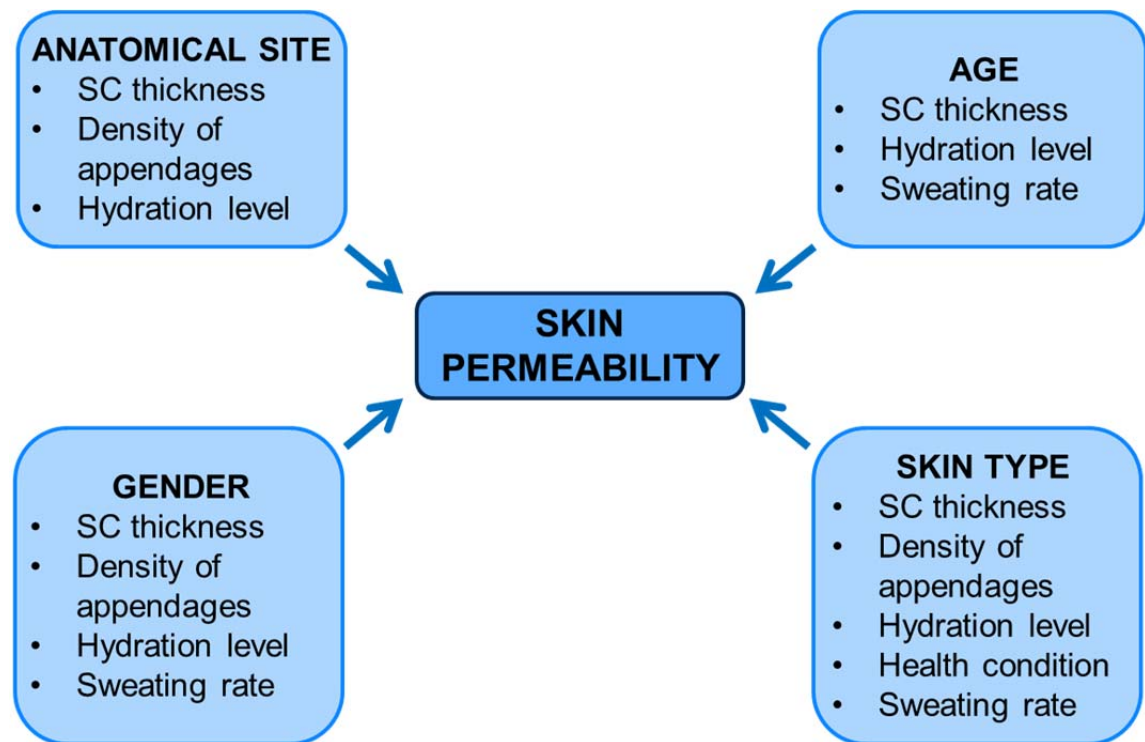

Figure 2. 5. Body-dependent factors influencing skin permeability.

The barrier properties of human skin vary significantly among body parts, as the anatomical site strongly influences the majority of skin characteristics, such as SC thickness, density of appendages and hydration level [1, 173]. Skin permeability is facilitated when the SC is thinner, due to a smaller distance having to be covered by penetrating substances [1]. The distribution, density and diameter of follicles have also a major influence on skin barrier properties [1]. The maximum density of follicles is characteristic of the forehead (292 follicles/cm^2 compared to 50 follicles/cm^2 in other body parts) whereas the maximum diameter of follicles has been reported for the calf (165 ± 45 μm) [1]. The water-diffusion rate varies depending on the body site. Diffusion rates of 2.1 mg/cm^2/h were reported for the SC on the sole, 0.4 mg/cm^2/h on the calf and 0.1 mg/cm^2/h on the thigh (isolated *dermis* showed very poor barrier properties and the diffusion rate persisted at a level of 5mg/cm^2/h) [174]. The hydration level of skin can vary significantly between body parts. An appropriate hydration level is necessary to avoid mechanical failure of skin [1]. Penetration of substances through impaired skin is significantly enhanced [162].

It was also observed that skin permeability decreases with age [1, 39]. It was found that sweating and high skin hydration result in increased water absorption [173, 175]. Both these parameters are reduced in older subjects [1, 99, 100].

Gender also has an influence on skin barrier function, as according to some researches, it is related to the SC thickness, the density of appendages, the hydration level and sweating rate [8, 51]. It was found that the presence of hair makes men's face more permeable than women's [70]. Men sweat to a greater extent than women (800 ml/h for men versus 450 ml/h for women during physical activity), which can also result in higher skin permeability in males [70]. Sex hormones influence the SC chemical composition and may also influence skin permeability [1].

All parameters contributing to personal variations in skin permeability are also dependent on the skin type, as all above mentioned characteristics, such as SC thickness, density of appendages, sweat rate and hydration level can vary among individuals of the same gender and at the same age. The health condition of the skin plays a very important role in its barrier properties, as the majority of nanoparticles present in the environment, or even bacteria, dust, viruses, and allergens cannot penetrate through healthy and non-disrupted human skin [39, 162]. However, skin mechanical failure or diseases can increase permeability of human skin significantly. For example, atopic skin was found to show up to a 2-fold higher permeability than healthy skin [173].

All the above-mentioned factors influencing human skin barrier properties are interlinked. Therefore, it is impossible to explicitly determine the importance of individual parameters. Moreover, different body-dependent factors will influence skin permeability to a different extent, depending on the penetration pathway preferable for a certain type of penetrating substances [1]. In addition, skin permeability can be also influence by the climate and environmental conditions [1, 19]. Increased hydration level of the skin, which can be caused by increased air humidity as well as increased temperature, for example, can act as penetration enhancers [1, 19]. This leads to the conclusion, that transdermal drug delivery should be personalized and consider individual skin characteristics and also the living environment of patients.

The transport of substances through the structure of human skin strongly depends on the substances themselves, as well as on the accompanying excipients [1]. It has been reported that elastic particles can migrate through human skin more efficiently than rigid ones [176]. While elastic particles could penetrate the SC and reach the border of viable *epidermis*, rigid particles were only accumulated in the superficial *stratum corneum* [177]. The solubility of the substance in the medium, the concentration of the solution and its pH are also important factors influencing the penetration process [1]. It is also assumed, that the molecular weight of the penetrating substance should not exceed 500 Da [162]. The size and shape of the molecule, in addition to other physicochemical descriptors, e.g. water-octanol partition coefficients and Abraham solute descriptors, is one of the factors that is decisive for its ability to

migrate through the skin structure and its penetration depth, the possible pathway and the diffusion coefficient [1, 178].

As the penetration of substances is quite often desired, (e.g. delivery or application of active substances in cosmetics), many compounds have been investigated as potential penetration enhancers [163]. Among the substances that could be successfully used as penetration enhancers are surfactants, esters, fatty acids, alcohols, amines, terpenes, alkanes, phospholipids, sulphoxides, amides or pyrrolidones [38, 163].

Besides chemical penetration enhancers, there are also some techniques enhancing skin penetration, such as electroporation, which leads to the creation of aqueous pores by the application of an electric pulse [179]. In addition, it has been observed that massage can increase the transappendageal penetration rate [39].

Skin permeability is an important area of science focusing on skin barrier and protective function as well as on drug delivery. Therefore many research groups have focused on human skin models and substitutes, such as animal skin, reconstructed *epidermis* (Skinethic™ HRE) or living skin equivalent (Graftskin™ LSE™), enabling simulations and predicting if, how and to what extent different substances can be transported through human skin layers [36, 180].

2.2.4. Conclusions

In this review we have discussed the major factors influencing skin properties and functions. The foregoing literature survey has disclosed how many factors can alter human skin in everyday life. The complexity of the skin cannot be neglected: the properties and performance of the skin are all interdependent and need to be considered as a system rather than as individual characteristics. Consequently, a change of one property can lead to a wide variety of effects.

Attributes influencing skin properties and functions can be divided into body-dependent factors and factors connected with the skin barrier function.

The majority of body-dependent factors influencing skin are congenital. Ethnicity and gender influence skin properties to a lesser extent than other factors. Skin type can influence UV protection and skin-ageing processes. Skin ageing results in, *inter alia*, a decrease in hydration level and elasticity. Generally, skin properties, such as thickness, roughness, hydration, TEWL, sweating rate, sebum secretion, elasticity or pH, vary with the body site.

Healthy diet and adequate body weight may slow the skin-ageing process, decrease the risk of skin disorders and accelerate the wound-healing process. Also the avoidance of excessive UV exposure allows the maintenance of better skin health.

Skin acts as a barrier that protects the body from the environment. However, certain substances can penetrate into deeper layers of the skin and even be absorbed into the bloodstream. This imperfection in skin's barrier properties leads to the need for adequate protection upon exposure to dangerous substances, but it is also an opportunity for new modalities of drug delivery. These do, however, bring the challenge that the pharmacokinetics is dependent on the location, type and health status of skin as well as on the age and gender of the patient.

Since skin is the biggest single organ in the human body, fulfilling a variety of very important functions, its properties have consequences in everyday life. All the above-mentioned factors can alter skin attributes, such as aesthetics, mechanical protection, resistance to external factors, wound healing or frictional behaviour of the skin.

Because of the diversity of skin properties and the complex relationship between skin permeability and other characteristics, individualized factors have to be taken into account for skin modeling or the design of transdermal-delivery-based treatment methods.

2.3.   Frictional behaviour of human skin

As skin is the first area of contact with the surroundings, skin friction plays an important function in everyday life. Friction coefficient of human skin rubbed against other objects depends on many factors, both external, like the roughness of the counterface, experimental or environmental conditions and internal factors, such as the specific body part, gender, skin health, age, and hydration level [4, 35, 181, 182]. Figure 2.6 shows possible factors influencing frictional behaviour of human skin.
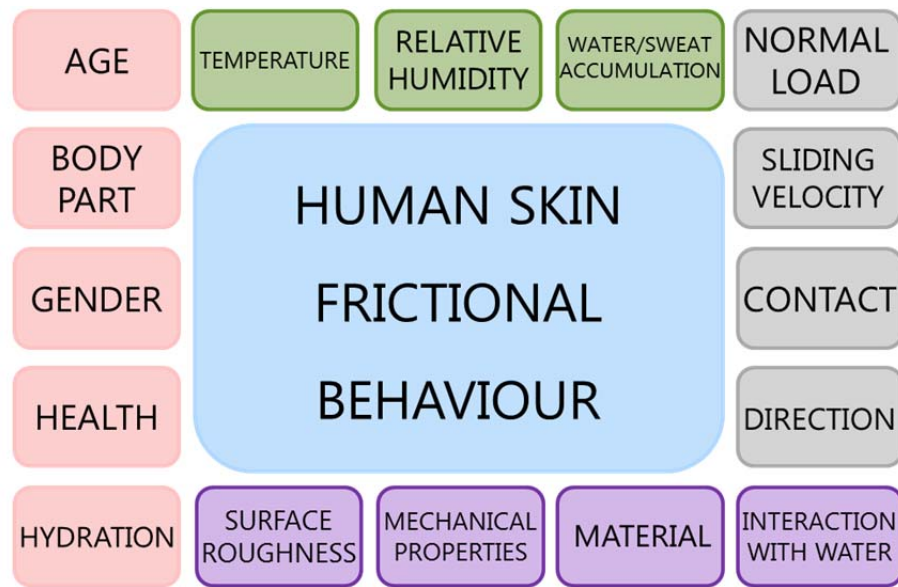

Figure 2. 6. Exemplary factors influencing human skin frictional behaviour: skin (pink) and counterface (purple) characteristics, environmental (green) and experimental (grey) conditions.

Skin is perceived as a soft viscoelastic material with the friction force F_f [N] being the sum of two components: an interfacial F_{int} [N] and a deformation component F_{def} [N], which is caused by incomplete recovery of the energy dissipated by the viscoelastic deformation [11, 183] :

$$F_f = Fint + Fdef \qquad (1)$$

It has been reported that the deformation component of the friction force is relatively small in comparison to the interfacial component and adds only around 0.04 to the final friction-coefficient value (being about one order of magnitude less than the values observed for dry skin, e.g. 0.46 for the forearm rubbed against a polypropylene sphere) [11] [184]. Therefore, to understand the mechanism of the frictional behaviour

of dry and wet skin, the deformation component can be neglected [11]. The interfacial component is related to molecular-scale attractive forces and is proportional to the real area of contact, A [m^2], over which the forces operate and the interfacial shear strength τ [Pa] [11]:

$$F_{int} = \tau A \qquad (2)$$

Interfacial shear strength has been found to depend linearly on the contact pressure for substances covered with a thin organic film, such as human skin in its natural environment [11]:

$$\tau = \tau_0 + \alpha p \qquad (3),$$

where τ_0 [Pa] is the intrinsic interfacial shear strength, p [Pa] is the contact pressure, being a quotient of the applied normal load and the real contact area and α is a pressure coefficient [11].

Combining Equations 1-3, another equation, describing coefficient of friction μ, can be derived:

$$\mu = \frac{F_f}{F_N} = \frac{F_{int}}{F_N} = \frac{\tau}{p} = \frac{\tau_0}{p} + \alpha = \frac{\tau_0 A}{F_N} + \alpha \qquad (4)$$

It has been demonstrated that the friction coefficient for dry skin can be perceived as independent or almost independent of the applied normal load [11, 21, 35, 185, 186].

Exemplary values of the friction coefficient for dry and untreated skin on the inner forearm are summarized in Table 2.2.

Table 2. 2. Friction coefficient of dry and untreated skin on the inner forearm, adapted from Derler et al.[35]

Counterface material	Friction coefficient	Normal applied load	Reference
Ruby sphere	0.7 ± 0.07	0.2 ± 0.1	Asserin [187]
Steel sphere	1.63 ± 0.07	0.05 ± 0.03	Elleuch [188]
Copper cylinder	0.45 - 0.65	0.2	Sivamani [189]
Gold cylinder	0.9 ± 0.5	0.08	Nakajima [190]
Steel slider	0.41 ± 0.08	0.49	Gupta [191]
Steel washer	0.19 ± 0.02	0.075 ± 0.005	Gerrard [192]
Steel washer	0.2 ± 0.01	0.075 ± 0.005	Batt [193]

Frictional behaviour of human skin changes in the presence of water, e.g. due to sweating, sweat accumulation or external sources of water being present in between skin and other objects, caused by rain, wet clothes, etc. The friction coefficient increases significantly in the presence of water, which is thought to be caused by swelling and softening of the *stratum corneum*, consequent increasing the real contact area and generating capillary bridges [20, 21, 23-25, 136].

The friction coefficient of human skin exposed to water is no longer load-independent, therefore in this work the name and symbol of the coefficient of friction will only be used for simplicity reasons and can be understood as a ratio between friction force and the normal applied load, not as a constant value. Wet skin, due to significant changes in its properties, follows different friction mechanisms [11]. While dry, human skin can be perceived as a multiple asperity surface, under wet conditions it becomes a smooth, elastic surface [11]. The real contact area is no longer directly proportional to the normal load and follows the Hertz equation, which has been found to be applicable for contact between hard and soft materials [11, 22, 194]:

$$A = \pi \left(\frac{3\,F_N R}{4\,E^*}\right)^{\frac{2}{3}} \qquad (5),$$

where R is the radius of the sphere and E^* is the effective Young's modulus, given by the equation:

$$E^* = \left(\frac{1-v_1^2}{E_1} + \frac{1-v_2^2}{E_2}\right)^{-1} \qquad (6),$$

where v and E are Poisson's ratio and Young's modulus of contacting materials.

As a consequence of Equations 2, 3 and 5, it can be clearly deduced that the friction coefficient of wet skin decreases with increasing applied normal load following the equation [22, 194]:

$$\mu_{wet} = \frac{F_{inf}}{F_N} = \pi\tau \left(\frac{3\,R}{4\,E^*}\right)^{\frac{2}{3}} F_N^{-\frac{1}{3}} \qquad (7)$$

Experimental results for in vivo measurements performed on the volar forearm rubbed against a reference textile under both dry and hydrated conditions presenting friction coefficient as a function of the normal applied load and the amount of applied water will be presented in detail as part of Chapter 4.

Another characteristic of human skin frictional behaviour is the so called "stick-slip" phenomenon, observed for the inner forearm and the finger pad [182, 195]. "Stick-slip" phenomena take place when the coefficient of friction decreases with increasing sliding velocity and contribute to the tactile sensation abilities of human skin [195, 196].

Human-skin frictional behaviour is an important topic, playing a substantial role in daily life. Therefore investigations focused on this issue are relevant not only to increase the comfort and safety of everyday activities, but also to help in the prevention of friction-related injuries, such as wear, friction burns or decubitus ulcers [4-6]. Also tactile properties of functional materials, such as textiles for sports, medical applications, materials for interiors or artificial leathers, are directly related to the friction of human skin [197].

2.4. Skin models

2.4.1. Motivation

Tests on animals, humans, cadavers and explants have traditionally been used to study skin-material interactions [11, 35, 198-201]. Such studies were useful in establishing safety margins and improved the characterization of skin. However, experiments on human and animal skin raise ethical issues, are difficult to perform and the results are highly variable due to inherent skin variability. In the last decades, significant progress has been made in the reproduction of skin by culturing cells *in vitro*. Cell cultures simulating skin are commercially available and used for research and testing as well as for clinical purposes [202, 203]. Despite their biological relevance, these skin models still have significant limitations. For example, most of their physical properties have not yet come close to those of real skin and are also characterized by large variations. In addition, they are expensive and difficult to store and handle. This type of skin models is not yet suitable for experiments under realistic physical conditions. Models based on biologically inactive materials, which we call *physical skin models* in the following, are often preferable. By physical skin models, we understand non-living materials or physical systems that are able to reproduce one or more of skin's properties, functions or behaviour. In the literature, such types of models are called skin model, skin phantom, skin equivalent, synthetic skin, skin substitute, artificial skin, skin replica, skin model substrate etc. depending on the research field.

Physical models of human skin have been proposed and described in numerous studies concerning testing and development of materials and methods. However, only in a few cases was the development and characterization of the models themselves the main research goal; usually, physical skin models were developed for the needs of testing, calibration, quality checking of devices or teaching.

Physical skin models allow long-term stability, lower costs, easy storage and manipulation and better control over their physical properties. Therefore, these models are usually characterized by better reproducibility and reliability. Moreover, they are devoid of the above-mentioned ethical issues.

2.4.2. Phases in the development of a skin model

The development of skin models comprises several distinct phases. First of all, the main requirements such as skin characteristics, properties and functions, and environmental and experimental conditions, have to be established. Table 2.3 summarises some of the most important requirements.

Table 2. 3 Physical skin models requirements.

Skin characteristics	Simulated properties	Simulated functions	Environmental factors	Experimental parameters
Age	Mechanical	Sensing	Temperature	Parameters:
Gender	Optical	Cooling	Relative humidity	-Speed
Body region	Thermal	Heating	Air flow	-Time
Physical status	Electrical	Protection	Precipitations	-Pressure
-Fitness	Chemical	Appearance etc.	Radiation etc.	-Frequency
-Health	Surface etc.			-Deformation
Physiological status				-Hysteresis etc.
-Skin temperature				Geometry:
-Sweating rate				-Anthropomorphic
-Hydration				-Simplified
-Sebum excretion rate				

The requirements can be based on the literature data and on the measurement systems specifications. Then, the materials and the processing methods have to be chosen accordingly. The third phase is the effective manufacturing and construction. This development phase takes place in feedback with the testing and characterization phase, in which simplified experiments are carried out to select the most promising skin models. The last phase in the development of the skin models is the validation. Validation of the skin models can be based on a comparison with *in vivo* skin, cadavers' skin, explants and excised skin, animals' skin (e.g. porcine skin), other validated skin models or on analytical calculations and theoretical modelling.

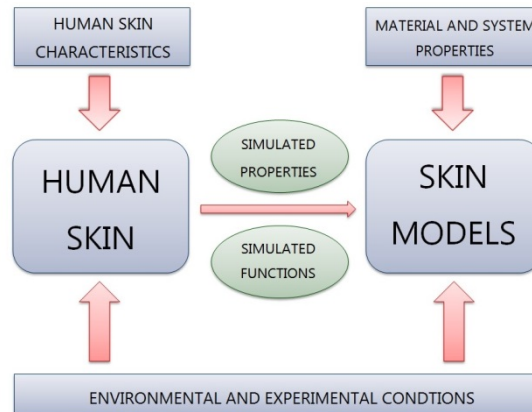Figure 2.7 shows schematically the interplay of the factors summarised in Table 2.3.

Figure 2. 7. Factors influencing the behaviour of human skin and skin models.

As discussed above, the properties of the human skin can vary over a wide range. For this reason, it is important to understand well the specifics of the skin to be simulated not only under all the relevant environmental and experimental conditions, but also the behaviour of the physical skin models and the materials they are made of.

2.4.3. Materials to simulate human skin

From the materials science point of view, skin is a very complex, active open system consisting of highly inhomogeneous and anisotropic composite materials. Furthermore, the skin actively exchanges mass and heat with the body and the environment. Due to this complexity, physical skin models are often aimed at providing similar results to human skin, while being highly simplified systems that do not reflect the structure and the composition of the human skin. Physical skin models can be produced based on numerous combinations of materials, structures and morphologies. There are skin models consisting of liquid suspensions, gelatinous substances, elastomers, resins, metals and textiles incorporating nano- and micro-fillers but also uncommon skin models such as those based on albumen, or engineered skin models.

Liquid suspensions

Various liquid suspensions have been used for simulating optical properties of tissues [204-207]. Implicitly, to some extent, scattering and absorption properties of the skin are simulated. Suspensions of lipid, polymeric and inorganic particles can be added

to liquids such as water, milk or oils to obtain scattering properties that are similar to those of skin. Liquid-based models can be produced using well-defined substances that are readily available commercially. Lipid solutions (used for intravenous delivery) [207], monodispersed polystyrene and titanium dioxide particles (used in various biomedical and chemical applications) [207, 208], are some of the most used scatterers. The light absorption is mainly determined by the liquid, but further control over it can be achieved by using absorbers and fluorophores of both biological and synthetic origin. Liquid skin models can provide good reproducibility for testing measurement systems and of theoretical models. However, as these models have to be embedded in solid recipients, care has to be taken as new interfaces are generated. Furthermore, these models are only useful for cases in which simulating the surface and mechanical properties are not critical.

Gelatinous substances

Skin models based on gelatinous substances have an ability to interact with water, leading to reversible creation of gels. This property allows modifying and controlling various physical, mechanical and chemical properties, such as elastic modulus, hardness, optical or surface properties. Specific behaviour of gelatine and related polymers can be influenced by pressure, pH and temperature, which can lead to further variability of properties [209, 210]. Representatives of this group used in the production of skin models are gelatine, agar and agarose, collagens and polyvinyl alcohol gels.

Gelatine

Gelatine is a protein produced by partial hydrolysis of collagen [211] and is an abundant component of the skin, bones and the connective tissue. Dry gelatine can be stored for a long time without a change in quality.

Water-gelatine solutions closely simulate the density and viscosity of human tissue. Ordinance gelatine or ballistic gelatine has become the standard for ballistic testing and for wound ballistic forensic reconstructions [212]. However, ballistic gelatine alone is not an accurate physical skin model. This is especially relevant at low kinetic energies, for example for the testing of less lethal ammunition [213, 214]. To

overcome these limitations in a multilayer approach, a second layer made of a different material simulating the *epidermis* can be combined with the gelatine block [213-215].

The gelatine-water solutions simulate the deformation and kinetic dissipation of the projectile and provide a similar behaviour of cavity formation and tissue deformation that allows extrapolation of the results to those obtained with human tissue [212].

Other important areas in which gelatine mixtures are used as skin models are in elastography [216], testing of sun creams, self-tanning formulations and moisturizers [217, 218] and testing of adhesives [219, 220]. Gelatine provides a matrix with density, stiffness, sound speed, absorption, and light scattering similar to that of human skin. Furthermore, through chemical or physical modification, it is possible to independently control each of these parameters that are essential for elastography.

Agar

Agar is a gelatinous substance made from seaweed polysaccharides. Skin models based on agar have been proposed first by Cubeddu et al. [221] as an alternative to resin and liquid-skin models. Since then, many groups have adopted agar skin models [222, 223].

Although not very stable and with a limited lifetime, agar-based skin models are versatile, easy to produce, with acoustic velocity, acoustic impedance and density similar to those of skin [224]. To produce the skin models, agar is mixed with deionised water or water-based solutions (e.g. saline solution). In addition, other substances that allow the control of various properties can be incorporated. Chromophores and scattering media (synthetic and biological) are used to obtain a broad range of optical properties. Sodium chloride can be added to control the conductivity [223]. The thermal transport can be studied by incorporating magnetic particles that are heated up using variable electro-magnetic fields [225].

Homogeneous mixtures of the substances are obtained in the liquid phase that can then be poured in 3d shaped moulds. Solidification occurs by polymerization, which can be initiated by heating up to the boiling point in microwave ovens followed by rapid cooling (e.g. by immersion in cold water [221]). The concentration of agar powder in solution is about a few percent and has a significant influence on the density and mechanical properties of the resulting skin model.

The applications of agar-based skin models are diverse, but limited to noncontact or light contact, where there is no necessity for long-term stability. Typical applications are related to optical imaging [221, 226, 227], thermal imaging and transport [228, 229], photoacoustic and ultrasound imaging [224], dosimetry [230], and body centric applications [222].

Polyvinyl alcohol gels

Poly(vinyl) alcohol (PVA) is a synthetic polymer commonly used in medical applications. It is highly soluble in water, but after crosslinking can form hydrogels [231]. PVA cryogels are especially suitable to simulate tissue in magnetic resonance studies [232]. Tissue-mimicking models are very important for optimization, testing or development of imaging-based diagnostic techniques. PVA is perceived as a skin and soft-tissue phantom e.g., for a wide group of magnetic resonance techniques [233], optical tomography [234] or x-ray examination [235]. PVA is also used as a matrix in which further substances can be integrated. For example, Mazzoli et al. [236] used PVA as a matrix containing scatterers and absorbers. In addition, Indian ink was added to simulate melanin and pigmented lesions of malignant melanoma. It is also possible to tune the optical properties of PVA-based products by adding nanoparticles [237].

Phantoms made of PVA are used in optoacoustics, such as acousto-optical elastography [238] or photoacoustic imaging [239]. They are important models for ultrasound systems for testing, optimizing and educational purposes [224]. PVA cryogels can be produced with properties similar to those of human skin [240]. The mechanical properties of PVA cryogels are tunable within the range of those of soft tissues [234]. Kim et al. proposed the usage of PVA thin films as a skin model to collect data for designing a computer-game controller [241].

A big advantage of PVA cryogels is the possibility of adapting their scattering coefficient and stiffness by changing the number of freeze/thaw cycles. PVA cryogels are relatively stable and easy to store.

Elastomers

Elastomers are polymers exhibiting rubber-like viscoelastic properties. The elastomers are either thermoplastics or thermosets, having a glass transition well below room temperature. This is directly related to their properties, which are similar to those

of human skin [242-244]. Moreover, elastomer-based composites allow the physical properties of skin models to be tailored within a wide range.

The elastomers comprise a broad spectrum of natural and synthetic materials, *inter alia* silicones, polyurethanes, polyether block amides, polyisoprene and polybutadiene. Human skin is primarily simulated by means of silicones and polyurethane.

Silicones

Silicones are inorganic-organic polymers containing Si, O, C and H as well as other secondary elements [245]. For skin models, silicone elastomers such as cross-linked polydimethylsiloxanes (PDMS) are widely used. Fillers are incorporated to strengthen and to tune the properties of silicone elastomers. Carbon black is added to control the electrical conductivity, titanium dioxide the dielectric constant, and barium sulphate the radiopacity [246]. Silicone is also applied for surface reproduction, allowing to produce surface morphologies with defined roughness as well as obtaining replicas directly from skin [5]. This possibility is used to investigate the role of roughness in measurements and to develop skin models for which the surface properties are important.

Silicone alone has a refractive index similar to that of skin (1.3-1.5), which can be further tuned by incorporating other substances and structures that can alter the interaction with light (see Nano- and micro-fillers section) and therefore simulate a broad range of human skin optical properties.

Skin models containing silicone are durable over long time periods and can be moulded to obtain various shapes from simple geometries to anthropomorphic, anatomical shapes.

The main advantages of silicone-based models are related to the broad range of properties that can be simulated, easy manipulation, nontoxicity during and after preparation, and long-time stability. Silicone-based skin models have been introduced to simulate skin in numerous applications such as optical imaging, measurement of the specific absorption rate (SAR) [247], drug delivery [248, 249], needle penetration [250, 251], acoustic and photoacoustic imaging [224], tactile assessment [252], indentation[253] and friction[254-256].

Polyurethanes

Polyurethanes are addition polymers that can be thermosetting (the majority) or thermoplastic. A skin model based on polyurethanes was considered for an intradermal injection training system by Graham and Sabelman [257].

The properties of polyurethane-based skin models can be influenced by using polyurethane elastomers with different soft-to-hard-phase ratio, polyurethane sponges, or by incorporating reinforcing particles. Such an approach has been used for instance to develop tactile sensing robotic skin [258, 259]. Due to their viscoelastic properties, polyurethanes can be used as mechanical skin models [188, 260], simulating the friction behaviour of human skin [5, 123, 125, 261]. Lorica® artificial leather, which consists of polyamide microfleece coated with polyurethane, has been shown to realistically simulate human skin friction against textiles under dry conditions [56]. In addition to friction properties, the Lorica® skin model reproduces many surface properties of human skin (roughness, topography, water contact angle) and shows similar force-deformation characteristics [6, 261].

Polyurethane skin models can be used for training in the medical area, e.g. in intradermal injection, skin surgery or prediction of softness of real human skin, where polyurethane simulates the *epidermis* [257, 262, 263]. Polyurethane sponges have been shown to simulate the human *dermis* during biomechanical modelling of non-ballistic skin wounding [264, 265]. Optical properties of polyurethanes (e.g. refractive index), make them an option also as optical skin models [263, 266].

Polyurethanes have a long shelf life and stability and due to their tunable properties, they could be useful in many other applications.

Epoxy resin

Epoxy resins are components for obtaining cross-linked or thermoset plastics with a wide range of properties [267]. As a skin model, they were proposed by White and Martin [268].

The properties of epoxy resins depend on the type of resin and can be controlled by mixing with other components, such as plasticizers and diluents [267].

The epoxy resins have a thermal diffusivity about 0.070-0.084 mm^2/s, close to that of human skin, which is about 0.11 mm^2/s, therefore making them a choice for

thermal skin models [269, 270] or skin-simulant temperature sensor models for skin burn prediction [271, 272]. Skin models based on epoxy resins have been used to observe the temperature profile inside or on the surface during cryogen spray cooling process and to analyse the dependence of temperature changes on different conditions [270, 273, 274].

The refractive index of epoxy resin (1.54) is close to that of human skin and can be further adjusted by adding e.g., titanium dioxide and aluminium oxide particles into the material [275, 276]. Epoxy-resin-based human skin models are used for Raman instrumentation calibration, validation of optical tomography (e.g. tomography of neonatal brain), or for calibration for near-infrared examinations [275-277]. Skin phantoms made of epoxy resins are also suitable as the outer layer of breast phantoms used for the quality control of x-ray imaging systems or in education for mammography[278].

Metals

Metal-based skin models are mainly used in systems to probe thermal properties of clothing [279]. The specific choice of the metal is not critical, as these types of skin models rely strongly on the design of the whole system. The main advantage of these models is their high thermal responsiveness, stable properties, robustness, and the availability of technologies to produce various shapes. Heating and cooling elements can be incorporated and controlled via modern electronic systems. In addition, sweating and moving capabilities have been implemented. For example, in ISO 11092:201 a porous sintered metal plate, heated to 35 °C is implemented as a "sweating guarded-hotplate" that is used to assess the textile-physiological effects under steady-state conditions simulating the evaporated sweat coming into contact with a textile.

Furthermore, such systems are often coupled with thermodynamic and thermophysiological models and placed in well-controlled climatic conditions [280]. Materials testing and development, body-monitoring systems, and human body thermophysiological response are the main areas of interest for these systems. Key parameters simulated by these models are skin temperature, sweating rate and heat transport. Some of the most important limitations are related to the mechanical properties and thermal inertia, which are not simulated realistically.

Textiles

Textile skin models based on natural (e.g., cotton, chamois) and synthetic materials (e.g., polytetrafluoroethylene, polyamide, polyester) are of great importance in systems simulating sweat distribution of humans [281-283]. In addition, synthetic and natural leather such as Lorica® and chamois simulate the mechanical and frictional contact behaviour of skin (see 'Polyurethanes' section).

There are three main types of sweating textile based skin models: pre-wetted textile skin, textile skin with water delivered by sweating nozzles, and waterproof textile skin that is vapour permeable [284]. Textile skin models are used to investigate the liquid and water vapour transport, thermal insulation as well as the combined effect on both the comfort and protective properties of clothing systems [283, 285]. The textiles are placed over thermophysiological devices (e.g., thermal manikins, sweating guarded hot plate) tightly fitted and their main function is related to redistribution and transport of moisture.

By appropriate choice of materials (fibre composition, surface properties, hygroscopicity, hydrophobicity etc.) and structural properties (thickness, construction, porosity, surface pattern etc.), the heat, moisture and vapour water transport can be controlled simulating various physiological conditions.

Another vibrant research area is the integration of sensing elements in textiles motivated by the requirements of continuous body monitoring. Textile-based and flexible sensors can take advantage of the large available surface of textiles, which is expected to provide unprecedented increase in spatial information for multiple parameters (e.g., heat flux, sweating rate, evaporative flux, skin temperature etc.) with minimum disturbance to the system.

Other materials used to model skin

The list of materials used to replicate human skin can be easily extended, especially if structure, morphology, surface properties or design are taken into account [257, 286]. From the less common solutions, but with important advantages, we mention albumin, which is able to simulate thermal damages of the skin [287]. There are also less common examples such as onion, peach and cellophane which were found

to simulate the diffusion mechanism of human skin [288]. A more systematic approach has been used to simulate the sweating of human skin in connection with water distribution in textiles using x-ray micro-computed tomography [289, 290]. Similarly, Hou et al. simulated the sweating of skin by using a multilayer design consisting of a polycarbonate porous membrane and a skin-replica membrane [291].

Nano- and micro-fillers

To obtain skin models with tailored properties and functionality, nano- and micro-fillers such as nanoparticles, nanowires, chromophores or fluorophores are added to a liquid or solid matrix. The incorporation of nanomaterials strongly influences various properties starting from the mechanical and thermal to optical, dielectric and magnetic properties. In addition, unique functionalities can be obtained by exploiting quantum effects occurring at nanoscale or using the coupling between nanomaterials and matrix properties [292, 293]. Sensing capabilities can be implemented into the skin models, allowing the improved monitoring of experiments, or to serve as sensing robotic skin for machine-human interfacing.

The choice of nanomaterials is vast, leading to a massive number of possible combinations to achieve a given property. Nano- and micro-particles such as metallic gold [294, 295], titanium dioxide [294], silicon dioxide [294], aluminium oxide [208], polystyrene [296], carbon black, graphite[247], lipid (Intra lipid) [207, 297-299] have been incorporated into solid and liquid matrices, to tune the optical properties of the skin models. Mechanical properties have been adjusted by using carbon black, dielectric and resistive properties by adding conductive (e.g., graphite [247], nickel [300]) and ferroelectric fillers [258].

2.4.4. Conclusions

The literature review reveals that a surprisingly large variety of materials has been used to simulate specific physical properties of the human skin. The spectrum ranges from liquids and gels such as water, milk, albumin, gelatine, and agar via soft materials such as polyurethane, silicones and polyvinyl alcohol gels to hard solids such as epoxy resins or metals. The role of skin models is to mimic chosen properties of

human skin in an appropriate way. Figure 2.8 illustrates and summarizes the main materials used to simulate different categories of skin properties according to this review.
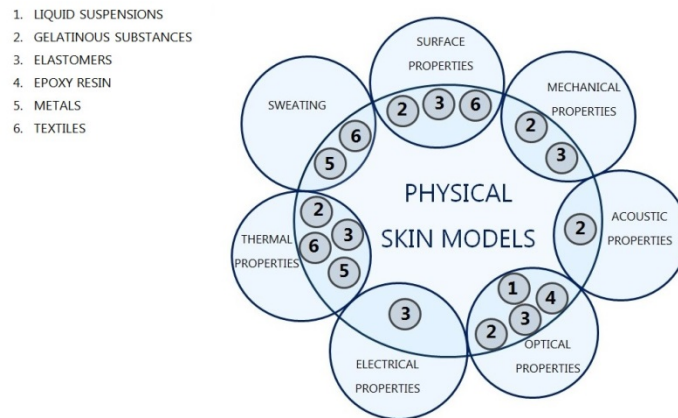

Figure 2. 8. Materials used to simulate skin properties and functions.

Historically, the development and adoption of physical skin models have been closely related to their applications, which inevitably led to a high diversity. Most of the skin models appear to be adopted through a trial and error process by using materials that look, feel, have a structure or composition similar to skin. In the empirical selection of materials, an important criterion often was to apply materials and systems with properties that can be adjusted conveniently or provide measurement results comparable to skin, even if the physical mechanisms involved in the material behaviour differed for the skin models and the skin.

Because of the complexity of the human skin, future skin models might still be based on empirical investigations in which incremental improvements of the existing solutions are achieved. For example, more realistic skin models can be obtained by combining suitable material compositions with skin-like structure, morphology and/or surface properties and topography. If scattering and absorption properties are important, titanium oxide, gold and aluminium oxide nanoparticles, polymer microspheres and chromophores (e.g. dyes, blood and yeast suspension) can be incorporated into the skin models.

The combination of different skin-like properties in the same skin model generally has high potential. Interdisciplinary or multiphysics approaches leading to more realistic models would be especially beneficial in materials science, as optimized materials have to meet different requirements. To be suitable for medical applications,

for example, biocompatible materials and surfaces are needed that combine specific functions with skin-adapted thermal, mechanical and tactile properties.

It is expected that the advance of new technologies and numerical simulation methods will stimulate the development of improved models that reproduce an increasing number of skin properties and functions and therefore are appropriate and valid for a wider range of conditions and applications. Another promising research area is related to tuneable and actively controllable skin models. Such systems would allow one to simulate the behaviour of skin in response to external influences more accurately and, thus, to better take into account the changes in the properties due to physiological and regulatory processes in objective measurements.

Chapter 3

Striving towards the skin model

The previous chapter gave an overview of the complex nature of human skin and circumstances influencing its properties and performance. Human skin frictional behaviour results from skin structure and characteristics but is also dependent on many other factors, such as environmental conditions or the properties of the countersurface.

Skin model to mimic frictional behaviour of human skin should follow similar trends and values as those reported for human skin under identical conditions. Following skin structure and properties, which are considered as important for friction, should lead to the development of the model that simulates friction of the skin against various materials.

In this chapter, we present our motivation and the line of thinking while developing a new bio-mimicking physical skin model. Detailed methods and results will be described while introducing the gelatine-based physical skin model (Chapter 5). Sections 3.1 and 3.2 define the choice of the materials and processing methods and section 3.3 describes the preparation of the potential skin models, while section 3.4 gives an overview of the friction-measurement procedure. Results given in section 3.5 lead to an outlook, which forms the basis for further investigations (section 3.6).

3.1. Chosen materials

The choice of materials to be examined as potential skin models was motivated by their physical properties, known applications and organoleptic observations. Commercially available materials were examined in order to define possibilities and limitations of using these materials as skin models. New materials, processed in three different ways, were proposed as potential skin models.

3.1.1. Commercially available materials

Two kinds of synthetic leather were examined according to their frictional behaviour: Lorica[®] Soft (Italvipla) and Stamskin Silicone (Tersuisse).

Lorica[®] is already used as a physical skin model and has been shown to simulate well the friction of the forearm skin against textiles in dry conditions. Lorica[®] has similar surface properties (water contact angle, roughness) and elastic properties to human skin [5] and is a synthetic leather composed of polyamide fleece with a polyurethane coating.

Stamskin Silicone is a polyamide jersey coated with silicone and seems to be very similar to the human skin, according to organoleptic observations (e.g. touch).

3.1.2. New candidates for the potential skin model

Based on the literature review, polyurethanes and polyether block amides (Pebax) were perceived as favorable polymers for the development of the new skin model mimicking human skin frictional behaviour.

Polyurethane (thermoplastic polyester-based polyurethane C95A55, BASF) was chosen due to its elastic properties and because it is largely responsible for the frictional properties of Lorica[®].

A group of three different Pebax block copolymers (polyether block amides) was used due to the wide range of mechanical properties (Pebax 2533, Pebax 400, Pebax 4033, Akema). Especially Pebax 2533 with elastic modulus of 12 MPa (whereas for the skin it is in the range of 15kPa -150 MPa) seemed to be a promising material [301, 302]. Pebax polymers are also known to have high breathability.

3.2. Chosen processing methods

The properties of the final product are conditioned not only by the used raw material, but also by the processing method. Hot pressing, electrospinning and bar coating were used in order to manufacture samples with different thicknesses and structures.

3.2.1. Electrospinning

Electrospinning provides membranes that are built up with very thin fibers (on the μm up to the nm scale). These membranes can have unique mechanical properties [303, 304]. Fibrous structure of electrospun membranes can be perceived as an analogy to the structure of human skin, containing collagen and elastin fibers [305]. A conventional electrospinning setup, equipped with one syringe filled with the polymer solution, is presented in Figure 3.1.
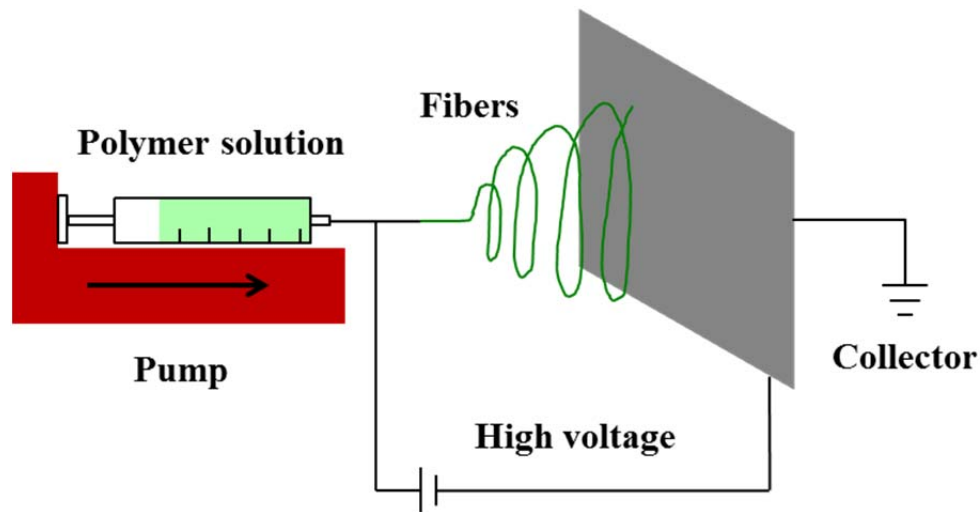
Figure 3. 1. Conventional electrospinning setup.

The polymer solution is pumped out from a syringe with a controlled speed, and therefore a controlled flow rate. A high positive voltage, typically tens of kV, is applied on the spinneret, whereas the collector is grounded or connected to a negative voltage. In a first step, a droplet of the electrically charged solution coming out from the needle elongates and forms a conical shape (Taylor cone). Further, because of the difference in the applied voltage, it is drawn and elongated till it hits the surface of the collector. The solvent evaporates on the way to the collector, so polymer fibers are created. The jet is

unstable and it whips chaotically, so it covers an extensive area on the collector. In this way an electrospun polymer non-woven membrane is fabricated [303, 304, 306].

In this work, a conventional electrospinning setup was only used for preliminary results, as its efficiency and working area is too small to obtain a robust sample with appropriate dimensions. In the next step, a Nanospider (Elmarco) was used as an alternative. The Nanospider is a multi-jet electrospinning device which instead of a syringe with one needle uses rods connected to a high voltage. A container filled up with polymer solution is moved with reciprocating motion on the rod, constantly wetting it with the solution. A moving substrate (e.g. paper or textile) acts as a collector. The schematic of the device is presented on Figure 3.2.
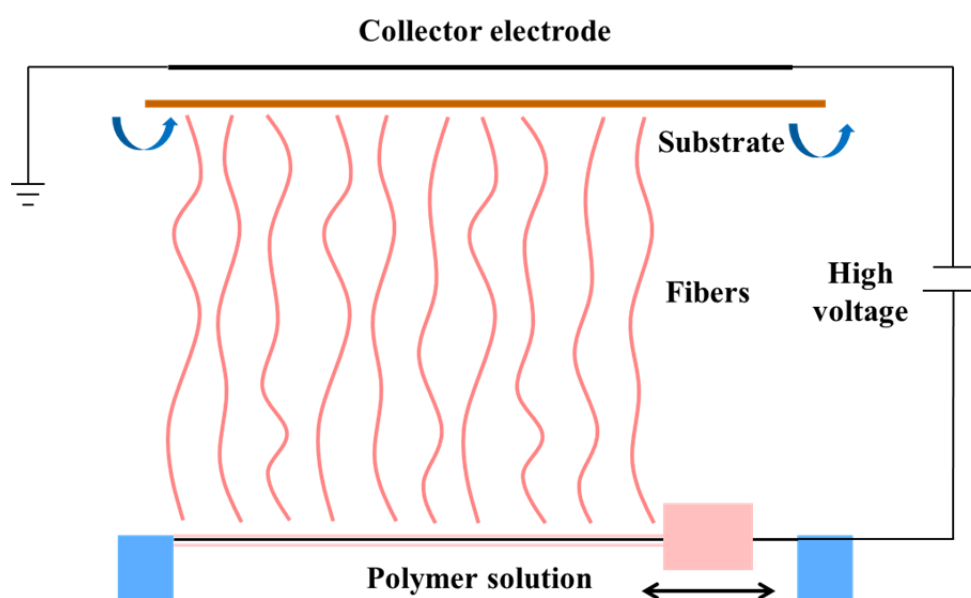
Figure 3. 2. Nanospider electrospinning setup.

3.2.2. Hot press

A hot press can provide thicker polymer films. It is a time-efficient method to process thermoplastic polymers [307, 308].

Figure 3.3 presents a schematic of the device. A square mold with defined thickness is filled with polymer pellets and placed between two flat steel plates, enabling easy and convenient transportation. In the next step, the whole set is placed in between two heated parts of the clamping form, and left until polymer melts, then pressed and cooled.
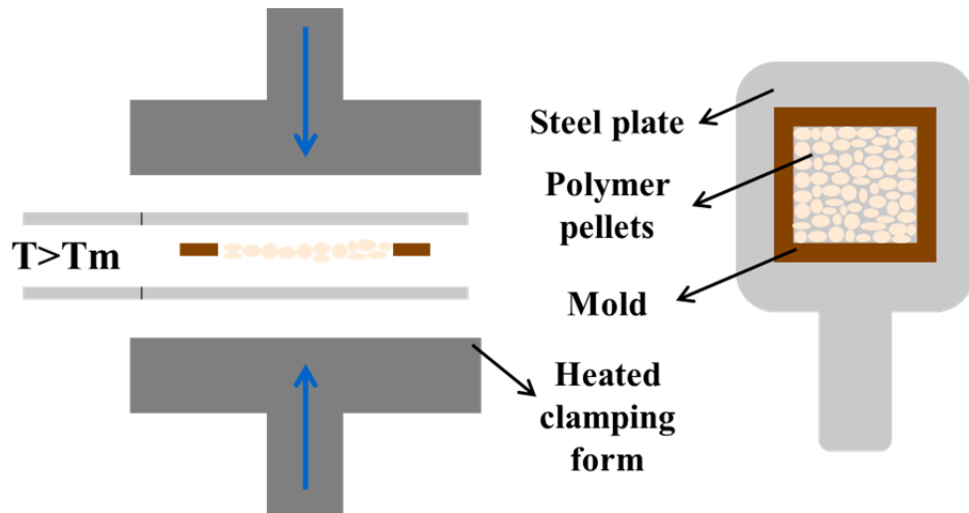
Figure 3. 3. Hot press schematic.

For this work, a Lindenberg hot press, equipped with a water cooling system, was used.

3.2.3. Bar coating

Bar coating can be used in order to obtain films from polymer solutions. It is a time-effective method allowing preparing samples of large area and controlled thickness [309]. The polymer solution is poured on top of the substrate, in front of the applicator with a slit of defined thickness. In the next step, the applicator moves forward, spreading an even layer of the solution behind. A schematic of a bar coated is presented on Figure 3.4.
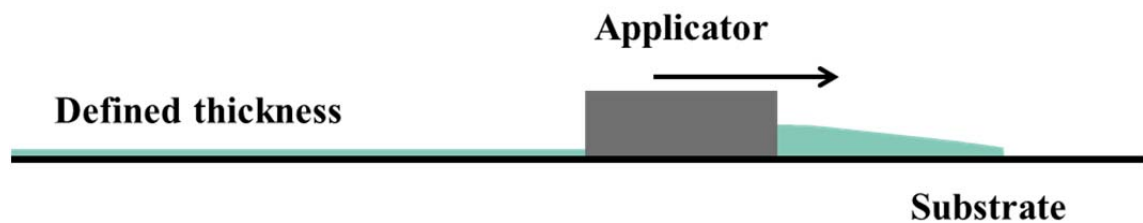
Figure 3. 4. Bar coater schematic.

For this work, an Erichstein Coatmaster 509 MC bar coater, was used.

3.3. Preparation of potential skin models

3.3.1. Electrospun membranes

The electrospinning process requires adapting crucial processing parameters in order to achieve an adequate spinning efficiency and high membrane quality.

As electrospinning of Pebax was not reported in the literature, even though the conventional electrospinning process is not efficient enough in order to prepare a robust skin model, in the first step, a conventional electrospinning setup (Figure 3.1) was used, in order to determine the best composition of the solutions and to set spinning parameters, such as applied voltage, needle-collector distance, pumping rate and spinning time.

Pebax polymers are known for their chemical resistance. Performed solubility trials resulted in the choice of concentrated formic acid (reagent grade $\geq$ 95%, Sigma Aldrich) as a necessary ingredient of the solution. The addition of dichloromethane (DCM, VWR chemicals) improved the efficiency of the process. Electrospinning trials, supported by on-going observations of the solutions and electrospun membrane properties, followed by the adaptation of the spinning parameters as well as components and concentration of the solution, led to the following specification (Table 3.1).

Table 3. 1. Conventional electrospinning process specification.

Polymer	Pebax 2533[a]	Pebax 400[a]	Pebax 4033[a]
Concentration [wt.%]	10	10	10
Solvent 1	Formic acid[b]	Formic acid[b]	Formic acid[b]
Solvent 2	DCM[c]	DCM[c]	DCM[c]
Solvent ratio	1:1	1:1	1:1
Needle-collector distance [cm]	15	15	15
Flow rate [μl/min]	10	10	10
Positive voltage [kV]	15	15	15
Negative voltage [kV]	5	5	5
Current [mA]	0.1	0.1	0.1

As mentioned above, simultaneously to the electrospinning trials, the characterization of the solutions and membranes was performed. Electrospun membranes were investigated by means of scanning electron microscopy (SEM) (Hitachi S-4800, Japan). The influence of the components and concentration of the solution on its conductivity (conductometer Methrohm 660, Switzerland), surface tension (drop shape analyzer, DSA25, Krüss, Germany) and viscosity (rheometer Anton Paar Physica MCR 300, Austria) was also investigated, as all these parameters influence the electrospinning process. Solution components and processing parameters were chosen that led to smooth, high-quality fibers.

The electrospinning process was performed at room temperature (22℃) at a relative humidity of 38%.

In the next step, the electrospinning process was transferred to the Nanospider setup (Elmarco), in order to obtain higher efficiency and robust membranes of larger area. The polyurethane solution was not tested by means of the conventional electrospinning setup, but electrospun by means of the Nanospider setup straightaway. The PUR (C95A55, BASF) solution in dimethylformamide (VWR chemicals) was enriched with a small addition (0.06 wt.%) of 3 wt.% Tetraethylammonium bromide (TEAB, Sigma Aldrich) solution in dimethylformamide (DMF, VWR Chemicals)) in order to increase the spinnability of the solution [310].

As in the case of the conventional electrospinning setup, processing parameters were adapted in order to obtain the best possible efficiency and quality of the membranes.

Table 3.2 shows the optimized specifications.

Table 3. 2. Nanospider electrospinning process specification.

Polymer	Pebax 2533 [a]	Pebax 400 [a]	Pebax 4033 [a]	PUR[b]
Concentration [wt.%]	10	10	10	13
Solvent 1	Formic acid[c]	Formic acid[c]	Formic acid[c]	DMF[d]
Solvent 2	DCM[e]	DCM[e]	DCM[e]	-

Solvent ratio	1:1	1:1	1:1	-
Cylinder diameter [mm]	0.7	0.8	0.7	0.7
Electrode distance [mm]	280	210	250	245
Relative humidity [%]	10	30	10	10
Temperature [℃]	20	19	20	20
Wire speed [mm/min]	72	55	75	48
EMV speed [mm/s]	350	256	350	250
Rewinding speed [mm/min]	18	18	18	18
Positive voltage [kV]	60	60	60	60
Negative voltage [kV]	20	20	20	10
Duration [min]	11x15	5x15	5x15	8x15

[a]Akema   [b]BASF   [c]Sigma Aldrich   [de]VWR Chemicals

A container filled with the solution was moving in a reciprocating motion with a defined speed (called EMV speed) and applying a layer of the solution on the wire that was also moving with a defined wire speed and connected to the high positive voltage.

Fibers were spun on the substrate (baking paper) connected to a negative voltage. The substrate was moving with a defined rewinding speed in 15-minute intervals. The substrate was moved to its initial position each time before the new spinning interval. The process was repeated until a required thickness of the membrane was achieved.

3.3.2. Hot-pressed films

Three different types of Pebax were processed into films via hot pressing (Pebax 2533, Pebax 400, Pebax 4033, Akema). The polymer was heated up to a temperature

above its melting point, maintained at this high temperature for 15 minutes and then pressed with gradually increasing pressure (up to around 180 bar). Processing parameters, such as temperature and weight of the material, were iteratively optimized.

Table 3.3 summarizes the processing temperatures and melting points (data from literature [302]) of the used polymers.

Table 3. 3. Processing temperatures and melting points of polymers processed via hot pressing.

Polymer	Melting point	Processing temperature
Pebax 2533	134℃	170℃
Pebax 400	159℃	190℃
Pebax 4033	160℃	190℃

Then, the polymer films were cooled at 25℃ using a set of water-cooled plates.

Polymers films of three different thicknesses (779 ± 53 μm, 1392 ± 49 μm and 1771 ± 33 μm) were manufactured, in order to investigate the influence of bulk properties of the material on its friction.

3.3.3. Bar-coated film

A 13 wt% solution of polyurethane (C95A55, BASF) in dimethylformamide (VWR chemicals) was prepared by continuous shaking at room temperature for 48 hours. With the use of a bar coater (Coatmaster 509 MC, Erichstein), a polymer solution was then spread on top of a stainless steel plate in three layers of 300 μm and left to dry for 24h at room temperature after the application of each layer. Afterwards, the polymeric film was peeled off from the stainless steel plate and cut up into pieces with dimensions appropriate for the following friction measurements.

3.4. Friction measurements

As already mentioned in the introduction, in this chapter only preliminary results, presenting our way of thinking and motivation for the choice of the materials, will be presented. This part of the work can be perceived as the introduction to Chapter 5, which concerns the preparation and characterization of the water-responsive, gelatine-based physical skin model. Therefore, in order to avoid unnecessary repetition and to ensure the completeness of the work, all necessary details will be explained in Chapter 5.

In vivo and *in vitro* measurements were performed under both dry and hydrated conditions. Dry conditions meant that no water was applied between the human forearm or skin model and the reference textile. Two different amounts of applied water can be distinguished among hydrated conditions: moist and wet. The premise was that moist conditions simulated physiological sweat accumulation (10 µl distilled water per 1 cm^2) [16] and wet conditions corresponded to the maximum water uptake of the reference textile (21.6 $µl/cm^2$ for the Martindale fabric and 50.31 $µl/cm^2$ for knitted cotton).

3.4.1. *In vivo* friction measurements

In vivo friction measurements provided information about the frictional behaviour of human skin rubbed against Martindale (worsted wool cloth) and knitted cotton in three different moisture states.

Experiments were performed using a force plate, Kistler 9254 [29, 197], a three-axis dynamometer based on piezoelectric force sensors. Figure 3.5 presents an exemplary experiment performed on the Kistler 9254 force plate.
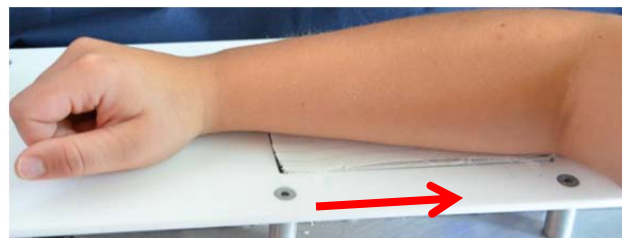
Figure 3. 5. In vivo friction measurement.

The textile sample is fixed on the force plate using double adhesive tape. For the case of wet conditions, water is evenly applied onto the textiles. Then, the forearm is rubbed repeatedly by performing movements towards the body at various normal loads.

The detailed methodology is presented in Chapter 5, where we present our final, gelatine-based skin model.

3.4.1. *In vitro* friction measurements

In vitro friction measurements were carried out using an in-house developed tribometer called the Textile Friction Analyzer (TFA). Figure 3.6 shows an overall view of TFA. The TFA is equipped with two quartz sensors for measuring the friction and the normal forces between the two materials in relative reciprocating motion [5].
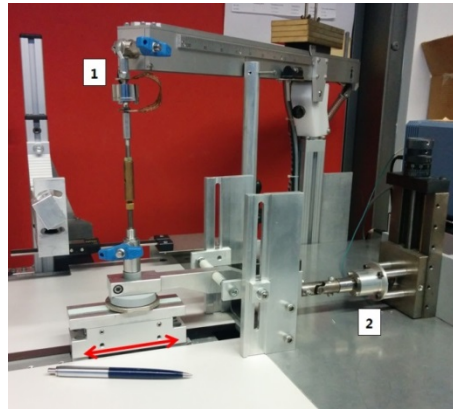
Figure 3. 6. Textile Friction Analyzer.

1-normal force load cell, 2- friction force load cell

The examined skin model is fixed on an aluminum sledge using double-sided adhesive tape, whereas textile swatches are fixed on a round shaped holder. The sledge moves in a reciprocating motion at a set speed and amplitude under various applied normal loads.

3.5. Results

A variety of samples was examined for their frictional behaviour. As already mentioned, besides the new proposed samples, two commercially available materials were tested as potential skin models. Figure 3.7 shows the summary of all examined potential skin models.

Figure 3. 7. Diversity of prepared potential skin models.

The final products can be divided into three groups (numbers given next to the skin models in the following correspond to the numbers in Figure 3.7):

- Commercially available materials
    1) Stamskin Silicone (Tersuisse)
    2) Lorica® Soft (Italvipla)
- Hot-pressed films
    3) Pebax 2553 (Akema)
    4) Pebax 4033 (Akema)
    5) Pebax 400 (Akema)
- Bar-coated films
    6) PUR (thermoplastic polyester-based polyurethane C95A55, BASF)
    7) PUR bar coated film mounted on top of a Lorica® Soft substrate
- Electrospun membranes
    8) Pebax 2533 electrospun membrane
    9) Pebax 4033 electrospun membrane
    10) Pebax 400 electrospun membrane

11) PUR electrospun membrane

3.5.1. Commercially available materials

Two investigated commercially available materials (Lorica® Soft and Stamskin Silicone) were investigated according to their frictional behaviour when rubbed against textiles under both dry and hydrated conditions. Both of them could be accepted as skin models only under restricted conditions.

The described potential skin models were compared to human skin based on the friction coefficient averaged from the values obtained from the measurements driven under five different applied normal loads (0.5N, 1N, 1.5N, 3N and 5N).

The average friction coefficient values for human skin (volar forearm) and Lorica® Soft were similar only in the case of friction measurements conducted with the use of the Martindale reference textile under dry conditions. The average friction coefficient was 0.47 ± 0.07 for the skin and 0.54 ± 0.36 for Lorica® Soft.

Stamskin Silicone was able to map friction coefficient values obtained via *in vivo* friction measurements under moist conditions with knitted cotton used as a reference textile. The average friction coefficient was 1.08 ± 0.09 for the skin and 1.11 ± 0.21 for the Stamskin Silicone skin model.

None of examined potential skin models could mimic the frictional behaviour of human skin under both dry and hydrated conditions. Therefore they could not be used as universal and functional physical skin models for friction-related purposes.

3.5.2. Electrospun membranes

Four different electrospun membranes were mounted on top of Lorica® substrate with the use of double-sided adhesive tape and examined as potential skin models.

Thanks to simultaneous adaptation of the processing parameters, it was also possible to conduct successful electrospinning of Pebax for the first time, according to the literature of that time.

Three Pebax electrospun membranes (Pebax 2533, 4033 and 400) and one polyurethane membrane were produced by means of the Nanospider setup according to the parameters leading to the highest spinning efficiency and allowing obtaining the

best looking and robust membranes. Figure 3.8 shows SEM pictures of investigated electrospun membranes: Pebax 2533 (Figure 3.8a), Pebax 4033 (Figure 3.8b) and Pebax 400 (Figure 3.8c).
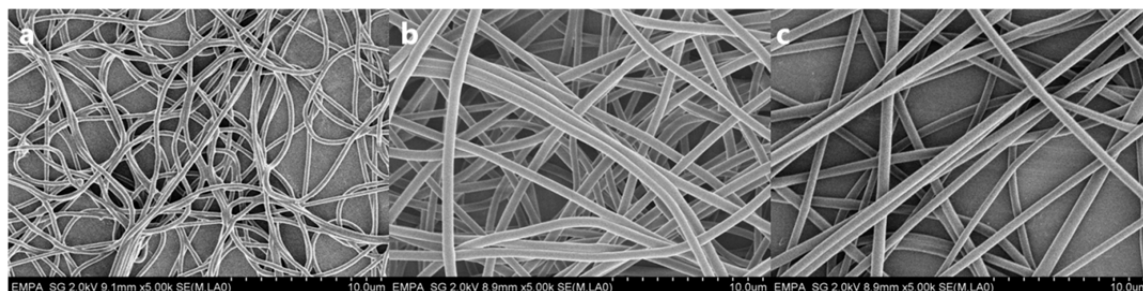
Figure 3. 8. SEM pictures of prepared electrospun membranes: Pebax 2533 (a), Pebax 4033 (b) and Pebax 400 (c).

The frictional behaviour of all prepared membranes rubbed against textiles under both dry and hydrated condition was investigated. Unfortunately, Pebax membranes were not durable enough to remain unaltered during friction measurements. They were destroyed after several dozen of cycles, which precluded further measurements. Figure 3.9 presents the appearance of Pebax 2533 (Figure 3.9a), Pebax 4033 (Figure 3.9b) and Pebax 400 (Figure 3.9c) electrospun membranes after friction-measurements trials.
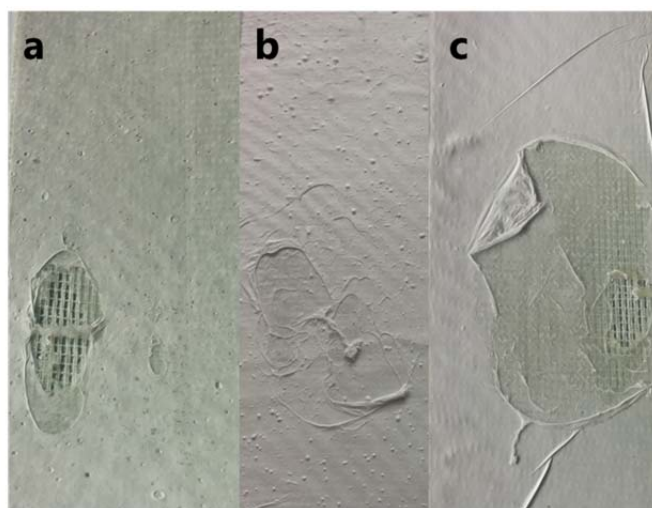
Figure 3. 9. Destruction of Pebax 2533 (a), Pebax 4033 (b) and Pebax 400 (c) electrospun membranes after friction measurements.

As in the case of the commercially available materials (section 3.5.1), the polyurethane electrospun membrane was able to mimic human skin friction within acceptable limits under certain conditions. Average friction coefficient values for human skin (volar forearm) rubbed against Martindale reference textile under moist and

wet conditions were 2.01 ± 0.41 and 2.27 ± 0.52, respectively. For the same conditions, the average friction coefficient values observed for the polyurethane electrospun membrane were 1.64 ± 0.76 and 1.75 ± 0.70, respectively.

It is also important to mention that the polyurethane electrospun membrane was often destroyed by the end of friction measurements (after few thousands of cycles).

3.5.3. Hot-pressed films

Three different Pebax-based (Pebax 2533, 4033 and 400, Akema) hot-pressed films were investigated as potential skin models. Samples were produced in three different thicknesses (779 ± 53 μm, 1392 ± 49 μm and 1771 ± 33 μm) in order to investigate the influence of bulk properties on the frictional behaviour of the final product.

Figure 3.10 presents the appearance of prepared Pebax 2533 films consisting of three different thicknesses (Figure 3.10a) and the results of friction measurements for these hot pressed films rubbed against Martindale under dry, moist and wet conditions (Figure 3.10b).
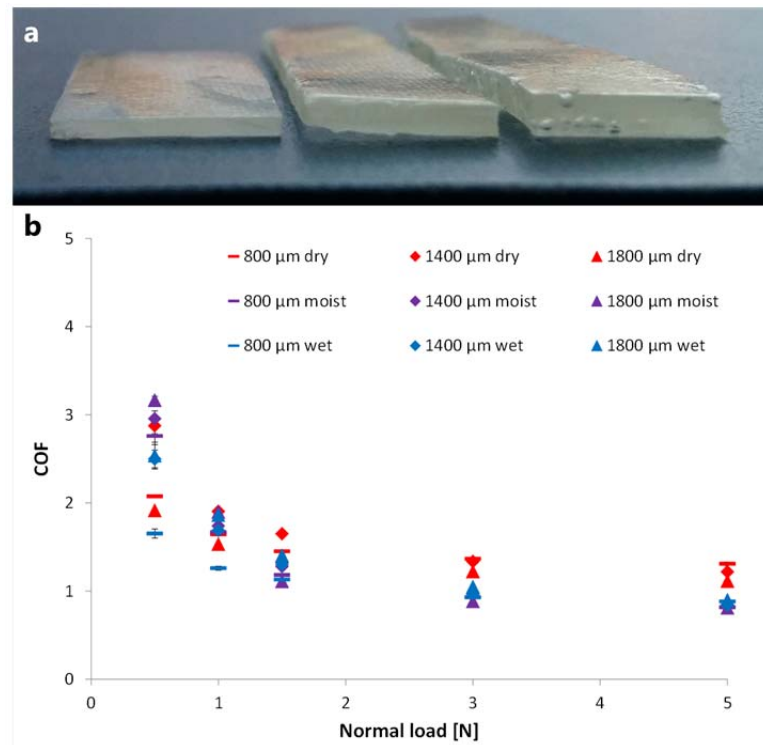
Figure 3. 10. Pebax 2533 hot-pressed films (a). Friction results for Pebax 2533 hot-pressed films (b).

As can be seen in Figure 3.10b, the thickness of the samples, within the examined range, has no significant influence on their frictional behaviour.

Among all examined hot-pressed films, only the one prepared from Pebax 2533 showed friction coefficient values similar to those reported for human skin, and only under certain conditions. The average friction coefficient for human skin (volar forearm) rubbed against Martindale under moist conditions was 2.01 ± 0.41. The average friction coefficient for a Pebax 2533 hot-pressed film examined under the same conditions was 1.47 ± 0.71. Moreover, when a Pebax 2533 hot-pressed film was rubbed against Martindale under dry conditions, it mimicked results obtained for human skin under moist conditions even better (average friction coefficient: 1.57 ± 0.28).

3.5.4. Bar-coated film

A polyurethane bar-coated film was examined according to its frictional behaviour. Measurements were only possible under dry conditions. In the presence of water, the polyurethane film was not durable enough and was destroyed after several dozen measurement cycles.

The average friction coefficient for human skin (volar forearm) rubbed against the Martindale reference textile under dry conditions was 0.47 ± 0.07, whereas for the polyurethane bar-coated film tested under the same conditions it was 0.73 ± 0.29.

3.6. Conclusions and outlook

Three groups of polymer-based potential skin models were prepared: electrospun membranes, hot pressed films and bar coated films. Samples were examined according to their frictional behaviour and compared with trends and values reported for human skin on the volar forearm tested under the same conditions.

As presented above, potential skin models could mimic human skin frictional behaviour only under certain conditions. None of the proposed materials could be used as a universal skin model, applicable for dry and hydrated conditions.

Besides their selectivity, electrospun membranes and bar-coated films were too fragile to outlast the complete series of friction measurements.

Figure 3.11 presents our way of thinking while developing the above-mentioned potential skin model. Our argumentation was that a material with mechanical properties and structure similar to those of human skin could lead to a functioning skin model. Experiments performed on the previously described samples showed that the mechanical properties are not the main factor responsible for the frictional behaviour of human skin. In addition, it is not sufficient to look for a material with a similar elasticity and structure. The parameter that was missing in the proposed potential skin models was the ability to interact with water. This conclusion was the basis for further investigations and the main motivation to develop the water-responsive, gelatine-based skin model, which will be described in Chapter 5.
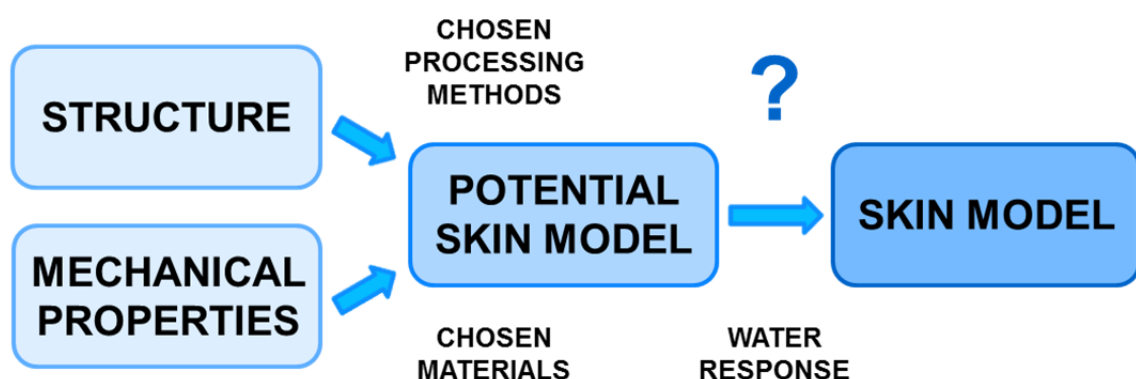
Figure 3. 11. Thinking process while developing a skin model.

Chapter 4

In vivo confirmation of hydration-induced changes in human-skin thickness, roughness and interaction with the environment

Results presented in Chapter 3 led to the conclusion that interaction with water is a very important parameter influencing human skin properties and performance. The need to understand, how water modifies human skin and what are the consequences of prolonged contact with water, which would be interesting from the tribological point of view, was the motivation for further research.

Chapter 4 focuses on the influence of water on human skin properties, such as hydration level, *stratum corneum* thickness, surface roughness and interaction with other materials. Section 4.1 focuses on the introduction and motivation for the study. Section 4.2 presents materials and techniques used to acquire and process the relevant data. Results are given in section 4.3 and discussed in section 4.4. Section 4.5 summarizes the study.

Chapter 4 is based on my contribution, under the supervision of Ch. Adlhart, F.Spano, G.M. Rotaru, R.M.Rossi and N.D. Spencer, to Ref. [19]:

Dąbrowska AK, Adlhart C, Spano F, Rotaru GM, Derler S,

Zhai L, Spencer ND and Rossi RM.

In vivo confirmation of hydration-induced changes in human-skin thickness, roughness and interaction with the environment.

Biointerphases. 2016;11:031015

All experimental work was carried out by myself under the supervision of Ch. Adlhart, F.Spano, G.M. Rotaru, R.M.Rossi and N.D. Spencer. All authors participated in the discussions and corrections of the manuscript.

The manuscript was the most read paper of the month in October and November 2016, and the Editor's Pick of the Biointerphases Journal.

4.1. Motivation

Skin is our protective armor in everyday life [35] and our primary interface with the environment. It has an area of some $2m^2$, and is thus the largest single organ in the human body. Human skin is a multilayer structure, consisting of the *epidermis*, being the outer layer of the skin, mostly exposed to the external factors, *dermis*, responsible for, *inter alia*, flexibility and durability of the skin and subcutaneous tissue, acting as additional insulation and mechanical protection [311-313]. One of the main functions of skin is to protect the body from external factors, such as mechanical injuries, extremes of temperature and radiation, as well as the transport of various substances [314, 315]. The barrier function of skin is mostly provided by the *stratum corneum* ("horny layer", SC) [316-318]. This thin layer, reaching a thickness of 15-20 μm at the volar forearm, is the most external of the sublayers of *epidermis* [35, 316]. Keratinocytes, comprising about 85% of the *epidermis*, migrate through the sublayers of the *epidermis*, gradually transforming to horny cells by changing their size, shape, composition and losing their nuclei. The SC consists of non-nucleated and flat cells named corneocytes[319, 320]. According to the "brick and mortar" model, corneocytes are described as bricks surrounded by lipid bi-layers as the mortar [317]. The hydration level of the SC can vary depending on environmental conditions, as corneocytes can take up water until the hydration level of the SC is in equilibrium with the environment [151]. The hydration level of the SC is responsible for the physiology and homeostasis of the skin [148]. Examples of the importance of hydration on the functions and properties of the skin are its influence on the mechanical toughness of skin, its barrier functions and the regulation of enzyme activity [112, 119, 316, 321] . As suggested by Egawa, daily routines can lead to visible changes in the skin [12]. Even a very short exposure to water, such as washing hands for 2 minutes, is enough to hydrate the SC *disjunctum* while a bath can contribute to changes in the SC *conjunctum*, and thus the influence of the environment on the properties of the skin are essential factors to be taken into account when studying skin-materials interactions [322, 323]. Moreover, seasonal changes in humidity are an important factor influencing the skin [324].

There is a variety of techniques that allow both *in vivo* and *in vitro* determination of the hydration level of skin, based on different principles, including chemical analysis and electrical methods [113, 325-328]. For the purposes of this paper, we have chosen

confocal Raman spectroscopy as a non-invasive, depth-resolved method that provides quantitative information concerning the skin's hydration level.

The results extracted from confocal Raman spectroscopy provide information on hydration and its variation with depth, the SC thickness and also, in combination with information on the real contact area of skin with the Raman instrument, inferences about the interaction of skin with other objects [11, 22, 112, 318, 329-331].

Given that skin is able to take up water, it is reasonable to assume that water should also change its morphology and surface properties. In order to analyze these changes over time, we have employed 3D laser scanning microscopy, which allowed us to observe the surface of a skin replica under high magnification and provided 3-D information [332-334].

In this paper, we present a pilot study focused on global changes in appearance and properties of human skin caused by exposure to water or humid conditions. In order to investigate the multifaceted response of skin to water we have examined the hydration level of the superficial *stratum corneum* (SSC), being the surface of skin, depth profiles of skin before and after exposure to external sources of water, the skin's water uptake abilities, the SC thickness, the real contact area against smooth CaF_2, the skin's surface roughness, and the evolution of the dimensions of the primary lines.

4.2. Materials and methods

4.2.1. Instrumentation

Confocal Raman Spectroscopy

The hydration level of skin was determined from *in vivo* Raman spectra that were acquired using an inverted confocal Raman spectrometer equipped with a 60x oil immersion objective, Skin Composition Analyzer (SCA), model 3510 (RiverD, Rotterdam, the Netherlands). Depth profiles were measured in 2 μm steps, from the surface of the skin to a depth of 60 μm. Laser excitation with a wavelength of 671 nm (laser power 19.5 ± 1.8 mW) was used for 1 s in order to obtain spectra in the region of 2550-4000 cm^{-1}, providing information about the amount of water and proteins in the skin [321, 335, 336]. The *z*-resolution of the optical setup was determined to be 4.7 μm by placing a water droplet on the CaF_2 window of the inverted microscope and fitting the slope of the Raman signal at the CaF_2/water interface with a Lorentz function, taking the full width at half maximum. To account for the known discrepancy between true confocal depth and mechanical displacement of the optical table [337], all depth profiles were corrected with the depth-correction factor $f_{depth} = 1.06$. f_{depth} was determined by comparing the confocal thickness of a NIST polystyrene standard film with its true thickness. Therefore, the film was placed onto the CaF_2 window with an additional water contact layer of approx. 5 μm and the Raman signal of polystyrene between 3040 and 3076 cm-1 was followed in steps of 0.5 μm. The true thickness of the polystyrene film was determined to be 52.7 μm as calculated from the infrared transmission interference pattern in the 3200 to 3600 cm^{-1} wavenumber region (refractive index $n_{polystyrene} = 1.59$).

3D Laser Scanning Confocal Microscopy

The surface morphology of polyvinylsiloxane (Profil novo light type 3, Heraeus Kulzer GmbH, Hanau, Germany) skin replicas was observed by means of a 3D Laser Scanning Confocal Microscope, model VK-X250 (Keyence, Osaka, Japan), using a violet laser with a wavelength of 408 nm (maximum laser power: 0.95 mW).

4.2.2. Measurements

The single-person pilot study was performed on a healthy, left-handed Caucasian woman aged 26 with a BMI of 21. For at least 48 hours before the measurements, the skin was not treated with moisturizers and heavy exercises were avoided. All measurements were performed on the left arm. For simplicity, the skin before water/humidity exposure is termed "dry", whereas the skin exposed to an external source of water is termed "hydrated". After exposure to water/humidity, the forearm was immediately placed on the CaF_2 acquisition window of the Raman instrument and maintained in this position throughout the entire measurement. After each depth profile, the lateral position of the laser was changed between 0.2 and 2.0 mm and another depth profile was collected. The measurements, consisting of 10 depth profiles collected at 10 different positions on the volar forearm, were repeated three times for each exposure time/set of conditions.

Influence of water on skin hydration

Hydration levels of skin under atmospheric conditions were measured at four different points that were equally distributed along a line from about 7 cm from the wrist up to the elbow (Figure 4.1a). Then the defined measuring points were exposed to water using patch-test chambers (Van der Bend, Brielle, the Netherlands) filled with 20 μl of distilled water. Exposure time was varied from 2 to 60 minutes. After unsticking the patch, excess water was removed with a paper towel.
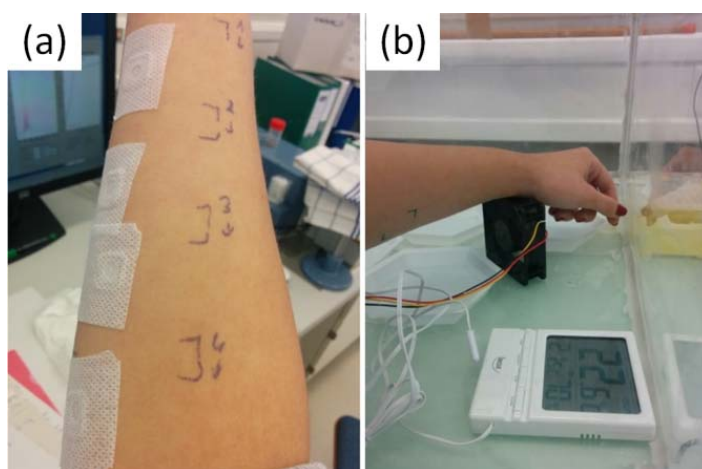
Figure 4. 1. (a) Forearm exposed to water with the use of patch test chambers. (b) Forearm inside the humidity box.

Influence of water vapor on skin hydration

Hydration levels of skin under atmospheric conditions as well as after exposure to air at a defined humidity were measured midway between the wrist and the elbow. To expose skin to an atmosphere at a specified humidity, the left arm was placed in a purpose-built PMMA humidity chamber with the dimensions of 60 x 50 x 30 cm for one hour (Figure 4.1b). Saturated NaCl solution or a travel air humidifier, both assisted by a fan to homogenize the air inside the chamber, were used in order to obtain a relative humidity of 70 or 90%, respectively [338, 339].

Surface morphology

Polyvinylsiloxane replicas of the skin taken before and after 2-60 minutes of exposure to water (according to the same procedures as explained above) were prepared in triplicate. The change in surface morphology due to exposure to water was investigated by means of a 3D laser scanning confocal microscope. Each replica was analyzed in three different spots using the 20 x objective lens.

4.2.3. Data processing

Hydration level

Hydration levels of skin were automatically determined from the Raman spectra using Skin Tools 2.0 software (RiverD, Rotterdam, the Netherlands), where the water content is calculated relative to keratin, based on the integrals of OH-vibration signals (W) in the range of 3350 to 3550 cm^{-1} and the integrals of the relevant CH-vibration signals (2910-2966 cm^{-1}), P) [113, 321, 335, 340], using the relation

$$hydration\ level\ (\%) = \frac{W/P}{W/P + R\prime} * 100\%$$

according to Caspers *et al [113]*, where *R' = 2* is a proportionality constant that was obtained by calibrating against protein solutions. To determine the integrals W and P, Raman spectra were baseline corrected with a first-order polynomial fitted through the spectral regions 2580 to 2620 and 3780 to 3820 cm^{-1}, see also Figure 4.2.

Both the absolute hydration level and the water uptake, understood as the difference between the hydration level before and after exposure to water, were taken into consideration in further investigations.

Biexponential fitting was applied to the data of time-dependent change in hydration level of superficial *stratum corneum* according to

$$hl(t) = hl_0 + hf_A \times [1 - e^{-D_A \times t}] + hf_B \times [1 - e^{-D_B \times t}]$$

where hl(t) and hl_0 are the respective hydration levels at time t and at $t = 0$ min. The variables hf and D are the hydration factor in % and the hydration rate coefficient in min^{-1} for the two exponential functions A and B, see also Figure 4.3.

Contact area

We propose a new non-invasive *in vivo* method to measure the influence of hydration on the contact area between skin and other objects. For each spectrum, an image of the contact between the skin and the CaF_2 acquisition window of the SCA was taken. Based on the images corresponding to each spectrum, the contact area could be calculated by means of CorelDRAW X6 software, supported with the Getarea macro.

Thickness of the *stratum corneum*

As proposed by Crowther, the thickness of the SC can be determined from each water profile by fitting with a Weibull curve [87, 321, 335]. This was performed with Matlab (The Mathworks, Natick, MA, U.S.A).

Surface morphology

Surface-roughness parameters: Sa, Sz, and the characteristic dimension of the profiles were extracted with VK-H1XME: VK-X AI-Analyzer Software, each measurement being the average of three profiles with the interval of 20 μm of replicas. Each image was inverted and artefacts as well as characteristic features, such as sweat glands, hair follicles etc. were not considered in further data processing.

4.3. Results

4.3.1. Raman spectra of the *stratum corneum* and viable *epidermis* before and after exposure to water
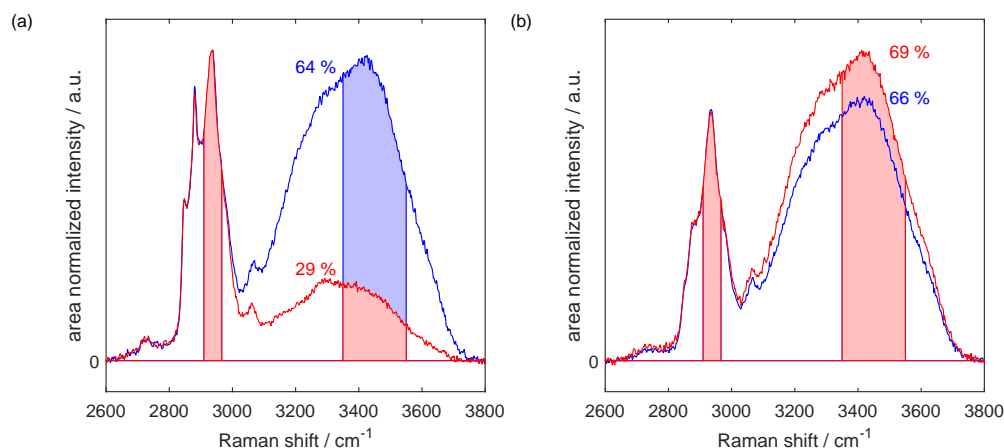
Figure 4. 2. Typical base line corrected Raman spectra and hydration levels of the superficial stratum corneum at 0 μm (a) and of the viable epidermis at 40 μm (b) captured before (dry, red) and after 1 h exposure to water (wet, blue). Hydration levels were determined based on the ratio of protein and water vibrations (shaded areas). The difference of 3 % in (b) reflects the uncertainty of skin hydration due to local variation of the hydration level.

Raman spectra of skin show characteristic features depending on the sampling depth and the preconditioning of the skin (Figure 4.2). For dry skin the Raman spectrum captured at the SSC (0 μm depth) level shows strong CH-vibration signals that are characteristic of proteins (2930 cm^{-1}) and lipids (2850 and 2880 cm^{-1}), as well as weak OH-vibration signals (3350 to 3550 cm^{-1}) characteristic of water (Figure 4.2a). This is in contrast to the spectrum captured in the VE (40 μm depth) (Figure 4.2b), where the strong lipid signals are absent, and the OH- signals are stronger, corresponding to a higher water content. After 1h exposure to water, the spectrum captured at the SSC level shows a strong water peak (Figure 4.2a) while no such significant change was observed in the VE-level spectrum (Figure 4.2b).

4.3.2. Environmentally dependent changes in the structure and properties of human skin

Hydration level of the *stratum corneum*
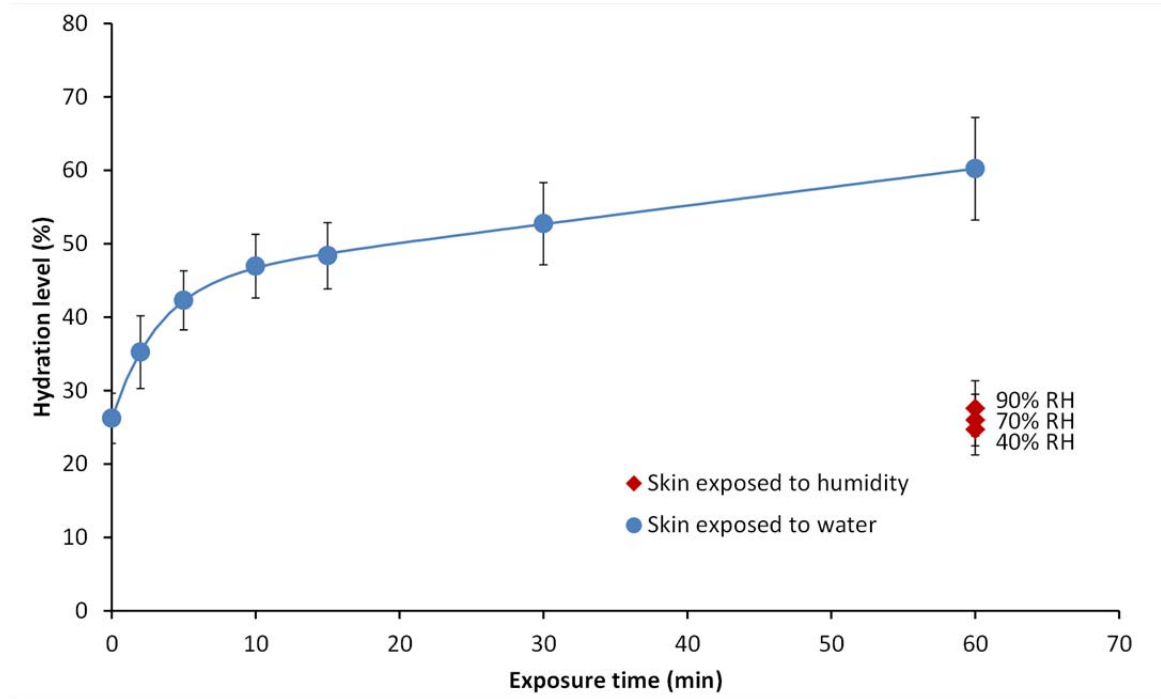
Figure 4. 3. Change of hydration level of the superficial stratum corneum (SSC) caused by the water and humidity exposure. The straight line shows the biexponential fit with $hl_0 = 26.2$ %, the hydration factors $hf_A = 18.8$ % and $hf_B = 494$ %, and the fast and slow hydration rate coefficients $D_A = 0.31$ min^{-1} and $D_B = 0.52*10^{-3}$ min^{-1}, $R^2=0.9998$.

Figure 4.3 shows the influence of the environment on the hydration level at the surface of the skin, at 0 μm depth (SSC). It can be clearly seen that water exposure influenced the hydration level of the SSC to a far higher extent than was observed for relative humidity up to 90%. The level of hydration gradually increased from 26.2 ± 3.4% to 60.2 ±7.0% after 60 minutes of water exposure. The extent of the forced hydration was significant, especially for short exposure time (up to 5 minutes).

Increase in relative humidity (RH) from 40% to 90% contributed towards an increase in the hydration level of the SSC from 24.7 ± 3.5% to 27.6 ± 3.8% after 60 minutes. In comparison, a significantly higher hydration level (35.2 ± 5.0 %) was observed after just 2 minutes exposure to liquid water.
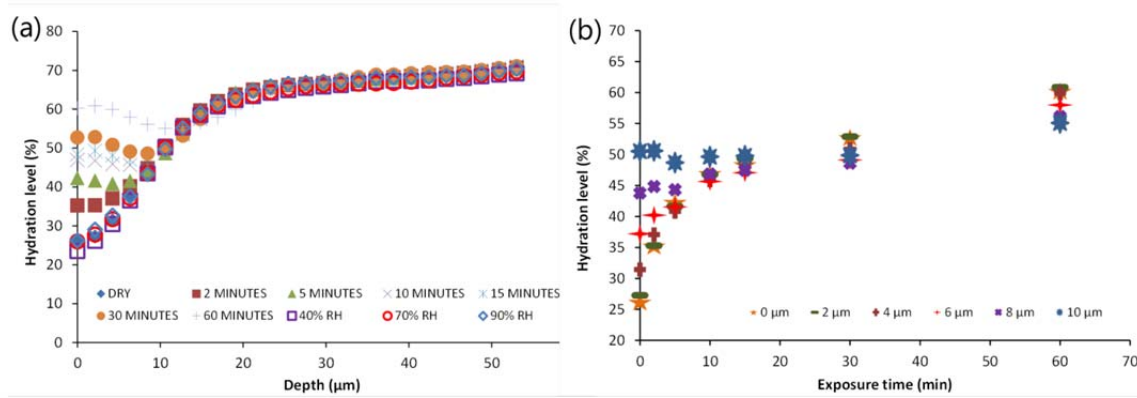
Figure 4. 4. (a) Change of the depth profiles of water content in the SSC caused by water and humidity exposure. (b) Time-dependent change in the hydration level at depths up to 10 μm caused by water exposure.

Consistent with the abovementioned phenomenon, it was also clear from the depth profiles of water content (Figure 4.4a) that the hydration level in the SSC increased most significantly after exposure to water. In addition to the results presented on the Figure 3, the depth profiles show that the largest change in hydration level caused by external factors could be observed within the first 10 μm. The hydration level of dry skin varied with depth from $26.2 \pm 3.4\%$ in the SSC to $70.3 \pm 2.9\%$ in the VE at a depth of 50 μm. Depth profiles before and after exposure to the external source of water coincide for deeper layers of the skin. In order to show this effect even more clearly, the hydration level measured at different depths of the skin from 0 to 10 μm were plotted as a function of the exposure time to water (Figure 4.4b). As presented in the graph, the influence of the exposure time to water on the hydration level was more marked for the (initially drier) outer layers of the skin. Water uptake, being the difference between the hydration level of the skin before and after water exposure for different depths of the skin, is presented on Figure 4.5. Confirming the effect visible on Figure 4.4, Figure 4.5 presents the uptake of water at different depths of the skin when the skin was exposed to water for 2, 30 and 60 minutes. It is clearly visible that the deeper the layer of skin that was investigated, the lower was the uptake of water. The hydration rate also decreased with exposure time. Considering the surface of the skin, the uptake of water after 2 minutes of exposure was 9.03 ± 6.03 %, changing to 26.53 ± 7.47 % after 30 minutes and 34.02 ± 8.95 % after 60 minutes.
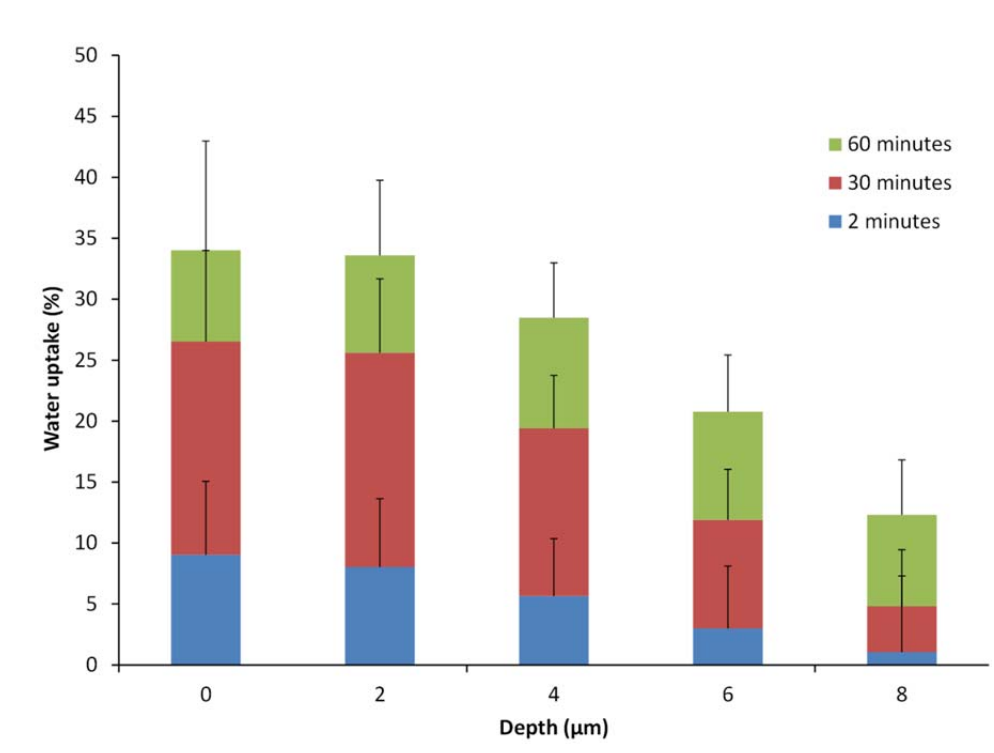
Figure 4. 5. Total uptake of water at different depths of the skin after different times of water exposure.

The evolution of contact area
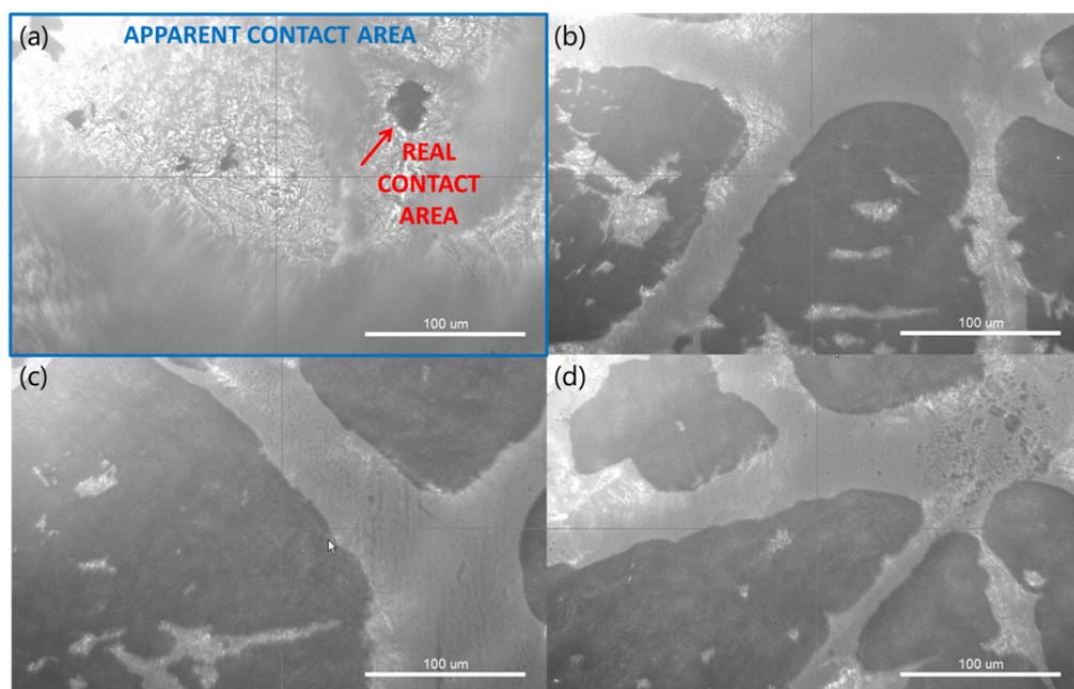
Figure 4. 6. Evolution of the skin/CaF$_2$ acquisition window contact area before (a) and after 2 (b), 30 (c) and 60 (d) minutes of water exposure.

The real contact area, which corresponds to direct contact between skin and the CaF$_2$ acquisition window, can be recognized as dark areas in Figures 4.6a-d, which were captured within the first few seconds after the forearm was placed on the CaF$_2$ window. The rapid acquisition was necessary in order to avoid the influence of sweating and relaxation process and to show the clear influence of the external source of water on the contact area. Apparent contact area is defined as the area of the apparent contact between the skin and the CaF$_2$ window, which itself had an area of 70 734 μm^2.

From the very low real contact area values, it is clear that dry skin has little direct contact area with the CaF$_2$ window values (Figure 4.6a). This is due to its roughness and limited elasticity. After only 2 minutes exposure to water there was a significant increase in real contact area (Figure 4.6b). Longer exposures, such as 30 (Figure 4.6c) or 60 minutes (Figure 4.6d) did not lead to a significantly greater real contact area value.
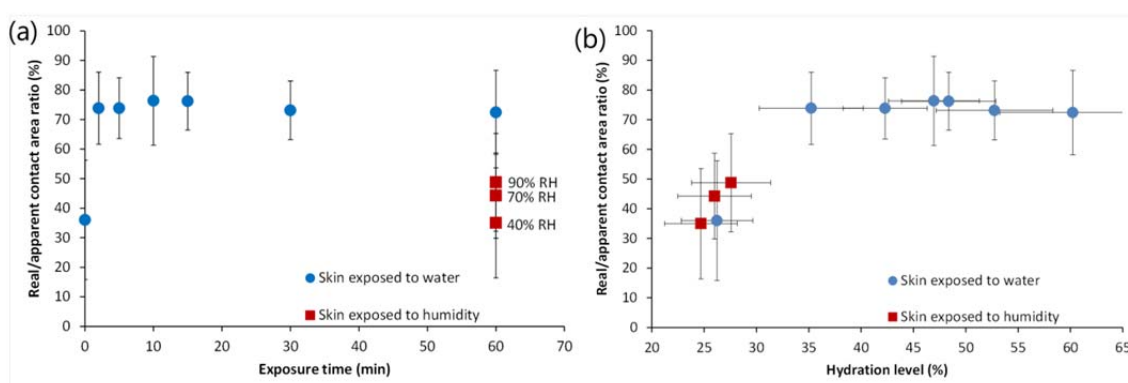
Figure 4. 7. Change in the real/apparent contact area ratio caused by the water and humidity exposure (a). Real/apparent contact area ratio as a function of the hydration level of the SSC (b).

The real/apparent contact area ratio for dry skin (hydration level: 26.2 ± 3.4%, as shown on Figure 4.2) had a value in the range of 36% (Figure 4.7a-b). Once the skin was exposed to water, the contact area significantly increased and real/apparent contact area ratio (hydration level 35.2 ± 5.0 %) reached 73% after 2 minutes exposure. Values of real contact area and real/apparent contact area ratio for skin exposed to water for 2-60 minutes were comparable.

In agreement with other analyses, the influence of humidity on the contact area was lower than it was measured for water. Real/apparent contact area ratio gradually increased from 35% for 40% RH to 48% for 90% RH.

Thickness of the *stratum corneum*

As presented above, hydration measurements showed that human skin absorbs water from the environment. To confirm this phenomenon, measurements of the change in structure and morphology of human skin were performed.

Figure 4.8 presents the influence of water absorption on the thickness of the SC. When the skin was exposed to water, the thickness of the SC, determined based on the Raman spectra, increased linearly with increasing exposure time. The SC thickness increased from 17.5 ± 2.5 μm measured for skin before water exposure to 21.2 ± 3.0 μm after 60 minutes exposure to water. The SC thickness increase after 30 and 60 minutes water exposure is statistically significant (accordingly $p=4 \times 10^{-4}$ and $p=3 \times 10^{-9}$). Exposure to humidity influenced the SC thickness to a smaller extent, causing an increase from 17.2 ± 2.0 μm for 40% RH to 18.5 ± 2.4 μm measured for the skin exposed to 90% RH for 60 minutes.
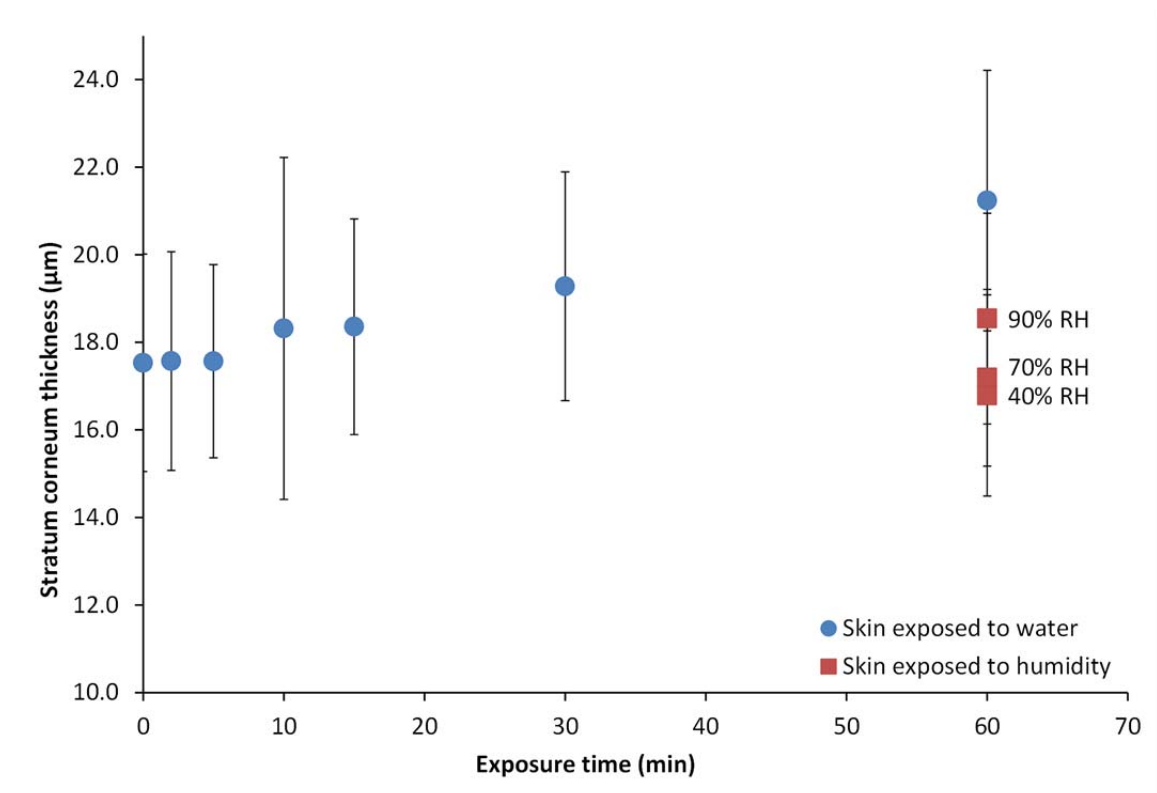
Figure 4. 8. SC thickness upon water and humidity exposure.

Morphology of the skin
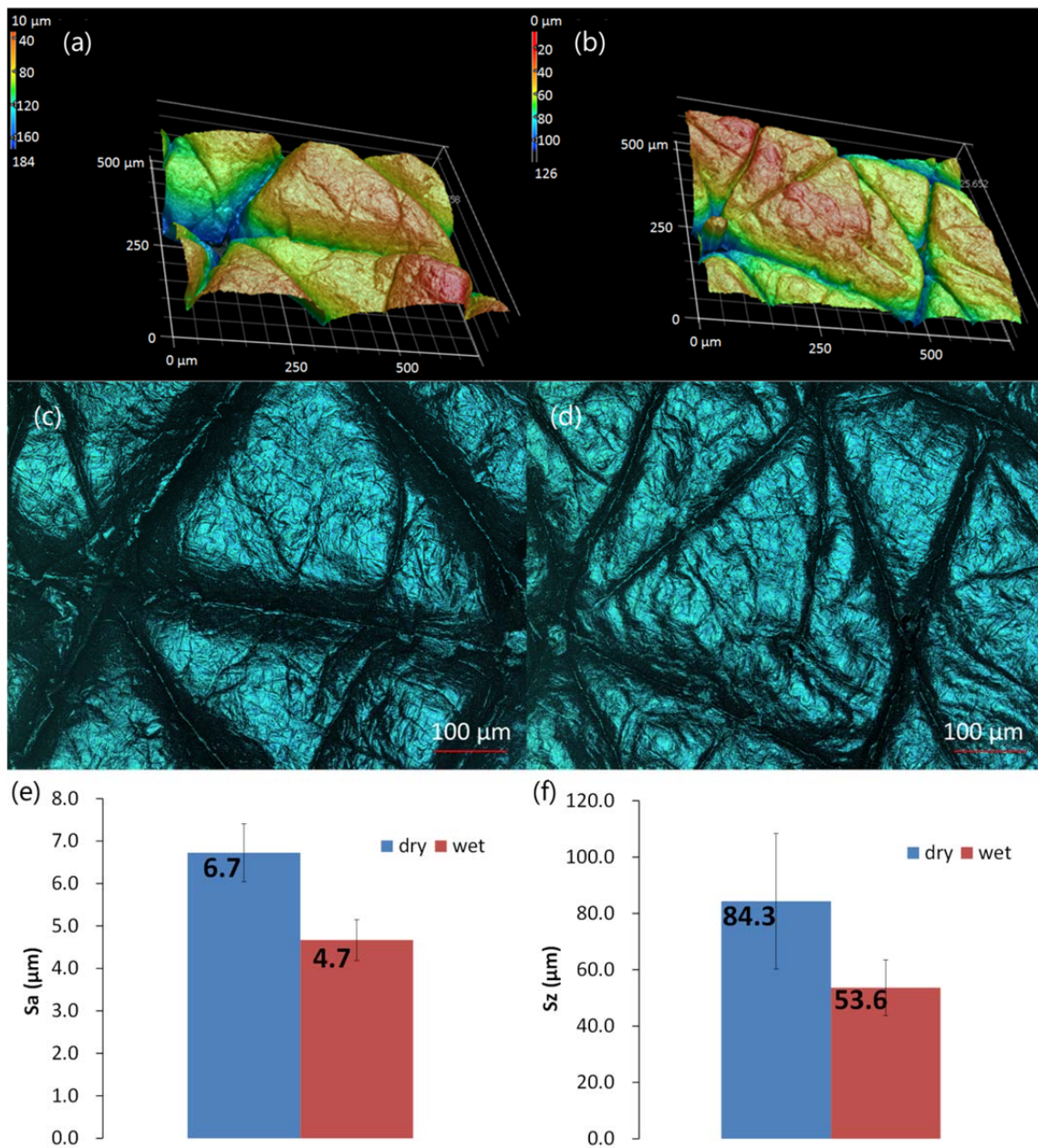
Figure 4. 9. Appearance of human skin before (a: 3D topographical view, c: 2D topographical view) and after 60 minutes exposure to water (b: 3D topographical view, d: 2D topographical view). Surface roughness: Sa (e) and Sz (f) of human skin before (dry) and after 60 minutes water exposure (wet).

Figure 4.9 presents the surface roughness values; Sa (Figure 4.9e) and Sz (Figure 4.9f) as well as two- and three-dimensional micrographs of skin replicas of the volar forearm before (Figure 4.9a, c) and after 60 minutes exposure to water (Figure 4.9b, d). It can be observed that water changed the appearance of human skin, making it

smoother. The Sa parameter decreased from 6.7 ± 0.7 μm measured for dry skin to 4.7 ± 0.5 μm measured after 60 minutes water exposure, due to the smoothening effect water uptake. Similarly, the value of the Sz parameter dropped from 84.3 ± 24.1 μm before to 53.6 ± 9.9 μm after exposure to water.

From the cross-section of the 3D microscopic pictures, surface profiles of dry (Figure 4.10a) and wet (Figure 4.10b) skin were extracted, in order to investigate the influence of exposure to water on the dimension of the clefts present on the skin. The average width of the primary lines decreased from 112.6 ± 30.7 μm before to 57.7 ± 16.0 μm after 60 minutes water exposure (Figure 4.10c). The depth of the primary lines also decreased, reducing from 44.5 ± 9.8 μm for dry skin to 20.5 ± 10.2 μm for skin exposed to water (Figure 4.10d).
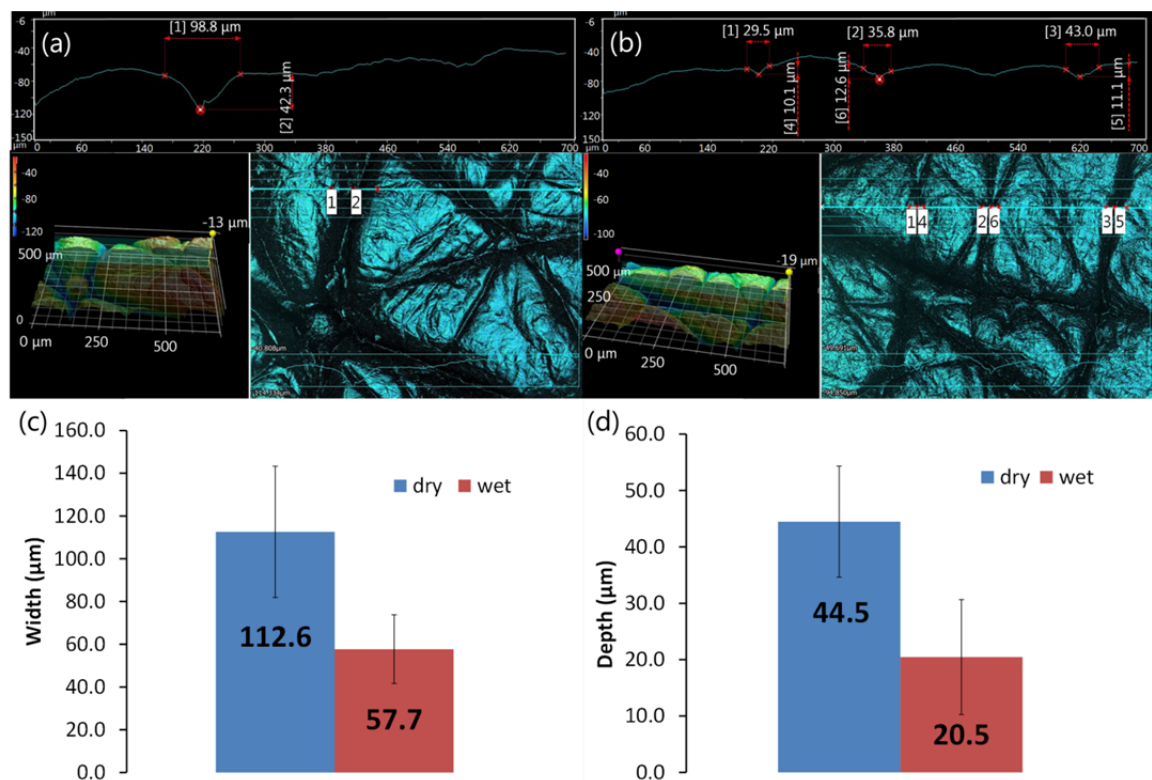
Figure 4. 10. *Surface profiles extraction from the 3D cross-section of the dry (a) and wet (b) skin replica. Width (c) and depth (d) of the primary lines before (dry) and after 60 minutes water exposure (wet).*

4.4. Discussion

In the present study we were able to demonstrate how hydration conditions influence human skin on several levels. Under dry conditions, human skin can be considered as a rough material [35]. Dry SC is characterized by high values of Young's modulus, reaching into the GPa range [341-344]. Therefore, as a rough and not easily deformable material, characterized by wide and deep primary lines [344], human skin in a dry state shows limited real contact area with the CaF_2 window. The hydration level of dry skin increased with the depth of the measurement, exhibiting the lowest value for the SC, consisting of dead and shriveled corneocytes [314] and the highest value for VE [87, 321, 336, 345]. The natural variation of the water content at different depths of the skin is the explanation for a clear difference in the ratio between protein and water peaks in Raman spectra for the SC and VE of the dry skin.

The hydration state has a major influence on the performance of the skin. As can be seen in the Raman spectra, when the skin was exposed to water for 60 minutes, the ratio between the protein and water peaks for the SSC changed drastically due to water uptake. However, the exposure to water did not influence the VE [336]. Depth profiles also confirmed that water can only influence the surface of the skin and showed that, below a certain depth, there was no difference between dry and hydrated skin. This behaviour can be explained by the barrier function of the SC, as the threshold depth corresponds to the location of the lower SC, known to act as a barrier layer for water [346-349]. Another threshold can be observed, suggesting that the skin was more accessible to penetration of water, and that it occurred faster at depths of the first few μm of the SC. The time dependent change of the hydration level of the SSC (Figure 4.3) fits well to a biexponential model with a fast and slow hydration rate coefficient $D_A =$ 0.31 min^{-1} and $D_B = 0.52*10^{-3}$ min^{-1}. This could indicate at least two different water diffusion mechanisms as expressed in the literature by multi-layer or multi-compartment skin models and the finding of true formation of water pools within the SC [350-352]. This observation is consistent with a statement by Loth, that the transport of water within the SC *disjunctum* takes place through spreading into the intercellular space due to the capillary forces, whereas the much slower and less straightforward water transport within the SC *conjunctum* is based only upon diffusion [322, 353-355]. This also explains the observation that the closer to the surface of the

skin, the faster and more significant is the water uptake as well as the fact that even a short exposure to water (2 minutes) caused appreciable changes in the SSC.

As the SC becomes hydrated, it is no longer stiff and rough. Due to the plasticizing effect of water, the Young's modulus of the SC may decrease by as much as three orders of magnitude [342, 344]. The dimensions of the primary lines decrease, making the surface of the skin smoother. Softer and smoother skin results in a significantly higher real contact area with the CaF_2 window. The uptake of water by corneocytes not only makes the main furrows shallower, but also leads to an increasing thickness of the SC [321, 336]. Water diffusion requires space and therefore leads to physical expansion, i.e. swelling [351, 352]. For all investigated parameters, an increase in relative humidity had a minor influence on the skin compared to direct contact with water. Skin hydrated through the exposure to humid conditions followed the same tendencies as the skin hydrated through direct exposure to water, but to a much lesser extent. In the case of our experiments, humid conditions can be compared with the amount of water in the air equal to 13,6 g/m^3 for the RH=70% and 19,6 g/m^3 for the RH=90% [356-358].

The observed effects caused by water on the skin are summarized in Figure 4.11.
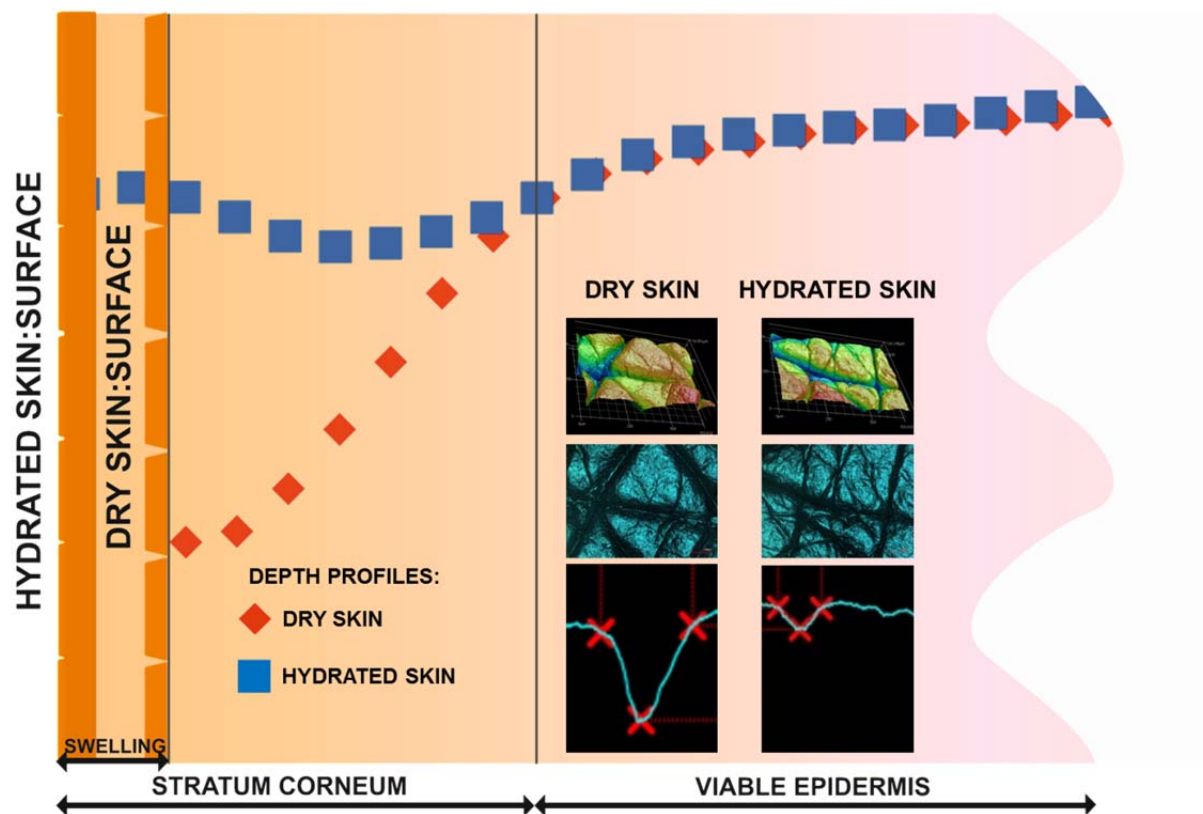
Figure 4. 11. The summary of observed changes in the structure and properties of skin caused by 60-minutes exposure to water.

4.5. Conclusions

In conclusion, although still consisting of the same cells and chemical components, hydrated skin can be perceived as a material with significantly different properties than skin in its usual dry state.

Our study shows that as a result of exposure to water, corneocytes take up the liquid, resulting not only in increased hydration on the SC, but also, due to swelling, in an increased SC thickness and a smoother surface. Moreover, plasticized SC exhibits a lower modulus, i.e. is more easily deformable, leading to a higher real contact area with the CaF_2 window and presumably other objects. This will clearly have tribological consequences.

Improved understanding of the influence of environmental conditions on the properties of human skin is important for various research areas. Barrier function of human skin is the focus of research useful for the drug delivery [359]. It was proven that hydration of the skin (and, consequently, environmental conditions) has a major impact on dermatological issues. Proper hydration is a requirement for the flawless wound healing process [360]. Various skin diseases are caused by skin dryness. Dermatological treatment of, example giving, Xerosis cutis or eczema, could be supported with monitoring and modification of the hydration level of skin [361]. Hydration of skin plays a key role also in ageing prevention [362]. Presented knowledge can be also useful for developing skin models or understanding skin-friction mechanisms, as skin friction is directly related to the skin hydration and environmental conditions and, as a consequence, skin roughness and real contact area with counter surfaces [11]. This could also contribute in the prevention of the decubitus ulcers, as the creation of ulcers depends on the friction between skin and the bedsheet [363].

Chapter 5

A Water-Responsive, Gelatine-Based Human Skin Model

Previous chapters have shown how strong the influence of water is on human skin properties and that the interaction with water is likely to be an important aspect of any accurate skin model that is to mimic the frictional behaviour of human skin under both dry and hydrated conditions.

Chapter 5 presents the development and characterization of a water-responsive, gelatine-based physical human skin model to mimic frictional behaviour of human skin under both dry and hydrated conditions. Section 5.1 presents the introduction and motivation for developing a water-responsive human skin model. Section 5.2 describes materials and methods used in order to develop and characterize gelatine-based skin model. Results are collected and discussed in section 5.3. Section 5.4 presents the conclusions of this study.

Chapter 5 is based on my contribution, under the supervision of F.Spano, G.M. Rotaru, R.M.Rossi and N.D. Spencer, to Ref. [21]

Dąbrowska AK, , Rotaru GM, Spano F,

Affolter Ch, Fortunato G, Lehmann S,

Derler S, Spencer ND and Rossi RM.

A Water-Responsive, Gelatine-Based Human Skin Model.

Submitted to Tribology International (June 2016)

Experimental work was carried out by myself under the supervision of F.Spano, G.M. Rotaru, Ch.Affolter, R.M.Rossi and N.D. Spencer. *In vivo* friction measurements were carried out by myself and S.Lehmann. All authors participated in the discussions and corrections of the manuscript.

The manuscript was awarded with the Dowson Prize during 43rd Leeds Lyon Symposium on Tribology.

5.1. Motivation

In everyday life, human skin continuously interacts with contacting materials, such as clothes, household items, sports equipment, medical devices, tools and instruments. Therefore, friction between human skin and other objects is a relevant topic of investigations that may not only lead to better ergonomics of these objects but also to the prevention of friction-related injuries, skin disorders or wear [4-6].

Methods to investigate the interaction between the skin and other objects can be divided into two main categories: *in vivo* and *in vitro* measurements. In vivo measurements, requiring the involvement of volunteers, can be challenging to perform, expensive and need many test repetitions for statistical significance [20, 364]. In vitro measurements involve the use of the skin models. There is a wide variety of biological or artificial skin models available that could be used in many kinds of investigations, such as cosmetology, drug delivery, biology, and medicine, as well as ballistic, optical or thermal analysis [4]. Among all possible materials, only a few can be considered to be skin models that mimic the frictional behaviour and friction-related properties of human skin [4, 126, 202, 203]. Some materials, such as the artificial leather Lorica®, polyurethanes or silicones were found to mimic the frictional behaviour of human skin under specific conditions [5, 123, 125, 126, 261, 365]. However, the existing models show clear limitations. Therefore, there is still a need for a skin model that simulates the frictional behaviour of human skin against everyday materials over a wide range of applied normal load and water amount, providing reliable and accurate results and at the same time being inexpensive and convenient to use and store.

The frictional behaviour of human skin depends on many factors, including factors such as age, gender, health conditions, anatomical region or hydration level [4, 28, 35]. The roughness as well as mechanical and other properties of the countersurface are also very important [35]. In addition, the frictional behaviour of human skin is strongly influenced by the amount of water in the tribosystem [11, 20]. Skin is a multilayer system with a horny upper layer (stratum corneum) that can be considered as a rough and stiff material under normal atmospheric conditions [35, 366]. However, hydration of this layer leads to smoothening and softening of the skin, with an associated increase of the real contact area between the skin and other objects, resulting in higher friction coefficient values [5, 11, 20, 367]. A realistic skin model simulating the frictional behaviour of human skin should respond to water in a similar way.

Gelatine, a proteinaceous product derived from collagen, is known to function as a skin model for many applications. Physical properties of gelatine, such as density, stiffness, sound speed, ballistic performance, energy dissipation, coincide with those of human skin [368-370]. Moreover, it can be made to absorb water without dissolving thanks to a facile crosslinking process [4, 371, 372]. The structure of skin itself served as the inspiration for the proposed physical model, the collagen and elastin fibers of the natural material being mimicked by a cotton-based textile, while the gelatine simulated the function of other components of the extracellular matrix [373, 374].

The new physical skin model not only simulates the frictional behaviour of human skin against a standard textile in dry and hydrated conditions over the entire range of applied normal load (0.5-5 N), but it also mimics the skin-specific change in the tensile Young's modulus, surface roughness and thickness by caused water uptake.

5.2. Materials and methods

5.2.1. Preparation of the skin model

Figure 5.1 shows schematically the preparation procedure of the gelatine-based skin model. In a first step, with the use of a bar coater (Coatmaster 509 MC, Erichstein), a 10 wt. % solution of gelatine (type A, bloom no 300, Sigma Aldrich) in distilled water (prepared by continuous stirring at 60˚C for 2 hours) was spread on top of knitted cotton fabric in three layers of 300 μm and left to dry for 24h at room temperature after the application of each layer. The knitted cotton was selected to be the bottom layer after preliminary tests, including six other textiles, as the skin model containing this substrate displayed frictional behaviour closest to human skin. Gelatine characterized by bloom no 300 was chosen after preliminary results, including lower bloom-numbered gelatines, such as 110 and 175, to be the best one for this application. The resulting composite material was then placed in 1 wt.% solution of glutaraldehyde (Sigma Aldrich) in Dulbecco's PBS buffer (DPBS, GIBCO) for 24 h at room temperature under continuous gentle stirring (130 rpm) in order to crosslink the gelatine. In the next step, the crosslinked skin model was rinsed with distilled water and slowly dried by wrapping in paper towels and squeezing between two boards with the use of a 4 kg weight, in order to avoid ripples caused by drying-related contraction. The paper towels were changed every day and the skin model was considered to be dry after about 6 days, at which point the mass had stabilized.
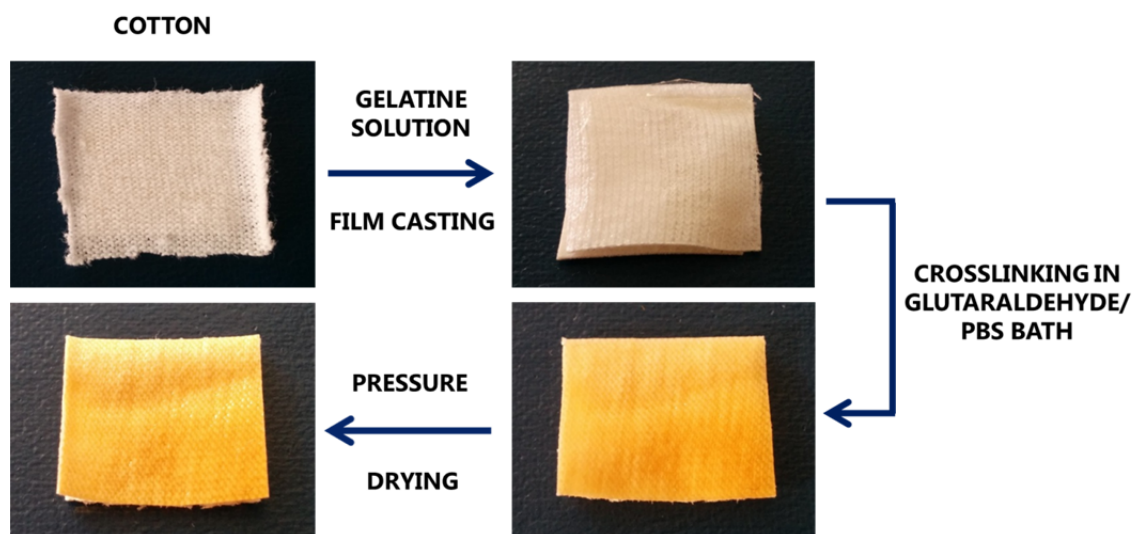
Figure 5. 1. Preparation procedure of the gelatine-based physical skin model.

5.2.2. Friction measurements

In order to determine whether the model mimics the frictional behaviour of human skin, identical procedures were used for both *in vivo* and *in vitro* friction measurements. Martindale test fabric (worsted wool cloth) was used as a reference textile. Measurements were performed in three different moisture states: dry and two hydrated conditions (moist and wet). In the case of dry conditions, samples were stored under ambient environmental conditions at a temperature of approximately 20 ˚C without any further addition of water. Moist conditions, simulating physiological sweat accumulation, were achieved by distributing to 10 μl distilled water per 1 cm^2 [16]. Wet conditions corresponded to the maximum water uptake of the textile (21.6 $μl/cm^2$ for the Martindale fabric), measured as a weight difference between the sample of the Martindale fabric before and after immersion in water. Besides these specific conditions, friction coefficients of the skin and the skin model were investigated as a function of the amount of water in the range of 0-100 $μl/cm^2$ in the reference textile.

5.2.2.1. *In vivo* friction measurements

The *in vivo* study was approved by the Ethics Committee of the Kanton St. Gallen (EKSG 13/156/1B). All measurements were performed in an environmentally controlled room at 23±1˚C temperature and relative humidity of 50±2%. In vivo measurements were performed on the volar forearm, which can also be considered as representative also of certain other skin areas. Furthermore, it is located in a relatively flat anatomical region, which makes measurements easier and provides better reproducibility [35].

In vivo measurements of the friction coefficient of the skin against Martindale fabric were performed as a function of the applied normal load on the right forearm of 6 healthy volunteers (3 men and 3 women with the average age of 27±4.5 years and with the average Body Mass Index (BMI) of 23±2.8) [375]. Friction-coefficient measurements were also performed against the Martindale reference textile as a function of the amount of water on the right forearm of one healthy male volunteer aged 36 years with a BMI of 28. For each investigated condition, volunteers were asked to rub their forearms against the reference textile at least ten times, consciously controlling

and modulating the applied load. The textile was fixed on a three-axis force plate (Kistler 9254) [5].

5.2.2.2. *In vitro* friction measurements

The frictional behaviour of the gelatine-based skin model against Martindale fabric was investigated in an environmentally controlled room (20±1˚C, 65±2% RH) by means of a purpose-built textile friction analyzer (TFA) [6]. Measurements were carried out with a frequency of 1.25 Hz over a distance of 50 mm for 350 cycles for each applied load. Additional experiments, concerning running in (applied load: 0.5 N) were performed under hydrated conditions until a stabilization of the friction coefficient was observed. Three independent series of measurements were performed, in order to calculate average values. Figure 5.2 shows representative results for the running-in process.
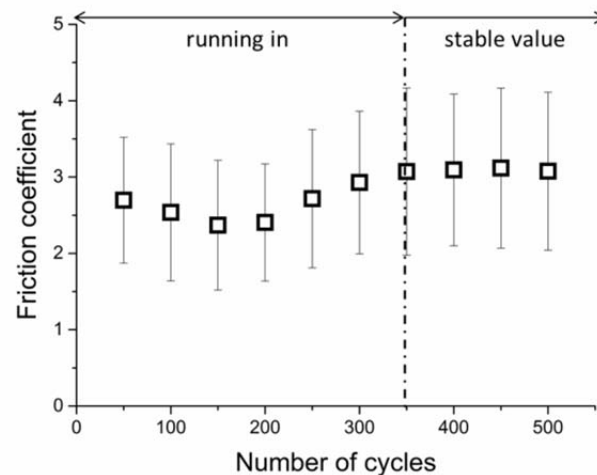
Figure 5. 2. Representative running in process for the skin model rubbed against Martindale under moist conditions.

5.2.3. Determination of the Young's modulus

The Young's modulus of the dry and hydrated (immersed in distilled water for 20 s to 60 min) gelatine-based physical skin model was evaluated in an environmentally controlled room (23±2 ˚C, 50±10 % RH) using a Zwick Roell Biaxial Testing Machine (Zwick-Roell GmbH Ulm, Germany) with optical strain measurement. Dry and hydrated samples with average dimensions of 40 x 5.5 x 0.45 mm were tested at a speed

of 1 mm/min and a 0.5 N preload was applied. The value of Young's modulus was obtained from the slope of the measured stress-strain curve, up to 1 % strain.   Three independent series of measurements were performed. Figure 3 shows the nominal stress as a function of nominal strain for a representative sample previously immersed in water for 15 minutes.
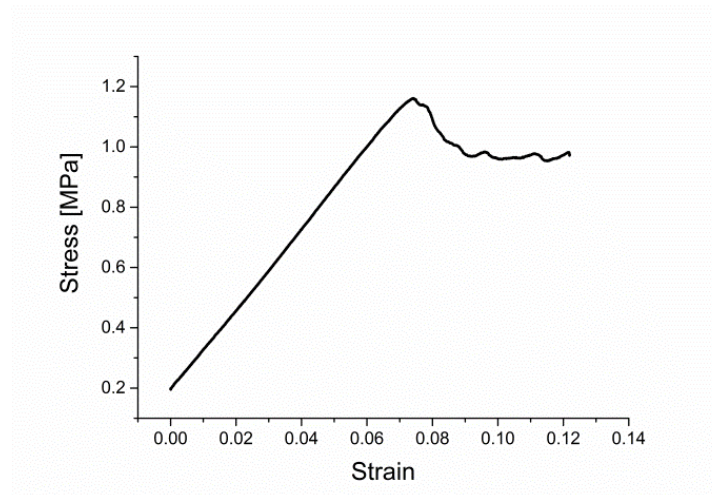
Figure 5. 3. Representative stress-strain curve for the skin model immersed in water for 15 minutes before the measurement.

5.2.4. Structural and surface characterization

Microscopic techniques were used to investigate the structure, surface morphology as well as the water response of the gelatine-based skin model.

The cross-section of the skin model was observed by means of scanning electron microscopy (SEM) (Hitachi S-4800, Japan) at 10 mA beam current and 2 kV accelerating voltage. Samples were plasma coated with a 5 nm Au/Pd layer before the measurement (Leica Microsystems EM ACE 600, Germany).

The surface of the gelatine-based skin model was observed before and after 20 minutes immersion in distilled water by means of a 3D Laser Scanning Confocal Microscope, model VK-X250 (Keyence, Osaka, Japan), equipped with a violet laser (λ= 408 nm). Each sample was analyzed at three different spots using a 20x objective lens. The surface roughness parameters Sa and Sz were extracted using VK-H1XME (VK-X AI-Analyzer Software, Osaka, Japan). All artefacts and characteristic surface features were avoided during subsequent data processing.

The thickness of the skin-model samples was measured by means of the Tesa Isomaster caliper with analogue indication. Measurements were performed for dry and hydrated (immersed in water for 20 minutes) skin models and repeated 10 times for each sample. Measurements were repeated on three independent samples both under dry and hydrated conditions and the average value was calculated. Thickness measurements were performed by a master's student, Patryk Spera. Before the actual measurement series, preliminary measurements indicating the immersion time for the maximum change in thickness were performed.

5.3. Results and discussion

5.3.1. Frictional behaviour of human skin and the skin model

Average friction coefficient (COF) values, calculated as the average values for the whole range of the normal load (0.5-5 N), for skin and the skin model rubbed against Martindale fabric in dry, moist and wet conditions, are given in Table 5.1.

Table 5. 1. Average friction coefficients for human skin and the skin model rubbed against Martindale fabric in dry, moist and wet conditions.

Conditions	COF (human skin)	COF (skin model)
dry	0.47 ± 0.07	0.68 ± 0.30
moist	2.01 ± 0.41	1.57 ± 0.79
wet	2.27 ± 0.52	2.25 ± 0.89

Based on the results of in vivo measurements, it can be observed that the friction coefficient values increased when water was applied at the interface between the skin and the reference textile. This observation is consistent with the adhesion theory of human skin friction [11, 367]. As skin is exposed to water, it becomes softer and easily deformable, what causes a higher real contact area between the skin and counterfaces [11, 366] . The value of the tensile Young's modulus of the skin is strongly influenced by the presence of water, which is evident for the stratum corneum, the tensile Young's modulus value falling in the range of GPa for RH=30% and decreasing into the range of MPa when humidity increases to 100% RH [341, 342, 376-381]. In addition to decreased Young's modulus values, the plasticizing effect of water on human skin leads to smaller surface roughness values [119, 367, 382]. The role of the textile in the investigated system cannot be neglected. As cotton-based textiles frequently respond to the presence of water by becoming swollen and plasticized, the effect of water will be particularly strong in the skin/textile tribological system [383, 384]. Lower surface roughness values and easier deformation for both the skin and the textile contribute to an increased real contact area and thus increased friction coefficient [187].

Figure 5.4 shows the results of the friction measurements for human skin and the skin model against Martindale fabric as a function of the applied load under dry (Figure 5.4a), moist (Figure 5.4b) and wet (Figure 5.4c) conditions.
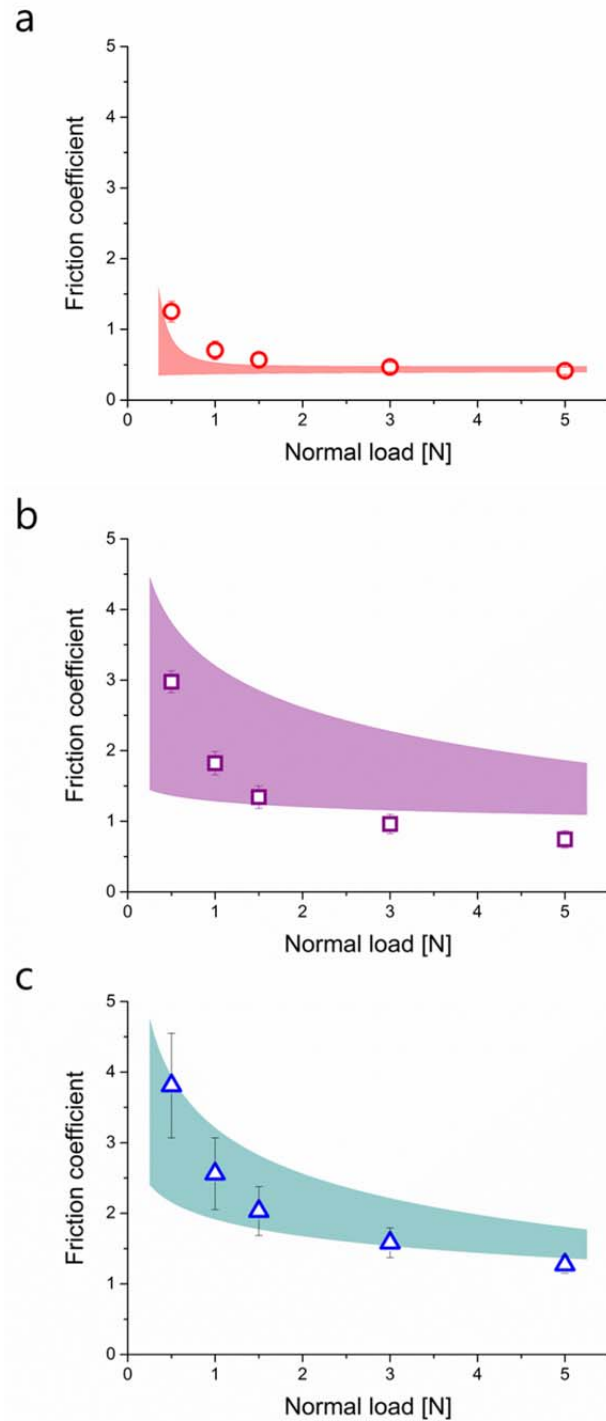
Figure 5. 4. COF of human skin (range of the values measured for the skin; shaded area) and the skin model (markers) against Martindale fabric as a function of the normal load in dry (a), moist (b) and wet (c) conditions.

As human skin is a very complex, anisotropic tissue with properties influenced by many factors, such as age, gender, ethnicity, health, lifestyle or physiological conditions, friction coefficient values of skin are given as a value range instead of the single values due to high standard deviations [4, 35]. As presented by Adams et al.,

2007 [11], the COF of dry skin, consistent with the conventional definition, can be understood as a constant value. Our results can in general support this statement, at normal loads below 1 N. The presence of water between skin and the counter-material changes the interfacial conditions significantly. The COF values not only increase, as mentioned above, but also depend on the normal load [11, 385-387]. The contact area of skin is not directly proportional to the normal load, but increases as a function of the normal load until it reaches a plateau. The COF decreases with increasing normal load, reaching a plateau for normal load values of 5 N and higher [388-390].

Another view of the characteristic frictional behaviour of human skin is presented in Figure 5.5. The average COF values for the entire range of applied load (0.5-5 N) are plotted as a function of the amount of water applied between skin and the textile and compared with corresponding COF values for the investigated gelatine-based composite material.
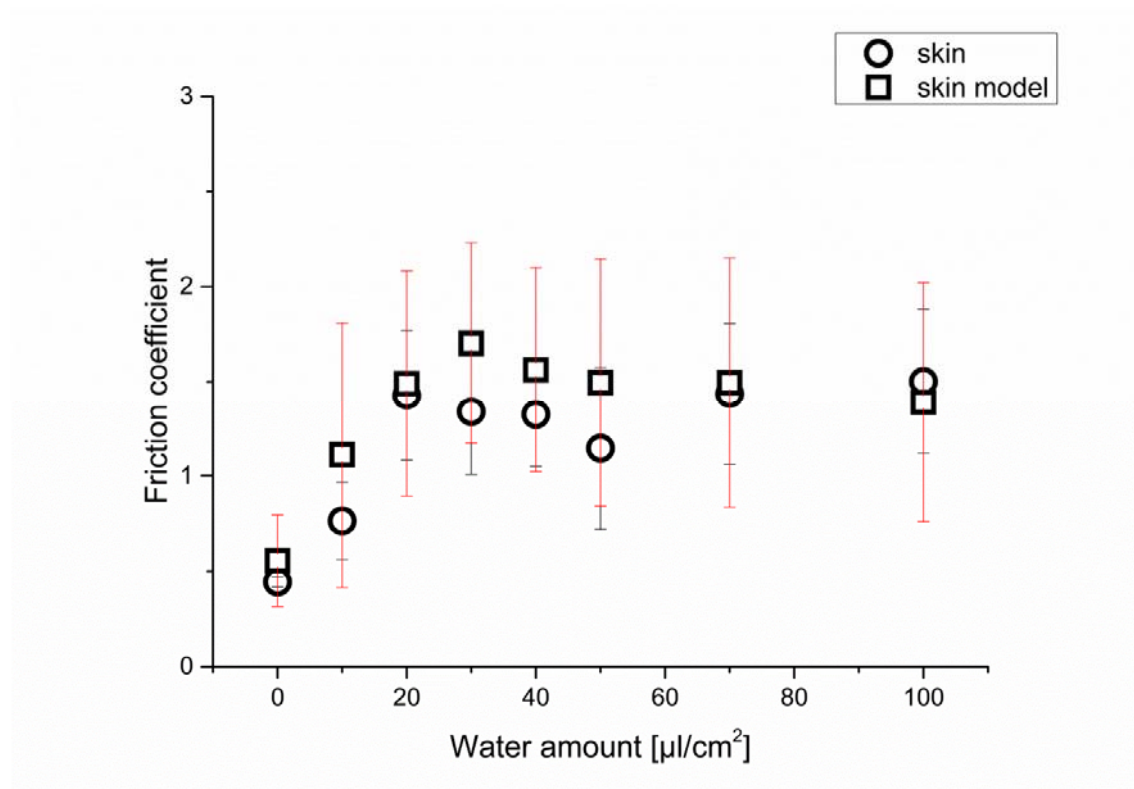
Figure 5. 5. COF of the gelatine-based skin model and of human skin against Martindale fabric as a function of the amount of applied water. Friction coefficient values are averaged for the entire range of normal load (0.5-5N).

As previously discussed by Derler et al., 2014 [158], the COF of human skin, due to the hydration and capillary adhesion, initially increases as a function of the

amount of water present in the system and decreases again after passing through a maximum value, as excess water creates lubricated regions leading to lower COF values.

The comparison between ranges of COF values obtained through in vivo measurements performed on skin of the volar forearm and COF values obtained for the gelatine-based composite material through in vitro measurements performed under similar conditions (Figure 5.4, Figure 5.5) suggests that the studied material is suitable as a physical skin model to simulate the frictional behaviour of human skin. The gelatine-based skin model is able to mimic the frictional behaviour of human skin against Martindale fabric over the entire range of investigated normal loads and in the presence of various amounts of water in the system. The COF of the skin model increases in the presence of a moderate amount of water (compared to dry conditions) and decreases as a function of the normal load, following the general trend and values reported for human skin (Fig. 4). When the influence of increasing amount of water on the COF values is investigated, the gelatine-based skin model mimics human skin according to general trends and COF values as well (Figure 5.5).

5.3.2. Tensile Young's modulus

The change in the Young's modulus of the gelatine-based skin model after up to 1 h water exposure was investigated (Figure 5.6).
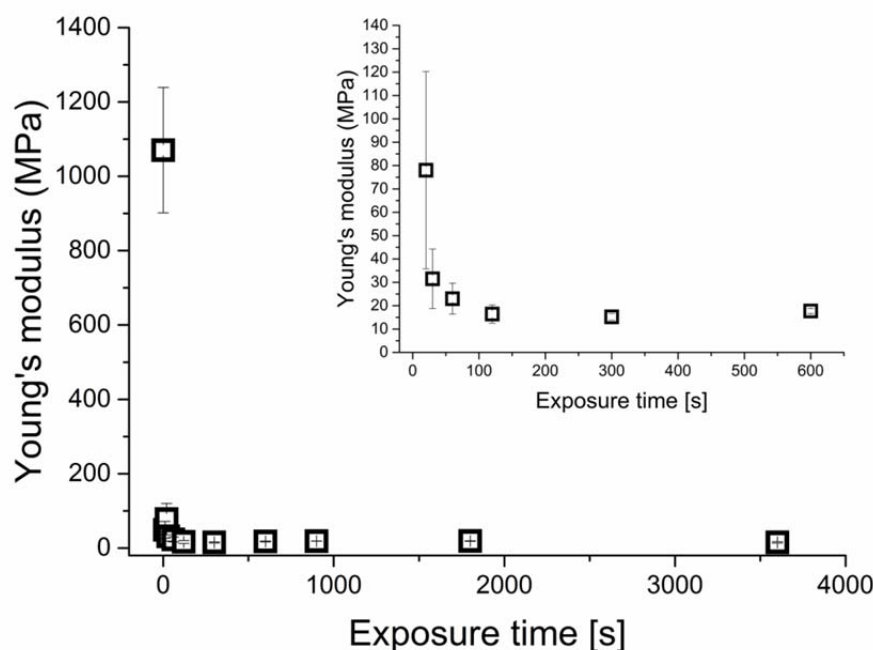
Figure 5. 6. Young's modulus of the gelatine-based skin model before and after water exposure. Inset: Influence of short water exposure (20-600s) on the Young's modulus value.

In analogy to human skin, hydration changed the stiffness of the investigated skin model significantly. The Young's modulus of the dry material reached a range between 0.9 and 1.2 GPa, whereas following brief immersion in water (20 s) it dropped to 78 ± 42 MPa and decreased further to 15.8 ± 1.8 MPa for longer (1 h) immersion time, showing a decrease by three orders of magnitude. After around 100 s exposure time there is no further clear influence of the increasing water content on Young's modulus values.

5.3.3. Structural and surface characterization

Figure 5.7 shows the cross-section micrographs of the gelatine-based skin model measured by means of SEM with 200 x (Fig. 7a), 500 x (Fig. 7b) and 1000 x (Fig. 7c) magnification. The knitted cotton, used as a substrate, is hydrophobic (WCA: $131 \pm 5°$) and hygroscopic, therefore it absorbs parts of the water-based gelatine solution during the process of bar coating. SEM pictures of a cross-section of the prepared skin model (Fig. 7) show that some cotton fibers are embedded in the gelatine coating. This leads to

a high degree of cohesion and therefore results in a robust and non-delaminating material.
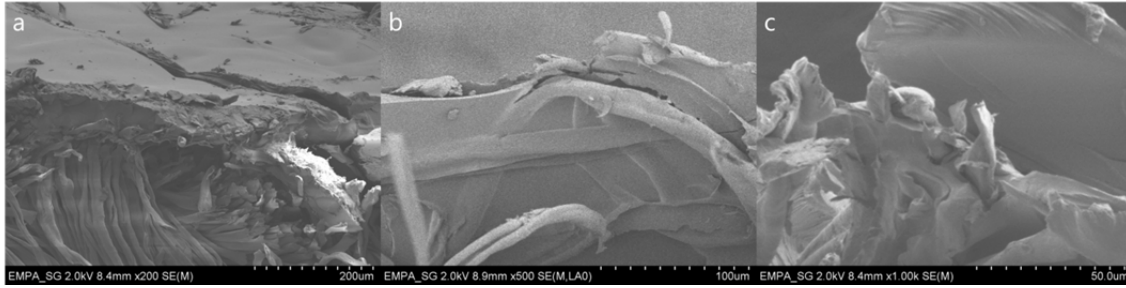
Figure 5. 7. SEM images of a cross-section of the gelatine-based physical skin model at 200 x (a), 500 x (b) and 1000 x (c) magnification.

Water acts as plasticizer in human skin, leading not only to a decrease in stiffness, but also to a smoother surface. It was shown that the surface roughness of human skin decreases significantly after exposure to water [19, 119, 367, 382]. In order to compare the specific water response of human skin with the gelatine-based physical skin model, a similar surface analysis was carried out.

The dry gelatine-based skin model is a stiff material with a ridged structure. When exposed to water, as both crosslinked gelatine and cotton absorb water, it became soft, flattened and smoothened, which was observed as a significant decrease in the measured surface roughness parameters; Sa decreases from 2.3 ± 0.3 μm for dry to 0.8 ± 0.1 μm for hydrated conditions (analogically, Sz decreased from 74.8 ± 13.5 μm to 8.6 ± 2.5 μm). Figure 5.8 shows three-dimensional microscopic pictures of the skin model before (Figure 5.8a) and after (Figure 5.8c) water exposure and the influence of the water exposure on the surface roughness parameters Sa (Figure 5.8b) and Sz (Figure 5.8d).
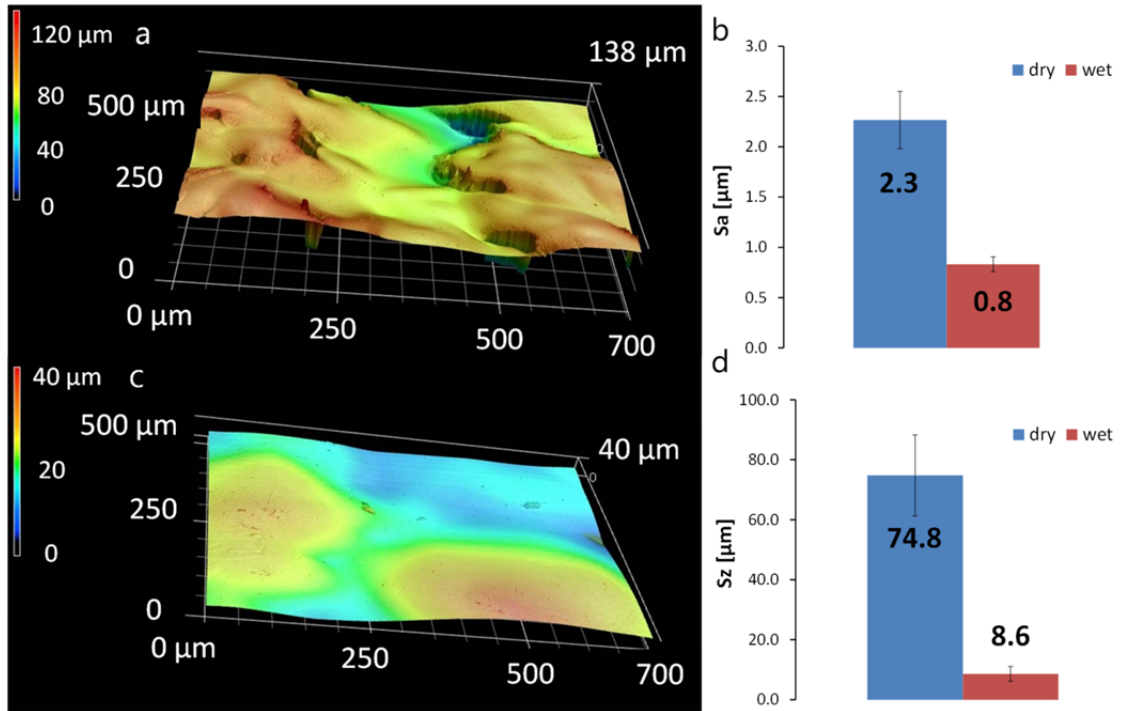
Figure 5. 8. Influence of water on the surface morphology of the gelatine-based physical skin model. Three-dimensional optical microscopic images of the gelatine-based physical skin model in the dry (a) and hydrated (c) state. Sa (b) and Sz (d) of the skin model in the dry and hydrated state.

Due to the water uptake and swelling, the *stratum corneum* thickness increases after prolonged water exposure [18, 19, 112]. Our recent study [19] showed that the maximum increase in the *stratum corneum* thickness was equal to 21% and was observed after 60 minutes of one-sided water exposure.

The maximum increase in thickness of the gelatine-based skin model was observed after 20 minutes of full immersion in water. Similarly to the *stratum corneum*, the thickness of the skin model also increased by 21% (from 0.66 ± 0.10 mm for dry skin model to 0.79 ± 0.11 after 20 minutes immersion in water). The measurement is statistically significant ($p=7\times10^{-6}$). Figure 5.9 shows the change in thickness of the examined skin model after 20 minutes of water immersion.
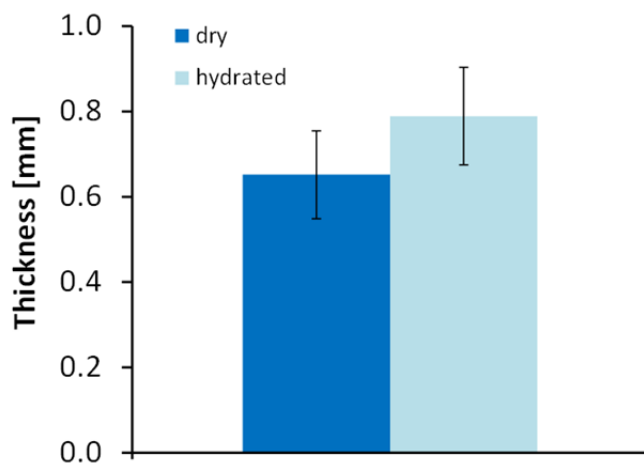
Figure 5. 9. Change in thickness of the gelatine-based skin model after 20-minutes immersion in water.

5.4. Conclusions

A new gelatine-based physical skin model was prepared and characterized regarding its frictional behaviour when in contact with a standard textile (Martindale fabric, worsted wool cloth) under both dry and hydrated conditions as well as with respect to the influence of water on the tensile Young's modulus and surface morphology. Friction coefficients for the skin model rubbed against Martindale fabric lie within the range of the values measured for human skin (volar forearm) under corresponding conditions over the entire range of investigated applied normal load. The gelatine-based skin model shows a similar behaviour to human skin when exposed to water, resulting in a significant decrease in the tensile Young's modulus value (from the GPa to the MPa range), surface smoothening and increase in thickness. All observed phenomena were in accordance with literature reports [19, 342, 366]. The new physical skin model mimics the general trends and values that are characteristic of the frictional behaviour, Young's modulus, change in thickness and surface morphology of human skin. Therefore, this material can potentially be used as a substitute for, or supplement to, conventional in vivo friction measurements, providing information concerning the interaction between human skin and examined objects.

Chapter 6

Conclusions and outlook

It has been demonstrated many times that nature usually provides scientists with the best possible solutions, the most effective mechanisms and an excellent choice of materials. No wonder, then, that recently, biomimetics is receiving more attention as an area of research. This thesis can be seen as a part of the biomimetic trend. In order to be able to develop a human skin model mimicking specific skin-water interactions and, consequently, the frictional behaviour of human skin under dry and hydrated conditions, skin properties had first to be characterised in detail, both based on a thorough literature review and laboratory experiments. Then, mimicking the most important characteristics of human skin, that are responsible for its friction properties, a water-responsive, gelatine-based human skin model was proposed.

Understanding the role of water in human skin functioning and properties

Skin properties, functioning and structure can be influenced by both internal (e.g. ethnicity, gender, age, skin type, anatomical site or lifestyle and diseases) and external (e.g. environmental conditions or contact with other materials and substances) factors.

In everyday life, skin remains in constant interaction with other objects and substances that are present in the environment. People wear clothes, use tools, kitchenware, sports equipment or medical items and also apply various cosmetics, such as moisturizers or sunscreen, as well as drugs, such as ointments, hormone or nicotine patches etc. Moreover, a variety of allergens, pathogens, microorganisms or chemical substances, which are present in the environment, can come into contact with human skin, having an influence on both its health and its performance.

Among all of these substances, one can distinguish water, which is practically always present on skin surface, either due to sweating or coming from the outside in the form of, e.g., air humidity or rain. A molecule of water, being one of the smallest molecules with a diameter of around 3 Ångström, can easily penetrate through first few μm of the skin.

Figure 6.1 demonstrates how water can penetrate human skin and what are the consequences of prolonged water exposure, and how the proposed gelatine-based skin model relates to this specific skin-water interaction.
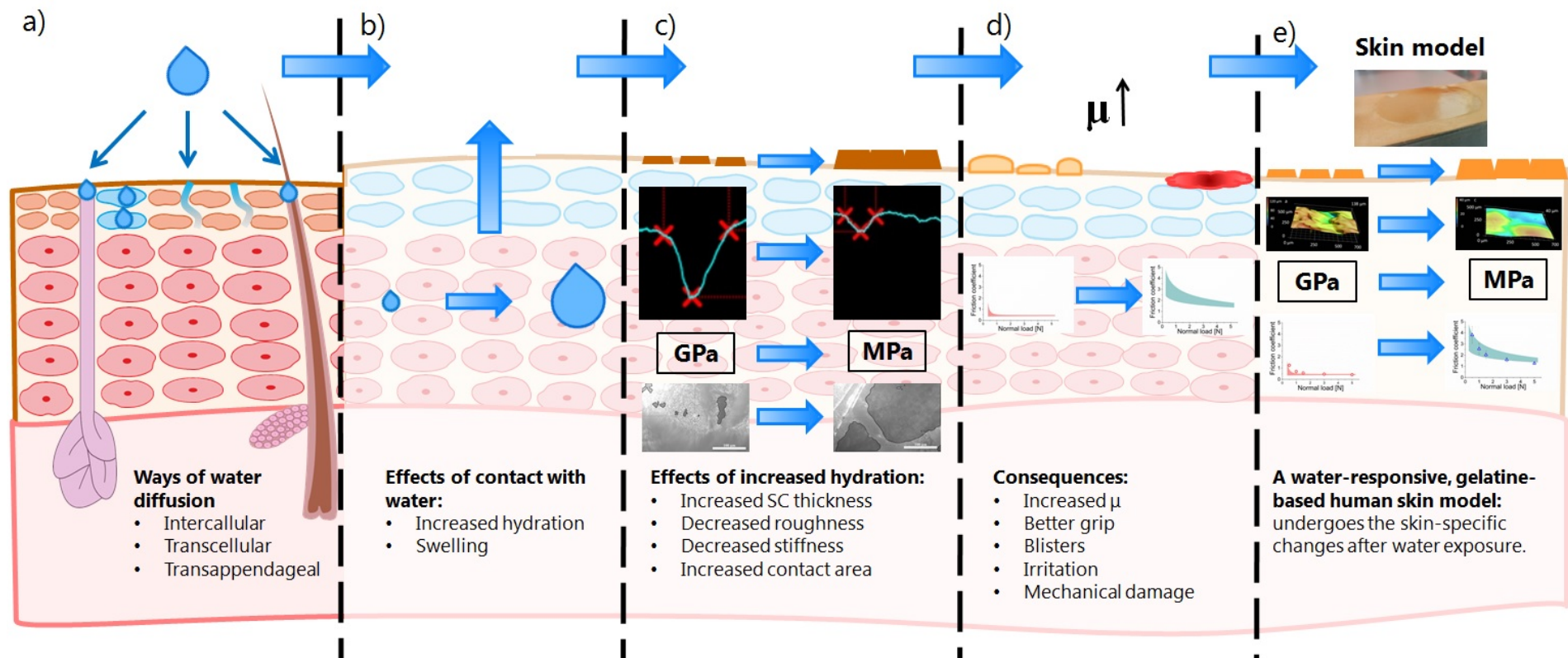
Figure 6. 1. Cause and effect chain for the example of skin water exposure: (a) three pathways of water diffusion, (b) effects of prolonged contact with water, (c) effects of increased skin hydration level, (d) friction-related consequences of increased skin hydration, (e) main characteristics of the gelatine-based human skin model. *μ-coefficient of friction.

There are three possible ways of passive diffusion within human skin (see Figure 6.1a): intercellular (between the cells of the *stratum corneum*), transcellular (with the involvement of keratinocytes) and transappendageal (through appendages, such as sweat and sebaceous glands and hair follicles). Even short water exposure, e.g. two minutes of contact with water during daily routine, can modify skin properties significantly.

Skin takes up water, which results in swelling and an increased hydration level of the *stratum corneum* (see Figure 6.1b).

Increase in skin hydration leads to a significant decrease in skin stiffness (the tensile Young's modulus of the *stratum corneum* drops from the GPa to the MPa range), a decrease in the surface roughness and an increase in *stratum corneum* thickness and real contact area with other objects (see Figure 6.1c).

As a result, the interaction between human skin and contacting objects may be clearly changed (see Figure 6.1d). Up to a certain limit, the presence of additional water on the skin surface leads to an increase in friction-coefficient values, which can lead to, for example, an improved grip when using tools but also skin irritation, blisters or mechanical damage after prolonged friction in the regime of high friction-coefficient values. The effect of water can be explicitly seen when skin interacts with other water-responsive materials, such as certain textiles. In this situation, water-dependent changes in human skin properties are escalated with analogous changes observed for the counter surface.

The main characteristics of the proposed gelatine-based, water-responsive human skin model are presented in Figure 6.1e. Following the specific interaction between human skin and water, the gelatine-based skin model responds to water, which leads to lower stiffness, a decrease in the surface roughness and an increase in thickness. All these modifications result in frictional behaviour that strongly depends on the presence of water and follows both the general friction trends as well as the friction-coefficient values observed for human skin.

Outlook: A tremendous number of possible interesting research areas related to the barrier properties of human skin can be listed, such as the effectiveness of topical moisturizers or the penetration abilities of various substances. Next to all these

subjects, penetration of steam through skin and related steam burns seems to be a very promising and still not very well-investigated direction. Skin permeability significantly increases at elevated temperatures. Steam burns are a common issue among workers exposed to high-humidity and high-temperature environments, such as firefighters. This type of injuries can also happen due to accidents, such as pipe ruptures. Investigation oriented to steam penetration and the mechanism of steam burns has already been performed in our group and there is an upcoming manuscript in preparation (Why does hot steam lead to severe skin burns?: in vitro Raman Spectroscopy of Porcine Skin after Steam Exposure, Zhai L, Adlhart C, Spano F, Dąbrowska AK, Li J and Rossi RM).

A water-responsive, gelatine-based human skin model

In the first step of development of a new physical skin model to mimic frictional behaviour of human skin, materials with similar properties to those of human skin were processed and examined as potential skin models. Although the proposed skin models, based on pebax, polyurethane, silicone or polyamide, could be used as skin models mimicking the frictional behaviour of human skin under some certain conditions, they did not respond to water in a similar way to skin. Preliminary results, supported by experiments demonstrating the influence of water on human skin properties and function, led to the idea of developing a gelatine-based, water-responsive skin model.

As a result, Chapter 5 presents a new bio-mimicking gelatine-based physical skin model. The proposed skin model simulates the frictional behaviour of human skin against a widely-used standard textile (Martindale worsted cloth) under both dry and wet conditions. It follows similar trends and friction-coefficient values to those observed for human skin over a broad range of applied normal load (0.5-5N) and amount of water at the interface (0-100 μl/cm^2). In addition, the tensile Young's modulus, thickness and surface roughness exhibit changes caused by prolonged contact with water, that are similar to those of human skin.

Outlook: There are various possibilities to modify properties of the gelatine-based human skin model in order to make it applicable for different tribosystems. After preliminary results, three parameters influencing the frictional behaviour of the final product were observed:

- *The choice of the substrate;*

- *The gel strength of the used gelatine;*

- *Variations in storage humidity.*

Knitted cotton was chosen to be the best substrate for the described application, in comparison to six other materials. The use of other substrates could allow developing a model mimicking the frictional behaviour of human skin under different conditions or rubbed against different counterfaces.

The same can be concluded about the choice of gelatine type. Bloom number 300 (high gel strength, average molecular mass of 50 000-100 000) provided the best results for this application.

Preliminary results performed by my master's student, Patryk Spera, have shown a significant influence of storage conditions on the frictional behaviour of the final product. Variation in storage humidity may modify the properties of the same material in order to make it applicable as a human skin model for different tribosystems.

In addition to optimizing the proposed gelatine-based skin model, more research on its friction mechanism and similarities to the friction mechanism of human skin would be an interesting research topic. Based on raw data from the tribometers, comparable data distribution can be seen both for human skin and gelatine-based skin model. This provides a hint that similar mechanisms of friction may be operating, but this requires further investigation. Figure 6.2 shows the data distribution for human skin (Figure 6.2a) and a skin model (Figure 6.2b) rubbed against a Martindale reference textile under dry, moist and wet conditions.
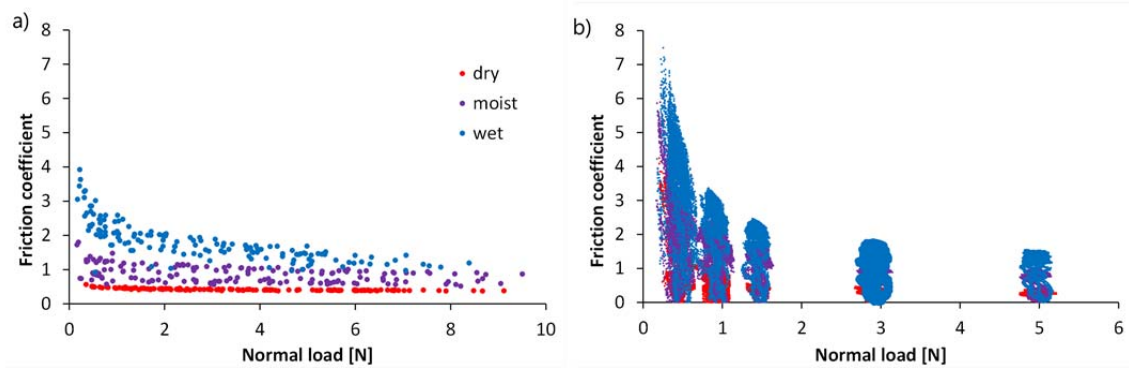
Figure 6. 2. Data distribution for human skin (a) and a skin model (b) rubbed against Martindale textile under dry, moist and wet conditions.

Mechanical damage of the samples after friction measurements seems to increase under hydrated conditions. This observation makes studies focused on the wear of the gelatine-based skin model as well as human skin as a function of conditions of friction measurements an interesting direction for further experiments. The appearance of the gelatine-based skin model before and after friction measurements under different conditions is presented in Figure 6.3.
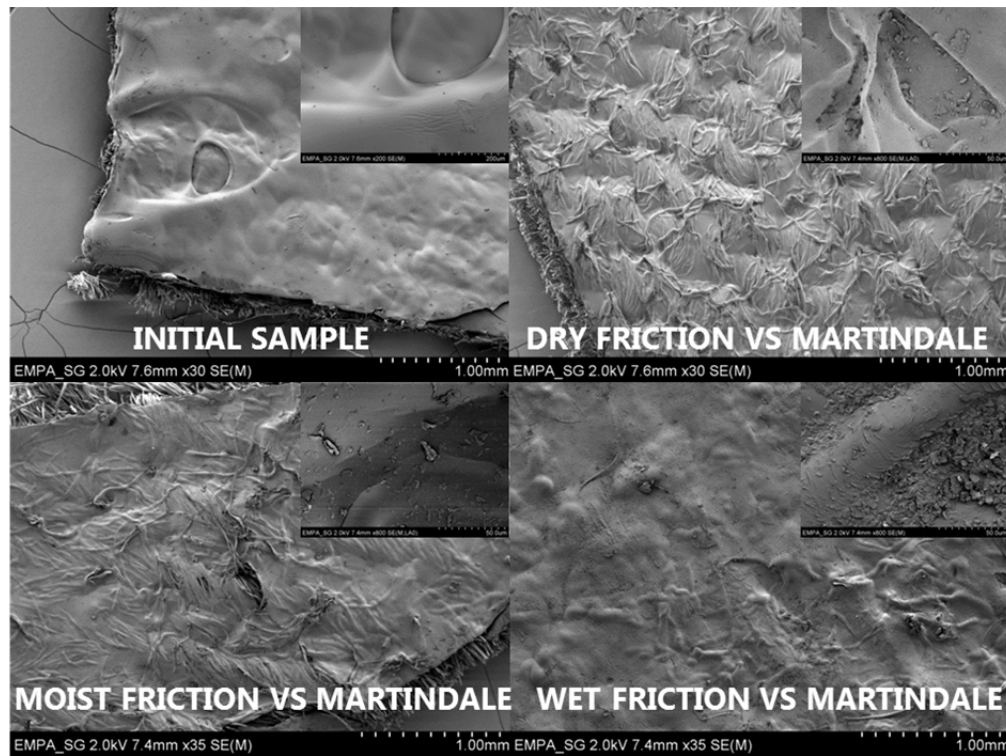
Figure 6. 3. Appearance of the gelatine-based skin model before and after friction measurements under different conditions.

Table of figures

Table of Tables

Abbreviations

Abbreviation	Definition
BMI	Body mass index, cf. 28, 35, 83, 103
COF	Coefficient of friction, cf. 107-110
DCM	Dichloromethane, cf. 66, 67
DMF	Dimethylformamide, cf. 67
EKSG	Ethics Committee of the Kanton St. Gallen, cf. 103
PBS	Phosphate buffered saline, cf. 102
PDMS	Polydimethylsiloxanes, cf. 53
PUR	Polyurethane, cf. 67, 72, 73
PVA	Poly(vinyl) alcohol, cf. 52
RH	Relative humidity, cf. 32, 87, 90, 91, 95, 104, 107
SAR	Specific absorption rate, cf. 53
SC	*Stratum corneum*, cf. 29, 30, 33-40, 80, 81, 85, 91, 94, 95, 97
SCA	Skin composition analyser, cf. 82, 85
SEM	Scanning electron microscopy, cf. 67, 74, 105, 111, 112
SSC	Superficial *stratum corneum*, cf. 33, 81, 86-88, 90, 94, 95
TEAB	Tetraethylammonium bromide, cf. 67
TEWL	Transepidermal water loss, cf. 30-35, 41
TFA	Textile friction analyser, cf. 71, 104
WCA	Water contact angle, cf. 111

Nomenclature

Symbol	Unit	Definition
A	[m^2]	Area of contact, cf. 44, 45
D	[s^{-1}]	Hydration rate coefficient, cf. 85, 87
E	[Pa]	Young's modulus, cf. 45
E*	[Pa]	Effective Young's modulus, cf. 45
F$_{def}$	[N]	Deformation component of friction force, cf. 43
f_{depth}		Depth-correction factor, cf. 82
F$_f$	[N]	Friction force, cf. 43, 44
F$_{int}$	[N]	Interfacial component of friction force, cf. 43, 44
F$_N$	[N]	Normal load, cf. 44, 45
hf	[%]	Hydration factor, cf. 85, 87
hl(t)	[%]	Skin hydration level at time t, cf. 85
hl_0	[%]	Skin hydration level at time $t = 0$ min. , cf. 85, 87
p	[Pa]	Contact pressure, cf. 44
P		Integrals of CH-vibration signals, cf. 84
R	[m]	The radius of the sphere, cf. 45
R'		Proportionality constant, cf. 84
W		Integrals of OH-vibration signals, cf. 84
α		Pressure coefficient, cf. 44
μ		Friction coefficient, cf. 44, 45
ν		Poisson's ratio, cf. 45
τ	[Pa]	Interfacial shear strength, cf. 44
τ$_0$	[Pa]	intrinsic interfacial shear strength, cf. 44, 45

Curriculum Vitae

Personal information

Date of birth: **11 March 1989**

Nationality: **Polish**

Address: **Burgstrasse 19**

9000 St. Gallen

Switzerland

Mobile phone: **+41 774 783 704**

Email: **dabrowska.agnieszka89@gmail.com**

Academic education

02.2014-12.2016	**ETH Zürich (Swiss Federal Institute of Technology in Zürich), Department of Materials** Doctor of Science Speciality: human skin characteristics and modelling Dowson Prize for the best paper and presentation: 43rd Leeds-Lyon Symposium on Tribology
02.2012–09.2013	**West Pomeranian University of Technology In Szczecin, Department of Mechanical Engineering and Mechatronics** Master of Science Major: Material Engineering; Speciality: Plastics Processing Medal for alumni with the highest average grade
10.2008–02.2012	**West Pomeranian University of Technology In Szczecin, Department of Chemical Technology and Engineering** Engineer Major: Chemical Technology; Speciality: Polymers Technology

Working experience

01.2014-06.2017   **Empa St. Gallen, Switzerland:** research assistant

- work on my own project: development and validation of the new physical skin model
- systematic publishing of papers and technical reports
- official presentations in front of an international audience
- full supervision of a master student

02-09.2013	**West Pomeranian University of Technology in Szczecin (ZUT), Poland:** research assistant

- work on the project „TransCond" no FP7-SME-2011 (conductive coatings with carbon nanofillers)
- responsible for an individual unit of a project (conductive epoxy coatings)

09.2011-06.2013	**Tutor** in chemistry, physics and mathematics (high school to college level)
09.2012	**BASF, Münster, Germany:** training; National Head Trainer (car painting)
06.2011	**DAAD and ZUT:** internship on tour
08.2011	**Furniture Factory AuraMeble in Kalisz Pomorski, Poland:** Internship
06.2008-02.2010	**Avon, Poland:** consultant and group leader

- responsible for the management and administration of a group of twenty direct-selling consultants

Extracullicular activities

03-12.2015	Empa PhD symposium: member of the organizing committee
	Responsible for the book of abstracts, invitation of the experts and evaluations for a scientific conference of over 100 participants
06.2013-	Youtube channel on healthy lifestyle: over 14 000 subscribers and over 3M views

Languages

- **Polish** – native
- **English** – working language (TOEFL score: 100 points)
- **German** – intermediate skills (currently learning)

Publications

2012 Composite lignin materials. Preparing and characteristics

Dąbrowska AK, Spychaj T and Wilpiszewska K

Przemysl Chemiczny. 2012;91(11):2219-2224.

2015 Materials used to simulate physical properties of human skin

Dąbrowska AK, Rotaru GM, Derler S, Spano F, Camenzind M, Annaheim S, Stämpfli R, Schmid M, Rossi RM

Skin Research and Technology. 2016;22:3-14.

2015 Flexible touch sensors based on nanocomposites embedding polymeric optical fibers for artificial skin applications

Spano F, Dąbrowska A, Quandt BM, Boesel L, Rossi RM, Massaro A, Lay-Ekuakille A

2015 IEEE 15th International Conference on Nanotechnology (IEEE-NANO), DOI: 10.1109/NANO.2015.7388870.

2016 In vivo confirmation of hydration-induced changes in human-skin thickness, roughness and interaction with the environment

Dąbrowska AK, Adlhart C, Spano F, Rotaru G-M, Derler S, Zhai L, Spencer ND, Rossi RM

Biointerphases. 2016;11:031015 (The manuscript was the most read paper of the month in October and November 2016, and the Editor's Pick of the Biointerphases Journal).

2016 A Water-Responsive, Gelatine-Based Human Skin Model

Dąbrowska A, Rotaru GM, Spano F, Affolter C, Fortunato G, Lehmann S, Derler S, Spencer ND, Rossi RM (submitted to Tribology International, awarded with the Dowson Prize).

2016 Relationship between skin functioning, barrier properties and body-dependent factors

Dąbrowska AK, Spano F, Rotaru GM, Derler S, Adlhart C, Spencer ND, Rossi RM (submitted to Colloids and Surfaces B: Biointerfaces)

2016 Why does hot steam lead to severe skin burns?: in vitro Raman Spectroscopy of Porcine Skin after Steam Exposure

Zhai L, Adlhart C, Spano F, Dąbrowska AK, Li J and Rossi RM (in preparation).

Oral talks

2016 In vivo evidence for the influence of hydration on human skin

Dąbrowska AK, Adlhart C, Spano F, Rotaru G-M, Derler S, Zhai L, Spencer ND, Rossi RM, 5th Swiss Raman Meeting, Wädenswil, Switzerland

2016 A Water-Responsive, Gelatine-Based Human Skin Model

Dąbrowska A, Rotaru GM, Spano F, Affolter C, Fortunato G, Lehmann S, Derler S, Spencer ND, Rossi RM, 43rd Leeds-Lyon Symposium on tribology, Leeds, England

Posters

2014 Friction of textiles against human skin and a skin model Dąbrowska AK, Spencer ND, Derler S, Fortunato G, Rossi RM, Rotaru GM, Swiss-Japanese Tribology Meeting, Zürich, Switzerland

2015 Bio-mimicking gelatine-based skin model

Dąbrowska AK, Spano F, Rotaru GM, Derler S, Spencer ND, Rossi RM, CCMX Summer School „Characterisation of Materials", Lausanne, Switzerland

Literature

[1] Baroli B. Penetration of nanoparticles and nanomaterials in the skin: fiction or reality? J Pharm Sci-Us. 2010;99:21-50.

[2] Elias PM. Stratum corneum defensive functions: An integrated view. J Invest Dermatol. 2005;125:183-200.

[3] Lee SH, Jeong SK, Ahn SK. An update of the defensive barrier function of skin. Yonsei Med J. 2006;47:293-306.

[4] Dabrowska AK, Rotaru GM, Derler S, Spano F, Camenzind M, Annaheim S, et al. Materials used to simulate physical properties of human skin. Skin Research and Technology. 2016;22:3-14.

[5] Derler S, Schrade U, Gerhardt LC. Tribology of human skin and mechanical skin equivalents in contact with textiles. Wear. 2007;263:1112-6.

[6] Gerhardt LC, Mattle N, Schrade GU, Spencer ND, Derler S. Study of skin-fabric interactions of relevance to decubitus: friction and contact-pressure measurements. Skin Research and Technology. 2008;14:77-88.

[7] Jung S, McCullough JL. Novel compounds for skin penetration enhancement. The UCI Undergraduate Research Journal. 2004;2:25-30.

[8] Firooz A, Sadr B, Babakoohi S, Sarraf-Yazdy M, Fanian F, Kazerouni-Timsar A, et al. Variation of Biophysical Parameters of the Skin with Age, Gender, and Body Region. Sci World J. 2012.

[9] Serup J, Jemec GB, Grove GL. Handbook of non-invasive methods and the skin: CRC press; 2006.

[10] Pailler-Mattei C, Bec S, Zahouani H. In vivo measurements of the elastic mechanical properties of human skin by indentation tests. Medical engineering & physics. 2008;30:599-606.

[11] Adams MJ, Briscoe BJ, Johnson SA. Friction and lubrication of human skin. Tribol Lett. 2007;26:239-53.

[12] Egawa M, Kajikawa T. Changes in the depth profile of water in the stratum corneum treated with water. Skin Research and Technology. 2009;15:242-9.

[13] Robinson S, Robinson AH. Chemical composition of sweat. Physiological reviews. 1954;34:202-20.

[14] Daroff RB, Fenichel GM, Jankovic J, Mazziotta JC. Neurology in clinical practice: Elsevier Health Sciences; 2012.

[15] Wilke K, Martin A, Terstegen L, Biel S. A short history of sweat gland biology. International journal of cosmetic science. 2007;29:169-79.

[16] Shapiro Y, Pandolf KB, Goldman RF. Predicting Sweat Loss Response to Exercise, Environment and Clothing. Eur J Appl Physiol O. 1982;48:83-96.

[17] Park A, Baddiel C. Rheology of stratum corneum. II. A physico-chemical investigation of factors influencing the water content of the corneum. J Soc Cosmet Chem. 1972;23:13-21.

[18] Crowther J, Sieg A, Blenkiron P, Marcott C, Matts P, Kaczvinsky J, et al. Measuring the effects of topical moisturizers on changes in stratum corneum thickness, water gradients and hydration in vivo. Brit J Dermatol. 2008;159:567-77.

[19] Dąbrowska AK, Adlhart C, Spano F, Rotaru G-M, Derler S, Zhai L, et al. In vivo confirmation of hydration-induced changes in human-skin thickness, roughness and interaction with the environment. Biointerphases. 2016;11:031015.

[20] Gerhardt LC, Strassle V, Lenz A, Spencer ND, Derler S. Influence of epidermal hydration on the friction of human skin against textiles. J R Soc Interface. 2008;5:1317-28.

[21] Dąbrowska AK, Rotaru GM, Spano F, Affolter Ch, Fortunato G, Lehmann S, Derler S, Spencer ND, Rossi RM. A Water-Responsive, Gelatine-Based Human Skin Model. submitted to Tribology International. 2016.

[22] Derler S, Rossi RM, Rotaru GM. Understanding the variation of friction coefficients of human skin as a function of skin hydration and interfacial water films. P I Mech Eng J-J Eng. 2015;229:285-93.

[23] Derler S, Rao A, Ballistreri P, Huber R, Scheel-Sailer A, Rossi RM. Medical textiles with low friction for decubitus prevention. Tribol Int. 2012;46:208-14.

[24] Pasumarty SM, Johnson SA, Watson SA, Adams MJ. Friction of the Human Finger Pad: Influence of Moisture, Occlusion and Velocity. Tribol Lett. 2011;44:117-37.

[25] Tomlinson SE, Lewis R, Liu X, Texier C, Carre MJ. Understanding the Friction Mechanisms Between the Human Finger and Flat Contacting Surfaces in Moist Conditions. Tribol Lett. 2011;41:283-94.

[26] Adelman S, Taylor CR, Heglund NC. Sweating on paws and palms: what is its function? American Journal of Physiology--Legacy Content. 1975;229:1400-2.

[27] Adams T, Hunter WS. Modification of Skin Mechanical Properties by Eccrine Sweat Gland Activity. J Appl Physiol. 1969;26:417-&.

[28] Skedung L, Arvidsson M, Chung JY, Stafford CM, Berglund B, Rutland MW. Feeling Small: Exploring the Tactile Perception Limits. Sci Rep-Uk. 2013;3.

[29] Gerhardt L-C. Tribology of human skin in contact with medical textiles for decubitus prevention: Diss., Eidgenössische Technische Hochschule ETH Zürich, Nr. 18027, 2008; 2008.

[30] Dąbrowska AK SF, Derler S, Adlhart C, Spencer ND and Rossi RM. Relationship between skin functioning, barrier properties and body-dependent factors. submitted to Colloids and Surfaces B Biointerfaces. 2016.

[31] Agache PG, Agache P, Humbert P. Measuring the skin: Springer Science & Business Media; 2004.

[32] Yudovsky D, Pilon L. Rapid and accurate estimation of blood saturation, melanin content, and epidermis thickness from spectral diffuse reflectance. Appl Optics. 2010;49:1707-19.

[33] Koehler MJ, Vogel T, Elsner P, Konig K, Buckle R, Kaatz M. In vivo measurement of the human epidermal thickness in different localizations by multiphoton laser tomography. Skin Research and Technology. 2010;16:259-64.

[34] Birgersson U, Birgersson E, Nicander I, Ollmar S. A methodology for extracting the electrical properties of human skin. Physiol Meas. 2013;34:723-36.

[35] Derler S, Gerhardt LC. Tribology of Skin: Review and Analysis of Experimental Results for the Friction Coefficient of Human Skin. Tribol Lett. 2012;45:1-27.

[36] Rauma M, Boman A, Johanson G. Predicting the absorption of chemical vapours. Adv Drug Deliver Rev. 2013;65:306-14.

[37] Asakura K, Nishiwaki Y, Milojevic A, Michikawa T, Kikuchi Y, Nakano M, et al. Lifestyle Factors and Visible Skin Aging in a Population of Japanese Elders. J Epidemiol. 2009;19:251-9.

[38] Desai P, Patlolla RR, Singh M. Interaction of nanoparticles and cell-penetrating peptides with skin for transdermal drug delivery. Mol Membr Biol. 2010;27:247-59.

[39] Prow TW, Grice JE, Lin LL, Faye R, Butler M, Becker W, et al. Nanoparticles and microparticles for skin drug delivery. Adv Drug Deliver Rev. 2011;63:470-91.

[40] Rawlings AV. Ethnic skin types: are there differences in skin structure and function? 1. International journal of cosmetic science. 2006;28:79-93.

[41] Taylor SC. Enhancing the care and treatment of skin color, Part 2: Understanding skin physiology. Cutis. 2005;76:302-6.

[42] Dayan N. Skin aging handbook. NewYork: William Andrew. 2008.

[43] Tschachler E, Morizot F. Ethnic differences in skin aging. Skin aging: Springer; 2006. p. 23-31.

[44] Diridollou S, de Rigal J, Querleux B, Leroy F, Barbosa VH. Comparative study of the hydration of the stratum corneum between four ethnic groups: influence of age. Int J Dermatol. 2007;46:11-4.

[45] Man MQ, Xin SJ, Song SP, Cho SY, Zhang XJ, Tu CX, et al. Variation of Skin Surface pH, Sebum Content and Stratum Corneum Hydration with Age and Gender in a Large Chinese Population. Skin Pharmacol Physi. 2009;22:190-9.

[46] Sugino K, Imokawa G, Maibach HI. Ethnic Difference of Stratum-Corneum Lipid in Relation to Stratum-Corneum Function. Clin Res. 1993;41:A488-A.

[47] Warrier A, Kligman A, Harper R. A comparison of black and white skin using. J Soc Cosmet Chem. 1996;47:229-40.

[48] Fotoh C, Elkhyat A, Mac S, Sainthillier JM, Humbert P. Cutaneous differences between Black, African or Caribbean Mixed-race and Caucasian women: biometrological approach of the hydrolipidic film. Skin Research and Technology. 2008;14:327-35.

[49] Gilchrest BA. Skin aging and photoaging: an overview. J Am Acad Dermatol. 1989;21:610-3.

[50] de Rigal J, Des Mazis I, Diridollou S, Querleux B, Yang G, Leroy F, et al. The effect of age on skin color and color heterogeneity in four ethnic groups. Skin Research and Technology. 2010;16:168-78.

[51] Sandby-Moller J, Poulsen T, Wulf HC. Epidermal thickness at different body sites: Relationship to age, gender, pigmentation, blood content, skin type and smoking habits. Acta Derm-Venereol. 2003;83:410-3.

[52] Weigand DA, Haygood C, Gaylor JR. Cell layer and density of Negro and Caucasian stratum corneum. J Invest Dermatol. 1974;62:563-8.

[53] Primavera G, Berardesca E. 11 Transepidermal Water l. oss and Racial Differences. Bioengineering of the skin: water and stratum corneum. 2005:129.

[54] Kompaore F, Tsuruta H. In vivo differences between Asian, black and white in the stratum corneum barrier function. Int Arch Occ Env Hea. 1993;65:S223-S5.

[55] Baker H. The skin as a barrier. Textbook of dermatology. 1986:355-65.

[56] Hillebrand G, Levine M, Miyamoto K. The age-dependent changes in skin condition in African Americans, Asian Indians, Caucasians, East Asians and Latinos. IFSCC Mag. 2001;4:2591266.

[57] Fluhr J, Pelosi A, Lazzerini S, Dikstein S, Berardesca E. Differences in corneocyte surface area in pre-and post-menopausal women. Skin Pharmacol Physi. 2001;14:10-6.

[58] Wilhelm K-P, Cua AB, Maibach HI. Skin aging: effect on transepidermal water loss, stratum corneum hydration, skin surface pH, and casual sebum content. Arch Dermatol. 1991;127:1806-9.

[59] Xin S-j, Liu Z-l, Shi Y-j, Feingold K, Elias P, Man M. Study on the sebum content and stratum corneum hydration in the normal Chinese population. JOURNAL OF CLINICAL DERMATOLOGY-NANJING-. 2007;36:131.

[60] Chilcott RP, Farrar R. Biophysical measurements of human forearm skin in vivo: effects of site, gender, chirality and time. Skin Research and Technology. 2000;6:64-9.

[61] Goh C, Chia S. Skin irritability to sodium lauryl sulphate—as measured by skin water vapour loss—by sex and race. Clin Exp Dermatol. 1988;13:16-9.

[62] Rogiers V, Houben E, De Paepe K. Transepidermal water loss measurements in dermato-cosmetic sciences. Bioengineering of the Skin: Water and the Stratum Corneum, ed. 2004;2:63-76.

[63] Rogiers V. Transepidermal water loss measurements in patch test assessment: the need for standardisation. 1995.

[64] Jacobi U, Gautier J, Sterry W, Lademann J. Gender-related differences in the physiology of the stratum corneum. Dermatology. 2005;211:312-7.

[65] Lammintausta K, Maibach H, Wilson D. Irritant reactivity in males and females. Contact Dermatitis. 1987;17:276-80.

[66] Aisen E, Shafran A, Gilhar A. Sebum and water content in the skin of aged immobilized patients. Acta Derm-Venereol. 1997;77:142-3.

[67] Wendling PA, Dell'Acqua G. Skin biophysical properties of a population living in Valais, Switzerland. Skin Research and Technology. 2003;9:331-8.

[68] Kim M-K, Choi S-Y, Byun H-J, Huh C-H, Park K-C, Patel RA, et al. Evaluation of gender difference in skin type and pH. J Dermatol Sci. 2006;41:153-6.

[69] Giltay E, Gooren L. Effects of sex steroid deprivation/administration on hair growth and skin sebum production in transsexual males and females. The Journal of Clinical Endocrinology & Metabolism. 2000;85:2913-21.

[70] Giacomoni PU, Mammone T, Teri M. Gender-linked differences in human skin. J Dermatol Sci. 2009;55:144-9.

[71] Ohman H, Vahlquist A. In vivo studies concerning a pH gradient in human stratum corneum and upper epidermis. Acta Derm-Venereol. 1994;74:375-9.

[72] Blank IH. Measurement of pH of the Skin Surface: II. pH of the Exposed Surfaces of Adults with No Apparent Skin Lesions. J Invest Dermatol. 1939;2:75-9.

[73] Ehlers C, Ivens UI, Moller ML, Senderovitz T, Serup J. Females have lower skin surface pH than men - A study on the influence of gender, forearm site variation, right/left difference and time of the day on the skin surface pH. Skin Research and Technology. 2001;7:90-4.

[74] Zlotogorski A. Distribution of skin surface pH on the forehead and cheek of adults. Arch Dermatol Res. 1987;279:398-401.

[75] Holbrook KA, Odland GF. Regional differences in the thickness (cell layers) of the human stratum corneum: an ultrastructural analysis. J Invest Dermatol. 1974;62:415-22.

[76] BLACK MM. A MODIFIED RADIOGRAPHIC METHOD FOR MEASURING SKIN THICKNESS*. Brit J Dermatol. 1969;81:661-6.

[77] Plewig G, Marples RR. Regional differences of cell sizes in the human stratum corneum. Part I. J Invest Dermatol. 1970;54:13-8.

[78] Humphries WT, Wildnauer RH. Thermomechanical Analysis of Stratum Corneum I. Technique. J Invest Dermatol. 1971;57:32-7.

[79] Huzaira M, Rius F, Rajadhyaksha M, Anderson RR, González S. Topographic variations in normal skin, as viewed by in vivo reflectance confocal microscopy. J Invest Dermatol. 2001;116:846-52.

[80] Lock-Andersen J, Therkildsen P, Olivarius F, Gniadecka M, Dahlstrem K, Poulsen T, et al. Epidermal thickness, skin pigmentation and constitutive photosensitivity. Photodermatology, photoimmunology & photomedicine. 1997;13:153-8.

[81] Whitton JT, Everall J. The thickness of the epidermis. Brit J Dermatol. 1973;89:467-76.

[82] Zhen YX, Suetake T, Tagami H. Number of cell layers of the stratum corneum in normal skin - relationship to the anatomical location on the body, age, sex and physical parameters. Arch Dermatol Res. 1999;291:555-9.

[83] Agache P, Humber P. Measuring the Skin: Non-invasive Investigation, Physiology, Normal Constants ed M Philipp. Berlin: Springer; 2004.

[84] Cua AB, Wilhelm KP, Maibach HI. Elastic Properties of Human Skin - Relation to Age, Sex and Anatomical Region. J Invest Dermatol. 1990;94:516-.

[85] Ishikawa T, Ishikawa O, Miyachi Y. Measurement of skin elastic properties with a new suction device (I): relationship to age, sex and the degree of obesity in normal individuals. The Journal of dermatology. 1995;22:713-7.

[86] Pedersen L, Hansen B, Jemec G. Mechanical properties of the skin: a comparison between two suction cup methods. Skin Research and Technology. 2003;9:111-5.

[87] Nakagawa N, Matsumoto M, Sakai S. In vivo measurement of the water content in the dermis by confocal Raman spectroscopy. Skin Research and Technology. 2010;16:137-41.

[88] Castelo-Branco C, Pons F, Gratacós E, Fortuny A, Vanrell JA, González-Merlo J. Relationship between skin collagen and bone changes during aging. Maturitas. 1994;18:199-206.

[89] Sumino H, Ichikawa S, Abe M, Endo Y, Ishikawa O, Kurabayashi M. Effects of aging, menopause, and hormone replacement therapy on forearm skin elasticity in women. Journal of the American Geriatrics Society. 2004;52:945-9.

[90] Ryu HS, Joo YH, Kim SO, Park KC, Youn SW. Influence of age and regional differences on skin elasticity as measured by the Cutometer (R). Skin Research and Technology. 2008;14:354-8.

[91] Leveque J, De Rigal J, Agache P, Monneur C. Influence of ageing on the in vivo extensibility of human skin at a low stress. Arch Dermatol Res. 1980;269:127-35.

[92] Lee M. Physical and structural age changes in human skin. The Anatomical Record. 1957;129:473-93.

[93] Holzmann H, Korting G, Kobelt D, Vogel H. Prüfung der mechanischen Eigenschaften von menschlicher Haut in Abhängigkeit von Alter und Geschlecht. Archiv für klinische und experimentelle Dermatologie. 1971;239:355-67.

[94] Yosipovitch G, Maayan-Metzger A, Merlob P, Sirota L. Skin barrier properties in different body areas in neonates. Pediatrics. 2000;106:105-8.

[95] Marrakchi S, Maibach HI. Biophysical parameters of skin: map of human face, regional, and age-related differences. Contact Dermatitis. 2007;57:28-34.

[96] Shriner D, Maibach H. Regional variation of nonimmunologic contact urticaria. Skin Pharmacol Physi. 1996;9:312-21.

[97] Mayes A, Murray P, Gunn D, Tomlin C, Catt S, Wen Y, et al. Ageing appearance in China: biophysical profile of facial skin and its relationship to perceived age. J Eur Acad Dermatol. 2010;24:341-8.

[98] Ohta H, Makita K, Kawashima T, Kinoshita S, Takenouchi M, Nozawa S. Relationship between dermato-physiological changes and hormonal status in pre-, peri-, and postmenopausal women. Maturitas. 1998;30:55-62.

[99] Inoue Y, Shibasaki M, Hirata K, Araki T. Relationship between skin blood flow and sweating rate, and age related regional differences. Eur J Appl Physiol O. 1998;79:17-23.

[100] Drinkwater B, Bedi J, Loucks A, Roche S, Horvath S. Sweating sensitivity and capacity of women in relation to age. J Appl Physiol. 1982;53:671-6.

[101] Choi EH, Man MQ, Xu P, Xin SJ, Liu ZL, Crumrine DA, et al. Stratum corneum acidification is impaired in moderately aged human and murine skin. J Invest Dermatol. 2007;127:2847-56.

[102] Lagarde JM, Rouvrais C, Black D. Topography and anisotropy of the skin surface with ageing. Skin Research and Technology. 2005;11:110-9.

[103] Jacobi U, Chen M, Frankowski G, Sinkgraven R, Hund M, Rzany B, et al. In vivo determination of skin surface topography using an optical 3D device. Skin Research and Technology. 2004;10:207-14.

[104] Boyer G, Laquieze L, Le Bot A, Laquieze S, Zahouani H. Dynamic indentation on human skin in vivo: ageing effects. Skin Research and Technology. 2009;15:55-67.

[105] Li L, Mac-Mary S, Marsaut D, Sainthillier JM, Nouveau S, Gharbi T, et al. Age-related changes in skin topography and microcirculation. Arch Dermatol Res. 2006;297:412-6.

[106] Akazaki S, Nakagawa H, Kazama H, Osanai O, Kawai M, Takema Y, et al. Age-related changes in skin wrinkles assessed by a novel three-dimensional morphometric analysis. Brit J Dermatol. 2002;147:689-95.

[107] Smith L. Histopathologic characteristics and ultrastructure of aging skin. Cutis. 1989;43:414-24.

[108] Johnston KJ, Oikarinen AI, Lowe NJ, Uitto J. Ultraviolet induced connective tissue changes in the skin: models for actinic damage and cutaneous aging. Models in dermatology. 1985;1:69-76.

[109] Fujimura T, Haketa K, Hotta M, Kitahara T. Loss of skin elasticity precedes to rapid increase of wrinkle levels. J Dermatol Sci. 2007;47:233-9.

[110] Dowson D. Bioengineering of the skin: skin surface imaging and analysis. CRC Press Boca Raton, RL; 1997.

[111] Derler S, Gerhardt LC, Lenz A, Bertaux E, Hadad M. Friction of human skin against smooth and rough glass as a function of the contact pressure. Tribol Int. 2009;42:1565-74.

[112] Egawa M, Hirao T, Takahashi M. In vivo estimation of stratum corneum thickness from water concentration profiles obtained with Raman spectroscopy. Acta Derm-Venereol. 2007;87:4-8.

[113] Caspers PJ, Lucassen GW, Carter EA, Bruining HA, Puppels GJ. In vivo confocal Raman microspectroscopy of the skin: Noninvasive determination of molecular concentration profiles. J Invest Dermatol. 2001;116:434-42.

[114] Zahouani H, Pailler-Mattei C, Sohm B, Vargiolu R, Cenizo V, Debret R. Characterization of the mechanical properties of a dermal equivalent compared with human skin in vivo by indentation and static friction tests. Skin Research and Technology. 2009;15:68-76.

[115] Agache PG, Monneur C, Leveque JL, Derigal J. Mechanical-Properties and Youngs Modulus of Human-Skin Invivo. Arch Dermatol Res. 1980;269:221-32.

[116] Diridollou S, Patat F, Gens F, Vaillant L, Black D, Lagarde JM, et al. In vivo model of the mechanical properties of the human skin under suction. Skin Research and Technology. 2000;6:214-21.

[117] Bohling A, Bielfeldt S, Himmelmann A, Keskin M, Wilhelm KP. Comparison of the stratum corneum thickness measured in vivo with confocal Raman spectroscopy and confocal reflectance microscopy. Skin Research and Technology. 2014;20:50-7.

[118] Schwindt DA, Wilhelm KP, Maibach HI. Water diffusion characteristics of human stratum corneum at different anatomical sites in vivo. J Invest Dermatol. 1998;111:385-9.

[119] Sato J, Yanai M, Hirao T, Denda M. Water content and thickness of the stratum corneum contribute to skin surface morphology. Arch Dermatol Res. 2000;292:412-7.

[120] Potts RO, Francoeur ML. The Influence of Stratum-Corneum Morphology on Water Permeability. J Invest Dermatol. 1991;96:495-9.

[121] Rougier A, Dupuis D, Lotte C, Roguet R, Wester RC, Maibach HI. Regional Variation in Percutaneous-Absorption in Man - Measurement by the Stripping Method. Arch Dermatol Res. 1986;278:465-9.

[122] Bronaugh RL, Hood HL, Kraeling ME, Yourick JJ. Determination of percutaneous absorption by in vitro techniques. Drugs and the pharmaceutical sciences. 1999;97:229-34.

[123] Gerhardt LC, Schiller A, Muller B, Spencer ND, Derler S. Fabrication, Characterisation and Tribological Investigation of Artificial Skin Surface Lipid Films. Tribol Lett. 2009;34:81-93.

[124] Egawa M, Oguri M, Kuwahara T, Takahashi M. Effect of exposure of human skin to a dry environment. Skin Research and Technology. 2002;8:212-8.

[125] Bhushan B, Wei GH, Haddad P. Friction and wear studies of human hair and skin. Wear. 2005;259:1012-21.

[126] Nachman M, Franklin S. Artificial Skin Model simulating dry and moist in vivo human skin friction and deformation behaviour. Tribol Int. 2016;97:431-9.

[127] Nicolaides N. Skin lipids. II. Lipid class composition of samples from various species and anatomical sites. Journal of the American Oil Chemists' Society. 1965;42:691-702.

[128] Gerhardt L-C. Tribology of human skin in contact with medical textiles for decubitus prevention. Zurich: ETH ZURICH; 2008.

[129] Conti A, Schiavi M, Seidenari S. Capacitance, transepidermal water loss and causal level of sebum in healthy subjects in relation to site, sex and age. International journal of cosmetic science. 1995;17:77-85.

[130] Fluhr J, Dickel H, Kuss O, Weyher I, Diepgen T, Berardesca E. Impact of anatomical location on barrier recovery, surface pH and stratum corneum hydration after acute barrier disruption. Brit J Dermatol. 2002;146:770-6.

[131] Taylor NA, Machado-Moreira CA. Regional variations in transepidermal water loss, eccrine sweat gland density, sweat secretion rates and electrolyte composition in resting and exercising humans. Extreme physiology & medicine. 2013;2:1.

[132] Sato K, Leidal R, Sato F. Morphology and development of an apoeccrine sweat gland in human axillae. American Journal of Physiology-Regulatory, Integrative and Comparative Physiology. 1987;252:R166-R80.

[133] Tagami H. Location-related differences in structure and function of the stratum corneum with special emphasis on those of the facial skin. International journal of cosmetic science. 2008;30:413-34.

[134] Gniadecka M, Gniadecki R, Serup J, Søndergaard J. Skin mechanical properties present adaptation to man's upright position. In vivo studies of young and aged individuals. Acta Derm-Venereol. 1994;74:188-90.

[135] Leveque J, Rasseneur L. Mechanical properties of stratum corneum: influence of water and lipids. The Physical Nature of the Skin: Springer; 1988. p. 155-61.

[136] Derler S, Preiswerk M, Rotaru GM, Kaiser JP, Rossi RM. Friction mechanisms and abrasion of the human finger pad in contact with rough surfaces. Tribol Int. 2015;89:119-27.

[137] Ramalho A, Silva CL, Pais AACC, Sousa JJS. In vivo friction study of human skin: Influence of moisturizers on different anatomical sites. Wear. 2007;263:1044-9.

[138] Darvin ME, Patzelt A, Knorr F, Blume-Peytavi U, Sterry W, Lademann J. One-year study on the variation of carotenoid antioxidant substances in living human skin: influence of dietary supplementation and stress factors. Journal of Biomedical Optics. 2008;13:044028--9.

[139] Akiba S, Shinkura R, Miyamoto K, Hillebrand G, Yamaguchi N, Ichihashi M. Influence of chronic UV exposure and lifestyle on facial skin photo-aging--results from a pilot study. J Epidemiol. 1999;9:136-42.

[140] Purba MB, Kouris-Blazos A, Wattanapenpaiboon N, Lukito W, Rothenberg EM, Steen BC, et al. Skin wrinkling: Can food make a difference? J Am Coll Nutr. 2001;20:71-80.

[141] Cosgrove MC, Franco OH, Granger SP, Murray PG, Mayes AE. Dietary nutrient intakes and skin-aging appearance among middle-aged American women. Am J Clin Nutr. 2007;86:1225-31.

[142] Mosely LH, Finseth F. Cigarette-Smoking - Impairment of Digital Blood-Flow and Wound-Healing in Hand. Hand. 1977;9:97-101.

[143] Wilson GR, Jones BM. The damaging effect of smoking on digital revascularisation: two further case reports. British journal of plastic surgery. 1984;37:613-4.

[144] Riefkohl R, Wolfe JA, Cox EB, McCarty Jr KS. Association between cutaneous occlusive vascular disease, cigarette smoking, and skin slough after rhytidectomy. Plastic and reconstructive surgery. 1986;77:592-5.

[145] Wulf HC, Sandby-Moller J, Kobayasi T, Gniadecki R. Skin aging and natural photoprotection. Micron. 2004;35:185-91.

[146] Löffler H, Aramaki J, Effendy I. The influence of body mass index on skin susceptibility to sodium lauryl sulphate. Skin Research and Technology. 2002;8:19-22.

[147] Yosipovitch G, DeVore A, Dawn A. Obesity and the skin: Skin physiology and skin manifestations of obesity. J Am Acad Dermatol. 2007;56:901-16.

[148] Fluhr JW, Elsner P, Berardesca E, Maibach HI. Bioengineering of the skin: water and the stratum corneum: CRC press; 2004.

[149] Verdier-Sévrain S, Bonte F. Skin hydration: a review on its molecular mechanisms. Journal of cosmetic dermatology. 2007;6:75-82.

[150] Dormenval V, Budtz-Jørgensen E, Mojon P, Bruyère A, Rapin C-H. Associations between malnutrition, poor general health and oral dryness in hospitalized elderly patients. Age and ageing. 1998;27:123-8.

[151] Silva CL, Topgaard D, Kocherbitov V, Sousa J, Pais AA, Sparr E. Stratum corneum hydration: phase transformations and mobility in stratum corneum, extracted lipids and isolated corneocytes. Biochimica et Biophysica Acta (BBA)-Biomembranes. 2007;1768:2647-59.

[152] Imokawa G, Abe A, Jin K, Higaki Y, Kawashima M, Hidano A. Decreased level of ceramides in stratum corneum of atopic dermatitis: an etiologic factor in atopic dry skin? J Invest Dermatol. 1991;96:523-6.

[153] Tupker R, Pinnagoda J, Coenraads P, Nater J. Susceptibility to irritants: role of barrier function, skin dryness and history of atopic dermatitis. Brit J Dermatol. 1990;123:199-205.

[154] Zulewski H, Müller B, Exer P, Miserez AR, Staub J-J. Estimation of Tissue Hypothyroidism by a New Clinical Score: Evaluation of Patients with Various Grades of Hypothyroidism and Controls 1. The Journal of Clinical Endocrinology & Metabolism. 1997;82:771-6.

[155] Cooper DS, HALPERN R, WOOD LC, LEVIN AA, Ridgway EC. L-thyroxine therapy in subclinical hypothyroidism: a double-blind, placebo-controlled trial. Annals of internal medicine. 1984;101:18-24.

[156] Egawa M, Tagami H. Comparison of the depth profiles of water and water-binding substances in the stratum corneum determined in vivo by Raman spectroscopy between the cheek and volar forearm skin: effects of age, seasonal changes and artificial forced hydration. Brit J Dermatol. 2008;158:251-60.

[157] Caspers P, Lucassen G, Bruining H, Puppels G. Automated depth-scanning confocal Raman microspectrometer for rapid in vivo determination of water concentration profiles in human skin. J Raman Spectrosc. 2000;31:813-8.

[158] Derler S, Rossi R, Rotaru G. Understanding the variation of friction coefficients of human skin as a function of skin hydration and interfacial water films. Proceedings of the Institution of Mechanical Engineers, Part J: Journal of Engineering Tribology. 2015;229:285-93.

[159] Scharf JE, Johnson GT, Harbison SC, McCluskey JD, Harbison RD. Dermal absorption of a dilute aqueous solution of malathion. Journal of Emergencies, Trauma and Shock. 2008;1:70.

[160] Barrett CW. Skin Penetration. J Soc Cosmet Chem. 1969;20:487-&.

[161] Elias PM. Epidermal Lipids, Barrier Function, and Desquamation. J Invest Dermatol. 1983;80:S44-S9.

[162] Bos JD, Meinardi MMHM. The 500 Dalton rule for the skin penetration of chemical compounds and drugs. Exp Dermatol. 2000;9:165-9.

[163] Williams AC, Barry BW. Penetration enhancers. Adv Drug Deliver Rev. 2004;56:603-18.

[164] Vogt A, Combadiere B, Hadam S, Stieler KM, Lademann J, Schaefer H, et al. 40 nm, but not 750 or 1,500 nm, Nanoparticles Enter Epidermal CD1a+ Cells after Transcutaneous Application on Human Skin. J Invest Dermatol. 2006;126:1316-22.

[165] Kitson N, Thewalt JL. Hypothesis: The epidermal permeability barrier is a porous medium. Acta Derm-Venereol. 2000:12-5.

[166] Elias PM, Menon GK. Structural and Lipid Biochemical Correlates of the Epidermal Permeability Barrier. Adv Lipid Res. 1991;24:1-26.

[167] van der Merwe D, Brooks JD, Gehring R, Baynes RE, Monteiro-Riviere NA, Riviere JE. A physiologically based pharmacokinetic model of organophosphate dermal absorption. Toxicol Sci. 2006;89:188-204.

[168] Hadgraft J. Modulation of the barrier function of the skin. Skin Pharmacol Physi. 2001;14:72-81.

[169] Albery W, HADGRAFT J. Percutaneous absorption: in vivo experiments. J Pharm Pharmacol. 1979;31:140-7.

[170] Potts RO, Francoeur ML. The influence of stratum corneum morphology on water permeability. J Invest Dermatol. 1991;96:495-9.

[171] Flynn GL, Banker G, Rhodes C. Cutaneous and transdermal delivery-processes and systems of delivery. Modern pharmaceutics, 4th ed, Banker GS, Rhodes Ch T, Eds. 2002:293-364.

[172] Mccarley KD, Bunge AL. Pharmacokinetic models of dermal absorption. J Pharm Sci-Us. 2001;90:1699-719.

[173] EFSA E. Panel on Plant Protection Products and their Residues (PPR). Guidance on Dermal Absorption. 2012;10.

[174] Vinson L, Singer E, Koehler W, Lehman M, Masurat T. The nature of the epidermal barrier and some factors influencing skin permeability. Toxicology and Applied Pharmacology. 1965;7:7-19.

[175] Loth H. Vehicular influence on transdermal drug penetration. Int J Pharm. 1991;68:1-10.

[176] Larese FF, D'Agostin F, Crosera M, Adami G, Renzi N, Bovenzi M, et al. Human skin penetration of silver nanoparticles through intact and damaged skin. Toxicology. 2009;255:33-7.

[177] van den Bergh BAI, Vroom J, Gerritsen H, Junginger HE, Bouwstra JA. Interactions of elastic and rigid vesicles with human skin in vitro: electron microscopy and two-photon excitation microscopy. Bba-Biomembranes. 1999;1461:155-73.

[178] Abraham MH, Chadha HS, Mitchell RC. The factors that influence skin penetration of solutes. J Pharm Pharmacol. 1995;47:8-16.

[179] Prausnitz MR, Bose VG, Langer R, Weaver JC. Electroporation of Mammalian Skin - a Mechanism to Enhance Transdermal Drug-Delivery. P Natl Acad Sci USA. 1993;90:10504-8.

[180] Schmook FP, Meingassner JG, Billich A. Comparison of human skin or epidermis models with human and animal skin in in-vitro percutaneous absorption. Int J Pharm. 2001;215:51-6.

[181] Skedung L, Danerlov K, Olofsson U, Aikala M, Niemi K, Kettle J, et al. Finger Friction Measurements on Coated and Uncoated Printing Papers. Tribol Lett. 2010;37:389-99.

[182] Skedung L, Danerlov K, Olofsson U, Johannesson CM, Aikala M, Kettle J, et al. Tactile perception: Finger friction, surface roughness and perceived coarseness. Tribol Int. 2011;44:505-12.

[183] van Kuilenburg J, Masen MA, van der Heide E. A Mechanistic Approach to Predicting the Friction Behaviour of Human Skin. Proceedings of the Asme/Stle International Joint Tribology Conference, Ijtc 2012. 2013:45-7.

[184] Tang W, Gel SR, Zhu H, Cao XC, Li N. The influence of normal load and sliding speed on frictional properties of skin. J Bionic Eng. 2008;5:33-8.

[185] Dowson D. Thin-Films in Tribology. Tribology S. 1993;25:3-12.

[186] Greenwoo.Ja, Williams.Jb. Contact of Nominally Flat Surfaces. Proc R Soc Lon Ser-A. 1966;295:300-&.

[187] Asserin J, Zahouani H, Humbert P, Couturaud V, Mougin D. Measurement of the friction coefficient of the human skin in vivo - Quantification of the cutaneous smoothness. Colloid Surface B. 2000;19:1-12.

[188] Elleuch K, Elleuch R, Zahouani H. Comparison of elastic and tactile behavior of human skin and elastomeric materials through tribological tests. Polym Eng Sci. 2006;46:1715-20.

[189] Sivamani RK, Wu GC, Gitis NV, Maibach HI. Tribological testing of skin products: gender, age, and ethnicity on the volar forearm. Skin Research and Technology. 2003;9:299-305.

[190] Nakajima K, Narasaka H. Evaluation of skin surface associated with morphology and coefficient of friction. International journal of cosmetic science. 1993;15:135-51.

[191] Gupta A, Haldar B, Bhattacharya M. A simple device for measuring skin friction. Indian Journal of Dermatology. 1995;40:116.

[192] Gerrard W. Friction and other measurements of the skin surface. Bioengineering and the skin. 1987;3:123-39.

[193] Batt M, Davis W, Fairhurst E, Gerrard W, Ridge B. Changes in the physical properties of the stratum corneum following treatment with glycerol. J Soc Cosmet Chem. 1988;39:367-81.

[194] Adams MJ, Johnson SA, Lefevre P, Levesque V, Hayward V, Andre T, et al. Finger pad friction and its role in grip and touch. J R Soc Interface. 2013;10.

[195] Derler S, Rotaru GM. Stick-slip phenomena in the friction of human skin. Wear. 2013;301:324-9.

[196] Berman AD, Ducker WA, Israelachvili JN. Origin and characterization of different stick-slip friction mechanisms. Langmuir. 1996;12:4559-63.

[197] Darden MA, Schwartz CJ. Investigation of skin tribology and its effects on the tactile attributes of polymer fabrics. Wear. 2009;267:1289-94.

[198] Bond JR, Barry BW. Hairless Mouse Skin Is Limited as a Model for Assessing the Effects of Penetration Enhancers in Human-Skin. Journal of Investigative Dermatology. 1988;90:810-3.

[199] Shergold OA, Fleck NA, Radford D. The uniaxial stress versus strain response of pig skin and silicone rubber at low and high strain rates. Int J Impact Eng. 2006;32:1384-402.

[200] Bush MA, Miller RG, Bush PJ, Dorion RBJ. Biomechanical Factors in Human Dermal Bitemarks in a Cadaver Model. J Forensic Sci. 2009;54:167-76.

[201] Maiden N. Historical overview of wound ballistics research. Forensic Sci Med Pat. 2009;5:85-9.

[202] Shevchenko RV, James SL, James SE. A review of tissue-engineered skin bioconstructs available for skin reconstruction. J R Soc Interface. 2010;7:229-58.

[203] Elliott NT, Yuan F. A review of three-dimensional in vitro tissue models for drug discovery and transport studies. J Pharm Sci-Us. 2011;100:59-74.

[204] Hull EL, Nichols MG, Foster TH. Quantitative broadband near-infrared spectroscopy of tissue-simulating phantoms containing erythrocytes. Physics in Medicine and Biology. 1998;43:3381-404.

[205] Pravdin AB, Utz SR, Kochubey VI. Physical modeling of human skin optical properties using milk and erythrocytes mixtures. Optical Biopsies, Proceedings Of. 1995;2627:221-6.

[206] Madsen SJ, Patterson MS, Wilson BC. The Use of India Ink as an Optical Absorber in Tissue-Simulating Phantoms. Physics in Medicine and Biology. 1992;37:985-93.

[207] Flock ST, Jacques SL, Wilson BC, Star WM, Vangemert MJC. Optical-Properties of Intralipid - a Phantom Medium for Light-Propagation Studies. Lasers in Surgery and Medicine. 1992;12:510-9.

[208] Lualdi M, Colombo A, Farina B, Tomatis S, Marchesini R. A phantom with tissue-like optical properties in the visible and near infrared for use in photomedicine. Lasers in Surgery and Medicine. 2001;28:237-43.

[209] Kozlov PV, Burdygina GI. The Structure and Properties of Solid Gelatin and the Principles of Their Modification. Polymer. 1983;24:651-66.

[210] Glicksman M. Gum technology in the food industry. 1969.

[211] Gomez-Guillen MC, Gimenez B, Lopez-Caballero ME, Montero MP. Functional and bioactive properties of collagen and gelatin from alternative sources: A review. Food Hydrocolloid. 2011;25:1813-27.

[212] Jussila J. Preparing ballistic gelatine - review and proposal for a standard method. Forensic Science International. 2004;141:91-8.

[213] Bir CA, Resslar M, Stewart S. Skin penetration surrogate for the evaluation of less lethal kinetic energy munitions. Forensic Science International. 2012;220:126-9.

[214] Jussila J, Leppaniemi A, Paronen M, Kulomaki E. Ballistic skin simulant. Forensic Sci Int. 2005;150:63-71.

[215] Perdekamp MG, Pollak S, Thierauf A, Strassburger E, Hunzinger M, Vennemann B. Experimental simulation of reentry shots using a skin-gelatine composite model. Int J Legal Med. 2009;123:419-25.

[216] Hall TJ, Bilgen M, Insana MF, Krouskop TA. Phantom materials for elastography. Ieee T Ultrason Ferr. 1997;44:1355-65.

[217] Jermann R, Toumiat M, Imfeld D. Development of an in vitro efficacy test for self-tanning formulations. International journal of cosmetic science. 2002;24:35-42.

[218] Chen S, Bhushan B. Nanomechanical and nanotribological characterization of two synthetic skins with and without skin cream treatment using atomic force microscopy. J Colloid Interf Sci. 2013;398:247-54.

[219] Renvoise J, Burlot D, Marin G, Derail C. Adherence performances of pressure sensitive adhesives on a model viscoelastic synthetic film: A tool for the understanding of adhesion on the human skin. International Journal of Pharmaceutics. 2009;368:83-8.

[220] Bait N, Grassl B, Derail C, Benaboura A. Hydrogel nanocomposites as pressure-sensitive adhesives for skin-contact applications. Soft Matter. 2011;7:2025-32.

[221] Cubeddu R, Pifferi A, Taroni P, Torricelli A, Valentini G. A solid tissue phantom for photon migration studies. Physics in Medicine and Biology. 1997;42:1971-9.

[222] Chahat N, Zhadobov M, Sauleau R, Alekseev SI. New Method for Determining Dielectric Properties of Skin and Phantoms at Millimeter Waves Based on Heating Kinetics. Ieee T Microw Theory. 2012;60:827-32.

[223] Nebuya S, Noshiro M, Brown BH, Smallwood RH, Milnes P. Detection of emboli in vessels using electrical impedance measurements - phantom and electrodes. Physiol Meas. 2005;26:S111-S8.

[224] Zell K, Sperl JI, Vogel MW, Niessner R, Haisch C. Acoustical properties of selected tissue phantom materials for ultrasound imaging. Physics in Medicine and Biology. 2007;52:N475-N84.

[225] Bante-Guerra J, Macias JD, Caballero-Aguilar L, Vales-Pinzon C, Alvarado-Gil JJ. Infrared thermography analysis of thermal diffusion induced by RF magnetic field on agar phantoms loaded with magnetic nanoparticles. Energy-Based Treatment of Tissue and Assessment Vii. 2013;8584.

[226] Nishidate I, Maeda T, Niizeki K, Aizu Y. Estimation of Melanin and Hemoglobin Using Spectral Reflectance Images Reconstructed from a Digital RGB Image by the Wiener Estimation Method. Sensors-Basel. 2013;13:7902-15.

[227] Nishidate I, Sasaoka K, Yuasa T, Niizeki K, Maeda T, Aizu Y. Visualizing of skin chromophore concentrations by use of RGB images. Opt Lett. 2008;33:2263-5.

[228] Cho J, Byun H, Lee S, Kim JK. Temperature distribution in deep tissue phantom during laser irradiation at 1,064 nm measured by thermocouples and thermal imaging technique. J Visual-Japan. 2011;14:265-72.

[229] Demura K, Morikawa S, Murakami K, Sato K, Shiomi H, Naka S, et al. An easy-to-use microwave hyperthermia system combined with spatially resolved MR temperature maps: Phantom and animal studies. Journal of Surgical Research. 2006;135:179-86.

[230] Jindra NM, Figueroa MA, Chavey LJ, Zohner JJ, Rockwell BA. An alternative method of evaluating 1540nm exposure laser damage using an optical tissue phantom - art. no. 60840D. Optical Interactions with Tissue and Cells XVII. 2006;6084:D840-D.

[231] Baker MI, Walsh SP, Schwartz Z, Boyan BD. A review of polyvinyl alcohol and its uses in cartilage and orthopedic applications. Journal of Biomedical Materials Research Part B: Applied Biomaterials. 2012;100:1451-7.

[232] Chu KC, Rutt BK. Polyvinyl alcohol cryogel: An ideal phantom material for MR studies of arterial flow and elasticity. Magnet Reson Med. 1997;37:314-9.

[233] Iravani A, Mueller J, Yousefi AM. Producing homogeneous cryogel phantoms for medical imaging: a finite-element approach. J Biomat Sci-Polym E. 2014;25:181-202.

[234] Lamouche G, Kennedy BF, Kennedy KM, Bisaillon CE, Curatolo A, Campbell G, et al. Review of tissue simulating phantoms with controllable optical, mechanical and structural properties for use in optical coherence tomography. Biomed Opt Express. 2012;3:1381-98.

[235] Price BD, Gibson AP, Tan LT, Royle GJ. An elastically compressible phantom material with mechanical and x-ray attenuation properties equivalent to breast tissue. Physics in Medicine and Biology. 2010;55:1177-88.

[236] Mazzoli A, Munaretto R, Scalise L. Preliminary results on the use of a noninvasive instrument for the evaluation of the depth of pigmented skin lesions: numerical simulations and experimental measurements. Laser Med Sci. 2010;25:403-10.

[237] Steenbergen W, de Mul F. Application of a novel laser Doppler tester including a sustainable tissue phantom. Optical Diagnostics of Biological Fluids Iii, Proceedings Of. 1998;3252:14-25.

[238] Kirkpatrick SJ, Wang RK, Duncan DD, Kulesz-Martin M, Lee K. Imaging the mechanical stiffness of skin lesions by in vivo acousto-optical elastography. Opt Express. 2006;14:9770-9.

[239] Manohar S, Kharine A, van Hespen JCG, Steenbergen W, de Mul FFM, van Leeuwen TG. Photoacoustic imaging of inhomogeneities embedded in breast tissue phantoms. Biomedical Optoacoustics Iv. 2003;4960:64-75.

[240] Pogue BW, Patterson MS. Review of tissue simulating phantoms for optical spectroscopy, imaging and dosimetry. J Biomed Opt. 2006;11.

[241] Kim DH, Lu NS, Ma R, Kim YS, Kim RH, Wang SD, et al. Epidermal Electronics. Science. 2011;333:838-43.

[242] Aleman J, Chadwick AV, He J, Hess M, Horie K, Jones RG, et al. Definitions of terms relating to the structure and processing of sols, gels, networks, and inorganic-organic hybrid materials (IUPAC Recommendations 2007). Pure Appl Chem. 2007;79:1801-27.

[243] AbdouSabet S, Puydak RC, Rader CP. Dynamically vulcanized thermoplastic elastomers. Rubber Chem Technol. 1996;69:476-94.

[244] Jachowicz J, McMullen R, Prettypaul D. Indentometric analysis of in vivo skin and comparison with artificial skin models. Skin Research and Technology. 2007;13:299-309.

[245] Levier RR, Harrison MC, Cook RR, Lane TH. What Is Silicone. Plastic and reconstructive surgery. 1993;92:163-7.

[246] Colas A, Curtis J. Silicone biomaterials: history and chemistry. Biomaterials science: an introduction to materials in medicine. 2004:80-5.

[247] Gabriel C. Tissue equivalent material for hand phantoms. Physics in Medicine and Biology. 2007;52:4205-10.

[248] Leveque N, Raghavan SL, Lane ME, Hadgraft J. Use of a molecular form technique for the penetration of supersaturated solutions of salicylic acid across silicone membranes and human skin in vitro. International Journal of Pharmaceutics. 2006;318:49-54.

[249] Khan GM, Frum Y, Sarheed O, Eccleston GM, Meidan VM. Assessment of drug permeability distributions in two different model skins. International Journal of Pharmaceutics. 2005;303:81-7.

[250] Aoyagi S, Izumi H, Fukuda M. Biodegradable polymer needle with various tip angles and consideration on insertion mechanism of mosquito's proboscis. Sensor Actuat a-Phys. 2008;143:20-8.

[251] Shergold OA, Fleck NA. Experimental investigation into the deep penetration of soft solids by sharp and blunt punches, with application to the piercing of skin. J Biomech Eng-T Asme. 2005;127:838-48.

[252] Tomimoto M. The frictional pattern of tactile sensations in anthropomorphic fingertip. Tribology International. 2011;44:1340-7.

[253] Morales-Hurtado M, Zeng X, Gonzalez-Rodriguez P, Ten Elshof J, van der Heide E. A new water absorbable mechanical Epidermal skin equivalent: The combination of Hydrophobic PDMS and Hydrophilic PVA Hydrogel. J Mech Behav Biomed. 2015.

[254] Van Der Heide E, Lossie CM, Van Bommel KJC, Reinders SAF, Lenting HBM. Experimental Investigation of a Polymer Coating in Sliding Contact with Skin-Equivalent Silicone Rubber in an Aqueous Environment. Tribology Transactions. 2010;53:842-7.

[255] FIFA. FIFA Quality Concept for Football Turf. Handbook of Test Methods. January ed: Zurich; 2012.

[256] Guerra C, Schwartz CJ. Development of a Synthetic Skin Simulant Platform for the Investigation of Dermal Blistering Mechanics. Tribology Letters. 2011;44:223-8.

[257] Graham TE, Sabelman EE. Human skin model for intradermal injection demonstration or training. Google Patents; 1984.

[258] Hwang HY. Piezoelectric Particle-Reinforced Polyurethane for Tactile Sensing Robot Skin. Mech Compos Mater. 2011;47:137-44.

[259] Krol P. Synthesis methods, chemical structures and phase structures of linear polyurethanes. Properties and applications of linear polyurethanes in polyurethane elastomers, copolymers and ionomers. Prog Mater Sci. 2007;52:915-1015.

[260] Cooper SL, Tobolsky AV. Properties of Linear Elastomeric Polyurethanes. J Appl Polym Sci. 1966;10:1837-&.

[261] Cottenden DJ, Cottenden AM. A study of friction mechanisms between a surrogate skin (Lorica soft) and nonwoven fabrics*. J Mech Behav Biomed. 2013;28:410-26.

[262] Bjellerup M. Novel method for training skin flap surgery: Polyurethane foam dressing used as a skin equivalent. Dermatol Surg. 2005;31:1107-11.

[263] Nakatani M, Fukuda T, Sasamoto H, Arakawa N, Otaka H, Kawasoe T, et al. Relationship between perceived softness of bilayered skin models and their mechanical properties measured with a dual-sensor probe. International journal of cosmetic science. 2013;35:84-8.

[264] Whittle K, Kieser J, Ichim I, Swain M, Waddell N, Livingstone V, et al. The biomechanical modelling of non-ballistic skin wounding: blunt-force injury. Forensic science, medicine, and pathology. 2008;4:33-9.

[265] Niedermann R, Wyss E, Annaheim S, Psikuta A, Davey S, Rossi RM. Prediction of human core body temperature using non-invasive measurement methods. Int J Biometeorol. 2014;58:7-15.

[266] Cruzado BM, Montiel SVY, Atencio JAD. Optical properties in simulated human skin at a wavelength of 633 nm. Optical Diagnostics and Sensing Xii: Toward Point-of-Care Diagnostics and Design and Performance Validation of Phantoms Used in Conjunction with Optical Measurement of Tissue Iv. 2012;8229.

[267] Muskopf JW, McCollister SB. Epoxy resins. Ullmann's encyclopedia of industrial chemistry. 1987.

[268] White DR, Martin RJ. Epoxy-Resin Based Tissue Substitutes. Brit J Radiol. 1977;50:814-21.

[269] Edris A, Choi B, Aguilar G, Nelson JS. Measurements of laser light attenuation following cryogen spray cooling spurt termination. Laser Surg Med. 2003;32:143-7.

[270] Pikkula BM, Domankevitz Y, Tunnell JW, Anvari B. Cryogen spray cooling: Effects of cryogen film on heat removal and light transmission. P Soc Photo-Opt Ins. 2002;4609:50-6.

[271] Mandal S, Song G. Thermal sensors for performance evaluation of protective clothing against heat and fire: a review. Text Res J. 2015;85:101-12.

[272] Camenzind MA, Dale DJ, Rossi RM. Manikin test for flame engulfment evaluation of protective clothing: Historical review and development of a new ISO standard. Fire Mater. 2007;31:285-95.

[273] Torres JH, Anvari B, Tanenbaum BS, Milner TE, Yu JC, Nelson JS. Internal temperature measurements in response to cryogen spray cooling of a skin phantom. Lasers in Surgery: Advanced Characterization, Therapeutics, and Systems Ix, Proceedings Of. 1999;3590:11-9.

[274] Ramirez-San-Juan JC, Aguilar G, Tuqan AT, Kelly KM, Nelson JS. Skin model surface temperatures during single and multiple cryogen spurts used in laser dermatologic surgery. Lasers in Surgery and Medicine. 2005;36:141-6.

[275] Tuchin VV, Bashkatov AN, Genina EA, Kochubey VI, Lychagov VV, Portnov SA, et al. Finger tissue model and blood perfused skin tissue phantom. Dynamics and Fluctuations in Biomedical Photonics Viii. 2011;7898.

[276] Gibson A, Yusof RM, Dehghani H, Riley J, Everdell N, Richards R, et al. Optical tomography of a realistic neonatal head phantom. Appl Optics. 2003;42:3109-16.

[277] Simpson CR, Kohl M, Essenpreis M, Cope M. Near-infrared optical properties of ex vivo human skin and subcutaneous tissues measured using the Monte Carlo inversion technique. Phys Med Biol. 1998;43:2465-78.

[278] Hoevel MK. Contoured mammography phantom with skin. Google Patents; 1987.

[279] Yoo HS, Hu YS, Kim EA. Effects of Heat and Moisture Transport in Fabrics and Garments Determined with a Vertical Plate Sweating Skin Model. Text Res J. 2000;70:542-9.

[280] Psikuta A, Richards M, Fiala D. Single-sector thermophysiological human simulator. Physiol Meas. 2008;29:181-92.

[281] Wang FM, Gao CS, Kuklane K, Holmer I. A Study on Evaporative Resistances of Two Skins Designed for Thermal Manikin Tore under Different Environmental Conditions. Textile Bioengineering and Informatics Symposium Proceedings, Vols 1 and 2. 2009:211-5.

[282] Kim JO. Dynamic moisture vapor transfer through textiles Part III: Effect of film characteristics on microclimate moisture and temperature changes. Text Res J. 1999;69:193-202.

[283] Zimmerli T, Weder MS. Protection and comfort - A sweating torso for the simultaneous measurement of protective and comfort properties of PPE. Am Soc Test Mater. 1997;1273:271-80.

[284] Wang F, Annaheim S, Morrissey M, Rossi R. Real evaporative cooling efficiency of one-layer tight-fitting sportswear in a hot environment. Scand J Med Sci Spor. 2014;24:e129-e39.

[285] Richards MG, Mattle NG. A sweating agile thermal manikin (SAM) developed to test complete clothing systems under normal and extreme conditions. DTIC Document; 2002.

[286] Lir I, Haber M, Dodiuk-Kenig H. Skin surface model material as a substrate for adhesion-to-skin testing. J Adhes Sci Technol. 2007;21:1497-512.

[287] Takegami K, Kaneko Y, Watanabe T, Maruyama T, Matsumoto Y, Nagawa H. Polyacrylamide gel containing egg white as new model for irradiation experiments using focused ultrasound. Ultrasound in Medicine and Biology. 2004;30:1419-22.

[288] Ansari M, Kazemipour M, Aklamli M. The study of drug permeation through natural membranes. International Journal of Pharmaceutics. 2006;327:6-11.

[289] Stampfli R, Bruhwiler PA, Rechsteiner I, Meyer VR, Rossi RM. X-ray tomographic investigation of water distribution in textiles under compression - Possibilities for data presentation. Measurement. 2013;46:1212-9.

[290] Weder M, Brühwiler PA, Laib A. X-Ray Tomography Measurements of the Moisture Distribution in Multilayered Clothing Systems. Text Res J. 2006;76:18-26.

[291] Hou LL, Hagen J, Wang X, Papautsky I, Naik R, Kelley-Loughnane N, et al. Artificial microfluidic skin for in vitro perspiration simulation and testing. Lab Chip. 2013;13:1868-75.

[292] Massaro A, Spano F, Cazzato P, La Tegola C, Cingolani R, Athanassiou A. Robot Tactile Sensing Gold Nanocomposites as Highly Sensitive Real-Time Optical Pressure Sensors. Ieee Robot Autom Mag. 2013;20:82-90.

[293] Massaro A, Spano F, Missori M, Malvindi MA, Cazzato P, Cingolani R, et al. Flexible nanocomposites with all-optical tactile sensing capability. Rsc Adv. 2014;4:2820-5.

[294] de Bruin DM, Bremmer RH, Kodach VM, de Kinkelder R, van Marle J, van Leeuwen TG, et al. Optical phantoms of varying geometry based on thin building blocks with controlled optical properties. J Biomed Opt. 2010;15.

[295] Zagaynova EV, Shirmanova MV, Kirillin MY, Khlebtsov BN, Orlova AG, Balalaeva IV, et al. Contrasting properties of gold nanoparticles for optical coherence

tomography: phantom, in vivo studies and Monte Carlo simulation. Physics in Medicine and Biology. 2008;53:4995-5009.

[296] Hao B, Liu W, Hu Z, Hong B, Li J. Metrology research on PDMS phantoms for evaluating resolution performance of OCT systems. 2014. p. 92820H-H-7.

[297] Allardice JT, Abulafi AM, Webb DG, Williams NS. Standardization of Intralipid for Light-Scattering in Clinical Photodynamic Therapy. Laser Med Sci. 1992;7:461-5.

[298] Bordier C, Andraud C, Charron E, Lafait J, Anastasiadou M, De Martino A. Illustration of a bimodal system in Intralipid-20% by polarized light scattering: experiments and modeling. Appl Phys a-Mater. 2009;94:347-55.

[299] van Staveren HJ, Moes CJ, van Marie J, Prahl SA, van Gemert MJ. Light scattering in Intralipid-10% in the wavelength range of 400-1100 nm. Appl Opt. 1991;30:4507-14.

[300] Canavese G, Stassi S, Stralla M, Bignardi C, Pirri CF. Stretchable and conformable metal-polymer piezoresistive hybrid system. Sensor Actuat a-Phys. 2012;186:191-7.

[301] Edwards C, Marks R. Evaluation of biomechanical properties of human skin. Clin Dermatol. 1995;13:375-80.

[302] www.pebax.com, 14.07.2016.

[303] Cui WG, Zhou Y, Chang J. Electrospun nanofibrous materials for tissue engineering and drug delivery. Sci Technol Adv Mat. 2010;11.

[304] Huang ZM, Zhang YZ, Kotaki M, Ramakrishna S. A review on polymer nanofibers by electrospinning and their applications in nanocomposites. Compos Sci Technol. 2003;63:2223-53.

[305] Wang XF, Ding B, Li BY. Biomimetic electrospun nanofibrous structures for tissue engineering. Mater Today. 2013;16:229-41.

[306] Bhardwaj N, Kundu SC. Electrospinning: A fascinating fiber fabrication technique. Biotechnol Adv. 2010;28:325-47.

[307] Lin CR, Chen RH, Hung C. The characterisation and finite-element analysis of a polymer under hot pressing. Int J Adv Manuf Tech. 2002;20:230-5.

[308] Appetecchi GB, Hassoun J, Scrosati B, Croce F, Cassel F, Salomon M. Hot-pressed, solvent-free, nanocomposite, PEO-based electrolyte membranes II. All solid-state Li/LiFePO4 polymer batteries. J Power Sources. 2003;124:246-53.

[309] Khim DY, Han H, Baeg KJ, Kim JW, Kwak SW, Kim DY, et al. Simple Bar-Coating Process for Large-Area, High-Performance Organic Field-Effect Transistors and Ambipolar Complementary Integrated Circuits. Adv Mater. 2013;25:4302-8.

[310] Cengiz-Çallioğlu F, Jirsak O, Dayik M. Electric current in polymer solution jet and spinnability in the needleless electrospinning process. Fibers and Polymers. 2012;13:1266-71.

[311] James W, Berger T, Elston D. Skin: basic structure and function. Andrews' Diseases of the Skin Clinical Dermatology, 10th Edition Phildelphia: Saunder Elsevier. 2006;12.

[312] Marks JG, Miller JJ. Lookingbill and Marks' principles of dermatology: Elsevier Health Sciences; 2013.

[313] Welzel J, Reinhardt C, Lankenau E, Winter C, Wolff H. Changes in function and morphology of normal human skin: evaluation using optical coherence tomography. Brit J Dermatol. 2004;150:220-5.

[314] Dąbrowska AK, Rotaru GM, Derler S, Spano F, Camenzind M, Annaheim S, et al. Materials used to simulate physical properties of human skin. Skin Research and Technology. 2015:n/a-n/a.

[315] Koepke P, Hess M, Bretl S, Seefeldner M. UV irradiance on the human skin: Effects of orientation and sky obstructions. CURRENT PROBLEMS IN ATMOSPHERIC RADIATION (IRS 2008): Proceedings of the International Radiation Symposium (IRC/IAMAS): AIP Publishing; 2009. p. 53-6.

[316] Caspers PJ, Lucassen GW, Bruining HA, Puppels GJ. Automated depth-scanning confocal Raman microspectrometer for rapid in vivo determination of water concentration profiles in human skin. J Raman Spectrosc. 2000;31:813-8.

[317] Elias PM. Epidermal lipids, barrier function, and desquamation. J Invest Dermatol. 1983;80.

[318] Fleischli FD, Mathes S, Adlhart C. Label free non-invasive imaging of topically applied actives in reconstructed human epidermis by confocal Raman spectroscopy. Vib Spectrosc. 2013;68:29-33.

[319] Elsner P. What textile engineers should know about the human skin. Textiles and the Skin: Karger Publishers; 2004. p. 24-34.

[320] Beele H. Artificial skin: past, present and future. The International journal of artificial organs. 2002;25:163-73.

[321] Crowther JM, Sieg A, Blenkiron P, Marcott C, Matts PJ, Kaczvinsky R, et al. Measuring the effects of topical moisturizers on changes in stratum corneum thickness, water gradients and hydration in vivo. Brit J Dermatol. 2008;159:567-77.

[322] Loth H. Vehicular Influence on Transdermal Drug Penetration. Int J Pharm. 1991;68:1-10.

[323] García JJO, Treviño-Palacios CG. Skin Effects Caused by the Use of Detergents. MEDICAL PHYSICS: Ninth Mexican Symposium on Medical Physics: AIP Publishing; 2006. p. 191-3.

[324] Wan MJ, Su XY, Zheng Y, Gong ZJ, Yi JL, Zhao Y, et al. Seasonal variability in the biophysical properties of forehead skin in women in Guangzhou City, China. Int J Dermatol. 2015;54:1319-24.

[325] Johnsen K, Mahonen M, Lunde P. Prevalence estimation and follow-up of aortic regurgitation subjects in a Norwegian Sami population. Scand Cardiovasc J. 2009;43:176-80.

[326] Zhang GJ, Papillon A, Ruvolo E, Bargo PR, Kollias N. In vivo Comparative Documentation of skin hydration by confocal Raman microscopy, Skin Sensor, Skicon and NovaMeter. Photonic Therapeutics and Diagnostics Vi. 2010;7548.

[327] Wichrowski K, Sore G, Khaiat A. Use of infrared spectroscopy for in vivo measurement of the stratum corneum moisturization after application of costmetic preparations. International journal of cosmetic science. 1995;17:1-11.

[328] Tagami H, Ohi M, Iwatsuki K, Kanamaru Y, Yamada M, Ichijo B. Evaluation of the Skin Surface Hydration Invivo by Electrical Measurement. J Invest Dermatol. 1980;75:500-7.

[329] Fleischli FD, Morf F, Adlhart C. Skin Concentrations of Topically Applied Substances in Reconstructed Human Epidermis (RHE) Compared with Human Skin Using in vivo Confocal Raman Microscopy. Chimia. 2015;69:147-51.

[330] Boncheva M, de Sterke J, Caspers PJ, Puppels GJ. Depth profiling of Stratum corneum hydration in vivo: a comparison between conductance and confocal Raman spectroscopic measurements. Exp Dermatol. 2009;18:870-6.

[331] Adlhart C, Baschong W. Surface distribution and depths profiling of particulate organic UV absorbers by Raman imaging and tape stripping. International Journal of Cosmetic Science. 2011;33:527-34.

[332] Shojo D, Sugimori H, Yamazaki S, Kimura K. Preparation of aromatic polyimide particles having clear morphology by polymerization of salt monomers. High Perform Polym. 2015:0954008315619998.

[333] Watanabe H, Furuyama T, Okazaki K. Carbon surface characteristics after electrochemical oxidation in a direct carbon fuel cell using a single carbon pellet and molten carbonates. Energy & Fuels. 2015;29:5415-22.

[334] Cznotka E, Jeschke S, Schmohl S, Johansson P, Wiemhöfer H-D. 3D laser scanning confocal microscopy of siloxane-based comb and double-comb polymers in PVDF-HFP thin films. Journal of Coatings Technology and Research.1-11.

[335] Schüttel M. Development of an in vivo screening method for moisturizer by Raman spectroscopy: Zurich University of Applied Sciences; 2013.

[336] Egawa M, Tagami H. Comparison of the depth profiles of water and water-binding substances in the stratum corneum determined in vivo by Raman spectroscopy between the cheek and volar forearm skin: effects of age, seasonal changes and artificial forced hydration. Brit J Dermatol. 2008;158:251-60.

[337] Everall NJ. Confocal Raman microscopy: why the depth resolution and spatial accuracy can be much worse than you think. Appl Spectrosc. 2000;54:1515-20.

[338] Greenspan L. Humidity fixed points of binary saturated aqueous solutions. Journal of research of the national bureau of standards. 1977;81:89-96.

[339] Wexler A, Hasegawa S. Relative humidity-temperature relationships of some saturated salt solutions in the temperature range 0 to 50 C. Journal of Research of the National Bureau of Standards. 1954;53:19-26.

[340] Swartzendruber DC, Wertz PW, Madison KC, Downing DT. Evidence That the Corneocyte Has a Chemically Bound Lipid Envelope. J Invest Dermatol. 1987;88:709-13.

[341] Park AC, Baddiel CB. Rheology of Stratum Corneum .1. Molecular Interpretation of Stress-Strain Curve. J Soc Cosmet Chem. 1972;23:3-&.

[342] Park AC, Baddiel CB. Rheology of Stratum Corneum .2. Physicochemical Investigation of Factors Influencing Water-Content of Corneum. J Soc Cosmet Chem. 1972;23:13-&.

[343] van Kuilenburg J, Masen MA, van der Heide E. Contact modelling of human skin: What value to use for the modulus of elasticity? P I Mech Eng J-J Eng. 2013;227:349-61.

[344] Geerligs M. In vitro mechanical characterization of human skin layers: stratum corneum, epidermis and hypodermis.: Technical University Eindhoven; 2009.

[345] Arimoto H, Egawa M. Imaging wavelength and light penetration depth for water content distribution measurement of skin. Skin Research and Technology. 2015;21:94-100.

[346] Bielfeldt S, Schoder V, Ely U, Van Der Pol A, De Sterke J, Wilhelm KP. Assessment of human stratum corneum thickness and its barrier properties by in-vivo confocal Raman spectroscopy2009.

[347] Elias PM, Feingold KR. Skin barrier: CRC Press; 2005.

[348] Elias PM. The skin barrier as an innate immune element. Semin Immunopathol. 2007;29:3-14.

[349] van Logtestijn MDA, Dominguez-Huttinger E, Stamatas GN, Tanaka RJ. Resistance to Water Diffusion in the Stratum Corneum Is Depth-Dependent. Plos One. 2015;10.

[350] van Logtestijn MD, Domínguez-Hüttinger E, Stamatas GN, Tanaka RJ. Resistance to water diffusion in the stratum corneum is depth-dependent. Plos One. 2015;10:e0117292.

[351] Li X, Johnson R, Kasting GB. On the Variation of Water Diffusion Coefficient in Stratum Corneum With Water Content. J Pharm Sci-Us. 2016;105:1141-7.

[352] Bouwstra JA, de Graaff A, Gooris GS, Nijsse J, Wiechers JW, van Aelst AC. Water distribution and related morphology in human stratum corneum at different hydration levels. J Invest Dermatol. 2003;120:750-8.

[353] Schatzlein A, Cevc G. Non-uniform cellular packing of the stratum corneum and permeability barrier function of intact skin: a high-resolution confocal laser scanning microscopy study using highly deformable vesicles (Transfersomes). Brit J Dermatol. 1998;138:583-92.

[354] Simonetti O, Hoogstraate AJ, Bialik W, Kempenaar JA, Schrijvers AHGJ, Bodde HE, et al. Visualization of Diffusion Pathways across the Stratum-Corneum of Native and in-Vitro-Reconstructed Epidermis by Confocal Laser-Scanning Microscopy. Arch Dermatol Res. 1995;287:465-73.

[355] vanderMolen RG, Spies F, vantNoordende JM, Boelsma E, Mommaas AM, Koerten HK. Tape stripping of human stratum corneum yields cell layers that originate from various depths because of furrows in the skin. Arch Dermatol Res. 1997;289:514-8.

[356] Haynes WM. CRC handbook of chemistry and physics: CRC press; 2014.

[357] O.Vaisala. Humidity Conversion Formulas. Helsinki2013.

[358] Lange NA, Forker GM, Burington RS. Handbook of chemistry. 1939.

[359] Benson HA. Transdermal drug delivery: penetration enhancement techniques. Current drug delivery. 2005;2:23-33.

[360] Field CK, Kerstein MD. Overview of wound healing in a moist environment. The American journal of surgery. 1994;167:S2-S6.

[361] Seyfarth F, Schliemann S, Antonov D, Elsner P. Dry skin, barrier function, and irritant contact dermatitis in the elderly. Clin Dermatol. 2011;29:31-6.

[362] Baumann L. Skin ageing and its treatment. The Journal of pathology. 2007;211:241-51.

[363] Gerhardt LC, Mattle N, Schrade G, Spencer N, Derler S. Study of skin–fabric interactions of relevance to decubitus: friction and contact-pressure measurements. Skin Research and Technology. 2008;14:77-88.

[364] El-Shimi A. In vivo skin friction measurements. J Soc Cosmet Chem. 1977;28:37-52.

[365] Curtis J, Colas A. Dow Corning® Silicone Biomaterials: History, Chemistry & Medical Applications of Silicones. Biomaterials Science. 2004;2.

[366] Geerligs M. In vitro mechanical characterization of human skin layers: stratum corneum, epidermis and hypodermis: Ph. D. Thesis, Technische Universiteit Eindhoven; 2006.

[367] Hendriks CP, Franklin SE. Influence of Surface Roughness, Material and Climate Conditions on the Friction of Human Skin. Tribol Lett. 2010;37:361-73.

[368] Bir CA, Resslar M, Stewart S. Skin penetration surrogate for the evaluation of less lethal kinetic energy munitions. Forensic science international. 2012;220:126-9.

[369] Renvoise J, Burlot D, Marin G, Derail C. Adherence performances of pressure sensitive adhesives on a model viscoelastic synthetic film: a tool for the understanding of adhesion on the human skin. Int J Pharm. 2009;368:83-8.

[370] Baït N, Grassl B, Derail C, Benaboura A. Hydrogel nanocomposites as pressure-sensitive adhesives for skin-contact applications. Soft Matter. 2011;7:2025-32.

[371] Bigi A, Cojazzi G, Panzavolta S, Rubini K, Roveri N. Mechanical and thermal properties of gelatin films at different degrees of glutaraldehyde crosslinking. Biomaterials. 2001;22:763-8.

[372] Bigi A, Cojazzi G, Panzavolta S, Roveri N, Rubini K. Stabilization of gelatin films by crosslinking with genipin. Biomaterials. 2002;23:4827-32.

[373] Rho KS, Jeong L, Lee G, Seo BM, Park YJ, Hong SD, et al. Electrospinning of collagen nanofibers: Effects on the behavior of normal human keratinocytes and early-stage wound healing. Biomaterials. 2006;27:1452-61.

[374] Frushour BG, Koenig JL. Raman scattering of collagen, gelatin, and elastin. Biopolymers. 1975;14:379-91.

[375] Deurenberg P, Weststrate JA, Seidell JC. Body-Mass Index as a Measure of Body Fatness - Age-Specific and Sex-Specific Prediction Formulas. Brit J Nutr. 1991;65:105-14.

[376] Agache P, Boyer JP, Laurent R. Biomechanical Properties and Microscopic Morphology of Human Stratum Corneum Incubated on a Wet Pad in-Vitro. Arch Dermatol Forsch. 1973;246:271-83.

[377] Wildnaue.Rh, Bothwell JW, Douglass AB. Stratum Corneum Biomechanical Properties .1. Influence of Relative Humidity on Normal and Extracted Human Stratum Corneum. J Invest Dermatol. 1971;56:72-&.

[378] Van Duzee BF. The influence of water content, chemical treatment and temperature on the rheological properties of stratum corneum. J Invest Dermatol. 1978;71:140-4.

[379] Wu KS, van Osdol WW, Dauskardt RH. Mechanical properties of human stratum corneum: effects of temperature, hydration, and chemical treatment. Biomaterials. 2006;27:785-95.

[380] Yuan YH, Verma R. Measuring microelastic properties of stratum corneum. Colloid Surface B. 2006;48:6-12.

[381] Yuan YH, Verma R. Mechanical properties of stratum corneum studied by nano-indentation. Spatially Resolved Characterization of Local Phenomena in Materials and Nanostructures. 2003;738:265-72.

[382] Kovalev AE, Dening K, Persson BNJ, Gorb SN. Surface topography and contact mechanics of dry and wet human skin. Beilstein J Nanotech. 2014;5:1341-8.

[383] Kenins P. Influence of Fiber-Type and Moisture on Measured Fabric-to-Skin Friction. Text Res J. 1994;64:722-8.

[384] Su CL, Fang JX, Chen XH, Wu WY. Moisture absorption and release of profiled polyester and cotton composite knitted fabrics. Text Res J. 2007;77:764-9.

[385] Kuilenburg Jv, Masen M, Heide E. A mechanistic approach to predicting the friction behaviour of human skin. ASME/STLE 2012 International Joint Tribology Conference, IJTC 2012, 7-10 October 2012, Denver, CO, USA American Society of Mechanical Engineers, Tribology Division, TRIB, 45-472012.

[386] Van Kuilenburg J, Masen M, Van Der Heide E. The role of the skin microrelief in the contact behaviour of human skin: Contact between the human finger and regular surface textures. Tribol Int. 2013;65:81-90.

[387] Pailler-Mattei C, Zahouani H. Study of adhesion forces and mechanical properties of human skin in vivo. Journal of Adhesion Science and Technology. 2004;18:1739-58.

[388] Wolfram L. Friction of skin. J Soc Cosmet Chem. 1983;34:465-76.

[389] Hertz H. Über die Berührung fester elastischer Körper. Journal für die reine und angewandte Mathematik. 1882;92:156-71.

[390] Derler S, Suess J, Rao A, Rotaru GM. Influence of variations in the pressure distribution on the friction of the finger pad. Tribol Int. 2013;63:14-20.